Rafael Vitorino

Production of high-value ingredients from *Raphidonema monicae* biomass and evaluation of their impact in aquafeed applications

UNIVERSIDADE DO ALGARVE

Faculdade de Ciências e Tecnologia

2023

Rafael Vitorino

Production of high-value ingredients from *Raphidonema monicae* biomass and evaluation of their impact in aquafeed applications

Mestrado em Biologia Molecular e Microbiana

Trabalho efetuado sob a orientação de:

Prof. Dr. João Varela – Ualg, CCMar, GreenCoLab

Dr. Hugo Pereira - GreenCoLab

UNIVERSIDADE DO ALGARVE

Faculdade de Ciências e Tecnologia

2023

Production of high-value ingredients from *Raphidonema monicae* biomass and evaluation of their impact in aquafeed applications

Declaração de autoria de trabalho

Declaro ser o autor deste trabalho, que é original e inédito. Autores e trabalhos consultados estão devidamente citados no texto e constam da listagem de referências incluído.

_____

(Rafael Vitorino)

Agradecimentos

Ao professor Dr. João Varela, gostaria de expressar o meu profundo agradecimento, que não só esteve presente desde a minha licenciatura em Bioquímica, como também me proporcionou a oportunidade de realizar esta tese. A sua valiosa orientação e encorajamento deram-me forças quando fraquejei, e foram cruciais para o meu progresso e para a conclusão desta tese.

Ao Dr. Hugo Pereira, que viu em mim alguém merecedor e me estendeu a mão que abriu caminho para esta tese. Agradeço a disponibilidade, tempo e paciência ao longo de todo este precurso, que foi atribulado e cheio de desafios.

À equipa do GreenCoLab, em particular ao Bernardo, à Monya e Sara, e à Ana, pelo vosso tempo, amizade e disponibilidade. Bernardo, muito me ouviste e me aturaste durante todo este caminho, sem ti não sei se teria conseguido ultrapassar os obstáculos que surgiram na tese. Monya e Sara, pelo conhecimento, apoio e carinho e pelas nossas conversas sempre a me puxarem para cima. Ana, pela energética orientação, se bem que exigente, e sem rodeios, mas que foi necessária para eu acordar para a vida e chegar a bom porto. Ao resto da equipa do GreenCoLab, pelo enorme apoio e amizade que tornaram os dias mais coloridos e me fizeram sentir em casa.

À equipa do MarBioTech, em particular à Inês, Beatriz e Melanie, pela paciência e motivação, por me ouvirem quando precisei, e pelos vossos preciosos conselhos. Inês, que paciência que tiveste, nem durante as férias te deixava descansar! Mas arranjaste sempre tempo para mim, muito obrigado! Beatriz, já caminhamos juntos há algum tempo, desde colegas de licenciatura a amigos nos tornámos. Estiveste lá em todos os meus melhores e piores momentos, sempre a apoiar-me com esse teu feitio especial, e a dar-me nas orelhas quando eu tinha ideias loucas. És como uma irmã para mim, e não trocaria por nada a nossa amizade, muito obrigado por tudo! Melanie, foi obra do acaso nos termos conhecido, mas fico feliz pela amizade, e pelo apoio que deste, que podes ter sentido que foi pouco, mas estavas lá quando precisei, e agradeço profundamente por isso. Ao resto da equipa do MarbioTech, por me acolherem como se fosse um colega de longa data e pela paciência que tiveram quando vos bombardeava com perguntas (e eu bem sei que foram muitas!).

Aos meus colegas de mestrado, especialmente a Ana e a Oda, por abraçarem a loucura comigo e estarem sempre lá quando precisava. Pelos momentos de convívio e alegria que foram muitos, e espero que sejam muitos mais!

À minha família, pelo amor incondicional, e conselhos indispensáveis que me guiaram no caminho certo. Os nossos momentos de convívio em muito me fortaleceram e deram forças para seguir em frente. Mas em particular à minha mãe, que sem ela nunca teria chegado onde cheguei. Por ser uma mãe galinha que conseguia stressar mais que eu na tese, e apesar de me chatear muito a cabeça, o fazer sempre do fundo do coração, cheio de amor.

Esta tese foi um percurso que não fiz sozinho, fi-lo com todos vós, e muito orgulho tenho em o ter percorrido convosco.

Abstract

Global problems including lack of food, clean water, and energy, are worsening, especially in aquaculture due to overfishing damaging ecosystems. Meanwhile, meeting a rising seafood demand while wild fisheries decline is a challenge. However, microalgae, highly adaptable and diverse microorganisms, could provide sustainable feed solutions, but to tap into their potential, it is necessary to optimize biorefinery processing methodologies.

In this thesis, a novel microalga, *Raphidonema monicae* (previously known as *Koliella antarctica*), was selected to produce fractions enriched in high-value compounds. By combining high-pressure homogenization and enzymatic hydrolysis techniques, a methodology comprised of 1 cycle of HPH at 1068 bars followed by a 1h alcalase treatment at 5% concentration (w/w), 50 ºC, pH 8 was optimized, achieving 71% disruption efficiency.

Using fractionation methodologies including micro and ultrafiltration, pH shifting and ethanolic extractions, six fractions were produced, found to be enriched in high-value compounds including PUFA, such as eicosapentaenoic acid (EPA), arachidonic acid (ARA), linoleic acid (LA), α-linolenic acid (ALA), and γ-linolenic acid (GLA), and certain bioactive pigments including lutein, neoxanthin, zeaxanthin and β-carotenes. These, and non-treated and disrupted fractions of *R. monicae*, to a total of 9 fractions, were evaluated in their potential to improve fish health by assessing the transcriptional response of genes related to the epithelial integrity (*OCL* and *TJP2*), antioxidant capacity (*GPx* and *CAT*) and immunostimulation (*COX2* and *IL1B*) in the intestine. While these fractions were found to have no significant influence on the transcription response, some up and down-regulatory expression trends were noticed regarding the antioxidant and immunostimulation genes, suggesting the fractions potentially contributed to the protection of the intestine. Further studies are however needed, to fully ascertain if these fractions hold any potential as feed ingredients for the amelioration of fish health.

Keywords: *Raphidonema monicae*; Biorefinery; Bioactive; High-value; PUFA; Gut performance.

Resumo

As microalgas são um grupo diverso de microrganismos que possuem notáveis capacidades de adaptação. Como causa e efeito, a composição bioquímica destes organismos também é bastante variada, incluindo um grande leque de diversos compostos com potencial bioatividade, incluindo aminoácidos, açúcares redutores, ácidos gordos polinsaturados (PUFA), proteínas, lípidos, açúcares, vitaminas, pigmentos e fenóis. Tendo em conta a vasta biodiversidade das microalgas, estas têm um elevado potencial como ferramenta para vários setores industriais, sendo utilizadas para o tratamento de águas residuais, bem como fontes sustentáveis de compostos de alto valor com potencial bioatividade para a produção de biocombustíveis, fertilizantes, nutracêuticos, alimentos, entre outros.

Com o agravamento de problemas a nível global, como a escassez de alimentos, água potável e energia, é cada vez mais imperativo a procura de soluções. Isto é particularmente importante no setor de aquacultura, que a cada ano que passa está cada vez mais sob pressão à medida que a humanidade tenta transitar da pesca para o cultivo controlado de produtos marinhos. No entanto, os produtos marinhos requerem vários recursos bem como um controlo muito preciso das suas condições de crescimento visto que estão bastante suscetíveis a adoecerem face condições de stress. Neste cenário, as microalgas podem ser utilizadas como recursos sustentáveis para a produção de alimentos de aquacultura ou substituir ingredientes não sustentáveis, bem como fornecer suplementos bioativos capazes de modular o sistema imunológico de forma a fortalecer a vitalidade dos organismos e prevenir o adoecimento. Todavia, para se maximizar o aproveitamento do potencial das microalgas nesta área industrial, é necessário desenvolver uma cadeia de processamento em bio-refinaria que combine técnicas de disrupção, fracionamento e estabilização de biomassa.

Nesta tese, a microalga *Raphidonema monicae* foi escolhida devido ao seu perfil bioquímico enriquecido em compostos bioativos incluindo PUFA e certos tipos de pigmentos. Em relação à sua disrupção, o processamento que combinou técnicas de disrupção via homogeneização de alta pressão (HPH) e hidrólise enzimática (EH) foi otimizado. Em relação à técnica de HPH, verificou-se que a condição mais eficiente para a disrupção da biomassa envolvia uma passagem no homogenizador a uma pressão de 1068 bars, levando a uma eficiência de disrupção de 50%. Em relação à técnica de hidrólise enzimática, verificou-se que das enzimas testadas a 4% (w/w), que

incluiu celulase, mananase, viscozyme, pectinase e alcalase, a mais eficiente na disrupção da biomassa foi a alcalase, com uma eficiência de disrupção de 63%. Ao combinar as duas técnicas de disrupção, tendo um tratamento inicial com HPH a 1068 bars, por 1 ciclo, seguido de uma disrupção enzimática com alcalase a 5% (w/w) por 90 minutos a 50 ºC, foi possível atingir uma eficiência de disrupção de 71%. Adicionalmente, foi possível concentrar em 2 vezes os açúcares solúveis e lípidos totais, e em 5 vezes os aminoácidos livres e proteínas solúveis.

Através de uma metodologia de fracionamento de solubilização alcalina, micro- e ultrafiltração e extração etanolica, foi possível fracionar esta biomassa em 6 frações enriquecidas em diferentes tipos de compostos de elevado valor. Em relação à extração de pigmentos, foi possível extrair neoxantina até 1,79 mg/g, luteína até 3,75 mg/g, zeaxantina até 0,56 mg/g, α-carotenos até 0,12 mg/g e β-carotenos até 9,84 mg/g. Em relação aos ácidos gordos polinsaturados, foi possível extrair, em abundância relativa de ácidos gordos totais, ácido eicosapentanóico (EPA) até 19.20±3.26 %, ácido linoleico (LA) até 16.27±0.25 %, ácido araquidónico (ARA), até 7.98±0.51 %, ácido α-linolénico (ALA) até 14.59±0.17 %, e ácido γ-linolénico (GLA) até 1.27±0.01 %.

As frações atrás mencionadas, assim como a biomassa hidrolisada e a biomassa não tratada foram testadas no seu potencial de melhorar a vitalidade dos peixes, através da avaliação da modulação transcricional destas frações em genes associados com a estabilidade epitelial (*OCL*; *TJP*1), resposta antioxidante (*GPx*; *CAT*) e imunoestimulação (*COX2*; *IL1B*) em células intestinais de dourada (*Sparus aurata*). No entanto, não foi possível identificar nenhuma influência indutora ou inibitória destas frações na expressão destes genes. Foram, no entanto, detetadas tendências inibitória ou amplificadoras destas frações nos genes associados à resposta antioxidante e imunoestimulação. Mais especificamente, em relação à resposta antioxidante, foi observado uma tendência não significativa amplificadora em ambos os genes. Esta resposta transcricional sugere que os compostos de alto valor presentes nas frações processadas possuíam atividade moduladora da resposta antioxidante, agindo como amplificadores/estimuladores da resposta antioxidante. Em relação à defesa imunológica, foi detetada uma tendência não significativa inibitória em relação ao gene *IL1B*. Isto sugere que as frações produzidas estariam enriquecidas em compostos anti-inflamatórios que sequestraram compostos inflamatórios e criaram um ambiente com reduzida atividade inflamatória que possibilitou a redução na resposta imunológica. No entanto, tendo em

conta que estas tendências observadas foram não significativas, será necessário recorrer a estudos mais aprofundados *ex-vivo* e *in-vivo* para avaliar o potencial destas frações no melhoramento da vitalidade dos peixes, como fonte de vários compostos bioativos de alto valor.

Palavras-chave: *Raphidonema monicae*; Bio-refinaria; Alto valor; Bioativo; PUFA.

Index

Figure index

Table index

1.Introduction

1.1. Microalgae

Microalgae are a biologically diverse group of microorganisms that can present unicellular and multicellular forms. They thrive in a wide range of habitats and have a remarkable ability to adapt to a wide spectrum of environmental conditions, including temperature, pH and salinity [1]. Most perform photosynthesis, a complex process where CO_2 and inorganic nutrients are converted into organic matter, producing O_2 as a byproduct [2]. They also remove high concentrations of sulfur, phosphorus, and nitrogen from water bodies, making them a resource with a high potential for bioremediation [3,4]. As microalgal biodiversity comprises more than 50,000 known species, their biochemical composition is very diverse, both in terms of primary metabolites (e.g., proteins, polyunsaturated fatty acids, carbohydrates, vitamins, carotenoids and amino acids) and secondary metabolites (e.g., terpenoids, and phenolics) (**Figure 1.1**) [1,5,6]. Some microalgae species are noteworthy for their high protein content, surpassing 50% of their total dry weight (DW) [7]. Notably, *Arthrospira platensis* currently stands out as one of the most protein-rich microalga identified to date, possessing a protein content of up to 77% DW [8]. Meanwhile, other microalgae species are known to have an impressive lipid content of up to 67% DW under stressful conditions, such as *Chlorella* spp., *Dunaliella* spp., and *Scenedesmus* spp. [9]. Furthermore, certain microalgae species are known to have more than 50% of their total content made up of carbohydrates. It is of particular attention that *Porphyridium purpureum* can have up to 72% of its total content composed of carbohydrates [10]. However, the mentioned content values and their specific composition profiles may vary depending on the cultivation parameters, including stress factors and extraction procedures to which microalgae were subjected [11–13].

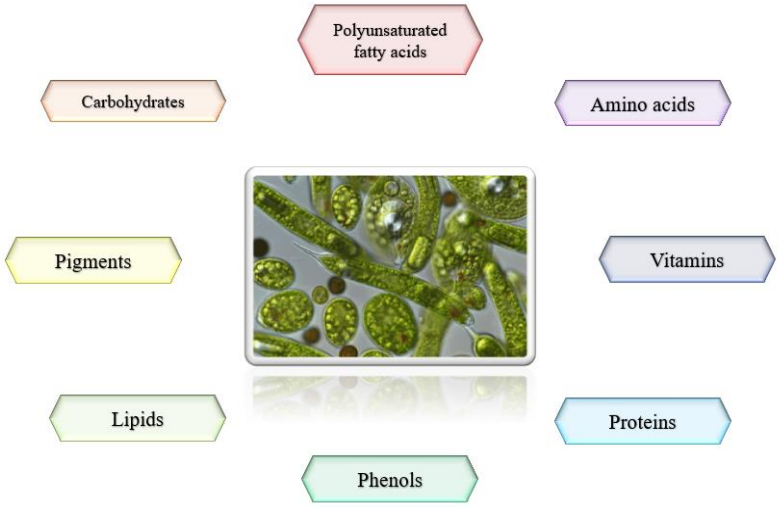

Figure 1.1: Potential compounds found in microalgal biomass. Microalgae are vastly diverse in biochemical composition, often correlated with their habitats.

Given the remarkable biodiversity of microalgae, their biomass has great potential for applications in a wide range of industrial sectors, some of which are already being actively implemented (**Figure 1.2**) [14]. In the water treatment industry, bioremediation techniques are employed to treat polluted or contaminated waters [15]. One project, ALGACYCLE (PT-INNOVATION-0023), aimed to research the use of microalgae as a bioremediation tool, to valorize drain water from hydroponic-based greenhouses, as a way of producing microalgal biomass while treating a waste stream. In the biotechnological field, microalgae have emerged as a sustainable bio-resource, yielding biomass rich in high-value compounds [1,16]. This biomass, in turn, can be used to produce nutraceuticals, biofuels, biofertilizers, cosmetics, food, and feed, with the type of biomass and the processing technologies varying according to the specific needs of each application [1,17–22]. For example, the medical industry has been researching microalgae as potential bio factories to produce recombinant proteins or antibiofilm agents against multidrug resistance bacteria, fungi, and cancerous tissues [23,24]. Microalgae are also being studied for their potential to produce bioplastics, in an effort to reduce fossil-based plastic waste, which has been linked to have vastly negative consequences in the global ecosystem [25].

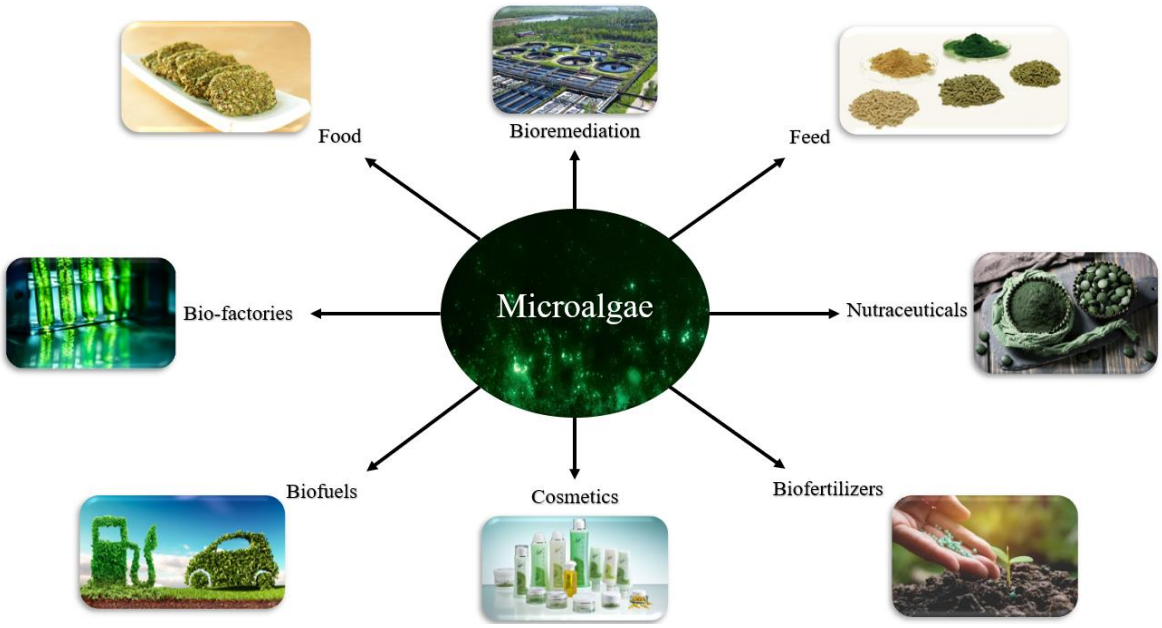

Figure 1.2: Example of microalgae applications. As microalgae possess a diverse biochemical composition, their biomass has a wide variety of potential applications.

With the intensification of global humanitarian challenges, such as climate change, population growth and the resulting scarcity of resources, particularly of food, clean water and energy, the need to find alternative sustainable solutions has never been more urgent [26–28]. Because of its untapped potential, microalgae are a very promising bioresource in helping to address the prevailing global challenges. Despite that, the utilization of microalgae-based technologies is significantly constrained in terms of its amplitude and scope [29]. These limitations stem from the existence of substantial knowledge gaps pertaining to the commercial viability of scaling up biomass production and processing methods [22,29,30]. One study found that the costs associated with the production of high-purity eicosapentaenoic acid (EPA) from the diatom *Phaeodactylum tricornutum* needed to be reduced by at least 80% to be considered economically viable [31]. Furthermore, the economic feasibility of microalgal products hinges on the efficient automatization of both microalgal biomass cultivation and processing in biorefineries.

Nevertheless, to effectively automate and scale-up these procedures, in-depth optimization efforts must be employed to ensure the consistent production of an economically viable end-product. However, establishing a financially sustainable and stable pipeline is hindered by the inherent variability in the biochemical composition of microalgal biomass. Not only are the microalgal biomass batches highly variable due to intra and inter-species variations, but their biochemical composition can also be influenced by cultivation methods and several abiotic factors

[11–13]. Furthermore, while microalgal biomass does not possess lignin, and is therefore easier to process when compared to lignocellulosic biomass, it is highly diverse in both proportions and types of polysaccharides. These can include rhamnose, arabinose, fucose, xylose, mannose, galactose, glucose, glucosamine, and more complex polymer-like substances formed from the combination of various polysaccharides, leading to the formation of a vast amount of cell wall types with widely different resistance capabilities [32]. Therefore, as microalgal cells demonstrate different degrees of resistance to similar processing treatments, they often require tailored processing methodologies to efficiently extract the desired compounds from the biomass, which is a time-consuming and costly endeavor [33]. As such, it is essential for the scientific community to persistently conduct research aimed at improving and/or innovating methodologies to overcome these obstacles [30].

1.2. Raphidonema monicae

Raphidonema monicae is a novel microalga, exhibiting great potential for industrial applications, particularly due to its biochemical composition abundant in polyunsaturated fatty acids (PUFA) and pigments [101,102]. Previously identified as *Koliella antarctica* (**Figure 1.3**) [103], this psychrophilic unicellular species was first isolated in 1989-1990, in the Ross Sea, Antarctica [104], and is remarkably adaptable, thriving at low temperatures (2 to 20 ºC) and in varying salinities and light conditions [101,105].

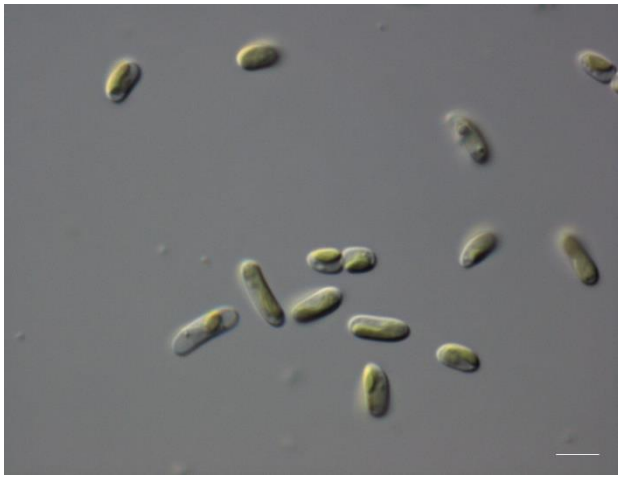

Figure 1.3: Microscopic observations of *Raphidonema monicae*, using DIC and a 100 x lens with an additional 1.6 x amplification provided by an Optvar module. Scale bar = 5µm.

The natural growth at lower temperatures has plausibly been the main driving factor for the development of a lipidic membrane enriched in PUFA to maintain fluidity, particularly of long-chain PUFA (LC-PUFA), with recent studies stating that they can constitute up to 46% of its total triacylglycerol content [102]. Among the LC-PUFA profile of *R. monicae*, some promising bioactive compounds have been identified, including eicosapentaenoic acid (EPA), comprising up to 14% of the total fatty acid content (TFA), and arachidonic acid (ARA), comprising up to 3.5% of the TFA content [102,106,107]. Of these, EPA is known for its anti-inflammatory properties and role in endothelium integrity [108]. ARA, conversely, is known as a precursor for various types of molecules including prostaglandins and possesses proinflammatory modulation properties [108]. In addition, it has been found that this microalga has a rich carotenoid profile, including lutein (up to 491.83 µg/g DW), violaxanthin (up to 18.80 µg/g DW), and neoxanthin (up to 9.53 µg/g DW) [106,107]. Of these, lutein is known to have relevant antioxidant and anti-inflammatory properties, with potential applications in food and health [109]. It has also been discovered that its cell wall is abundant in glucosyl residues, some minor sugars (rhamnose and mannose), and linkages, particularly of β-1,4-linked glucans [101]. In terms of its biochemical composition, *R. monicae* contains up to 21.90% of its dry weight in protein content, 41.18% in carbohydrates and 15.06% in lipids [102,107]. The biochemical composition of microalgae is a fundamental aspect to know before attempting to valorize its biomass, as a microalga poor in high-value and potentially bioactive compounds will have less beneficial effects if incorporated into other products such as food, feed, and fertilizers [110]. By knowing if the biomass is rich in high-value compounds or not, its potential applications will shift accordingly. For example, it's been reported that incorporating high-value compounds in animal nutrition can contribute to the augmentation of bioactive compounds which play a role in the modulation of gut function and the reduction of oxidative stress [111]. In this matter, as *R. monicae* was found to be rich in certain high-value compounds, it could be, once processed in biorefineries, potentially incorporated into feed for animal nutrition.

1.3. Biorefinery

"Biorefinery" is a concept first introduced around the 1990s, closely associated with "green chemistry" [34]. It can be defined as an advanced processing facility engineered to convert or extract biomass feedstock into a wide array of products, such as various bio-compounds, biofuels, renewable energy, and other high-value materials [35], through a multitude of physical, chemical,

biochemical, and microbial processes (**Figure 1.4**) [36]. Unlike the original refineries in the petrochemical industry, which refine non-renewable fossil raw materials, biorefineries aim to use renewable feedstocks, offering a more sustainable approach in the production of the targeted compounds [34]. Several classification systems exist for biorefineries, some based on the feedstock or material they process (e.g., first, second and third-generation biorefineries), others based on the number of feedstocks and end-products (e.g., phase 1, phase 2 and phase 3 biorefineries), and some are based around the conversion platform that is being used (e.g., biochemical, biological, thermochemical and hybrid conversion platforms) [34,36,37].

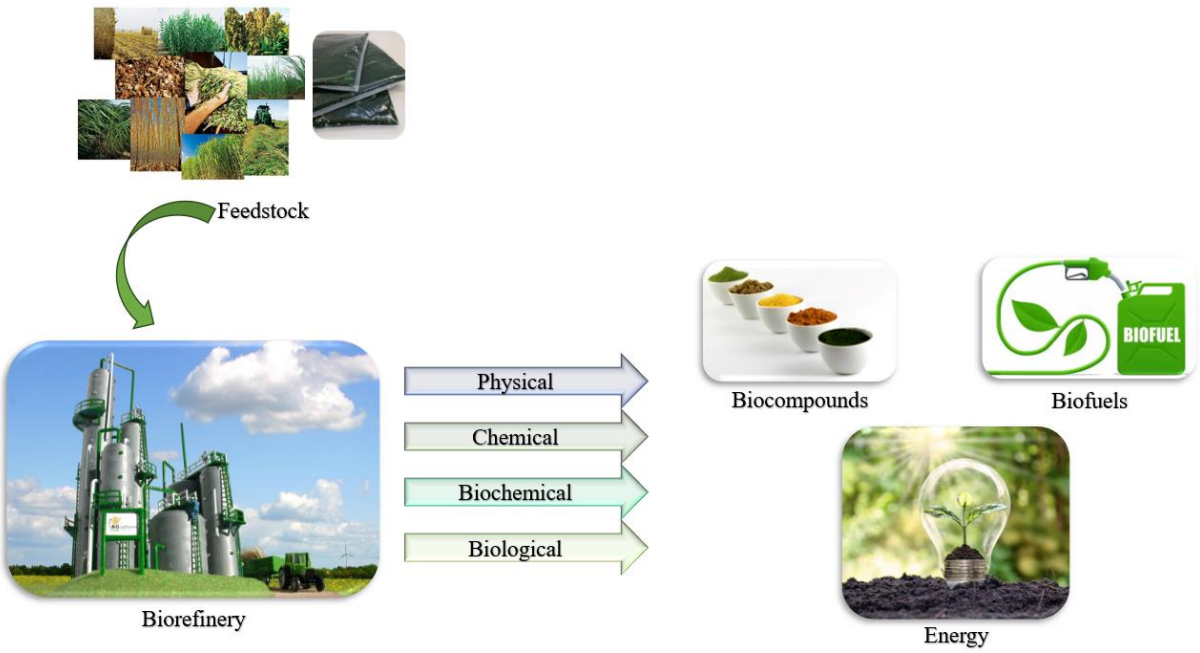

Figure 1.4: Example of a conceptual biorefinery in how it can harness feedstock, and through either physical, chemical, biochemical, or biological treatments, can produce a wide array of products, including energy, biofuels, and bio compounds.

First-generation biorefineries deal with sugary, oil-based, and starch-containing substrate feedstocks, with the aim of producing fuels and chemicals. Second-generation biorefineries work with lignocellulosic-containing sustainable residual/waste-based feedstocks. Third-generation biorefineries aim to use sustainable and renewable non-lignocellulosic feedstock sources to produce a diverse range of products, through the usage of microbial cell factories [36]. Irrespective of the type of biorefinery, they all share a common goal, to refine the feedstock(s) and extract target compounds/products, which is accomplished through a tailored methodology or processing pipeline (**Figure 1.5**), specifically designed with the physical and biochemical characteristics of

the raw material(s) in mind, and also considering the desired output(s) [35,36,38,39]. These pipelines encompass a series of distinct processing steps through which the biomass is subjected, typically including pre-treatment, cellular disruption, fractionation, and stabilization, among other steps, all of which are strategically designed to facilitate and maximize the extraction and production of the intended end-product, thus ensuring its commercial viability [38].

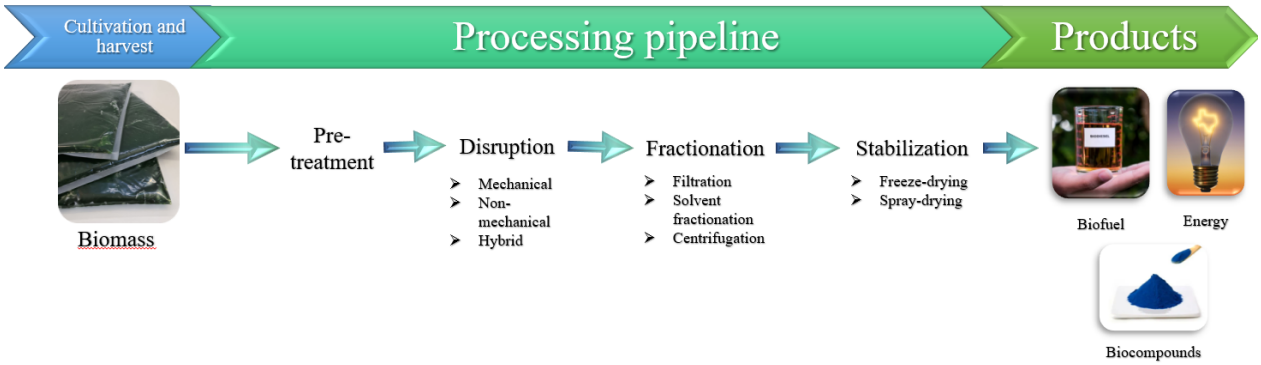

Figure 1.5: Example of a processing pipeline in biorefineries, including the previous cultivation and harvesting step of microalgal biomass and potential products obtained.

1.4. Biomass Disruption

Biomass disruption is often paramount for biorefineries that work with microalgae-based feedstocks, as it directly influences the extraction efficiency of the targeted compounds [40,41]. It aims to disrupt the cell wall to increase the bioavailability of the desired (intracellular) compounds, which would otherwise be inaccessible [42,43]. This step is highly dependent on the chemical composition of the biomass, particularly of the cell wall, which acts as the barrier that protects cells from most external lysing agents. However, the microalgal cell wall is highly diverse, varying both in the types and proportions of polysaccharides that it is composed of. This variation can be observed between and within microalgal species and strains [33,40]. Consequently, this processing stage is often time-consuming, energy-intensive and costly, requiring the development of a tailor-made disruption methodology targeted at that specific microalga species [40]. Various methodologies have been studied to achieve this goal (**Figure 1.6**), such as: a) mechanical approaches, including bead milling, grinding, irradiation, high-pressure homogenization (HPH), high-speed homogenization, ultrasonication, microwave-assisted extractions and pulse electric

field, and b) non-mechanical approaches, comprised of enzymatic hydrolysis and chemical hydrolysis (e.g. acidic or alkaline hydrolysis) [42–44].

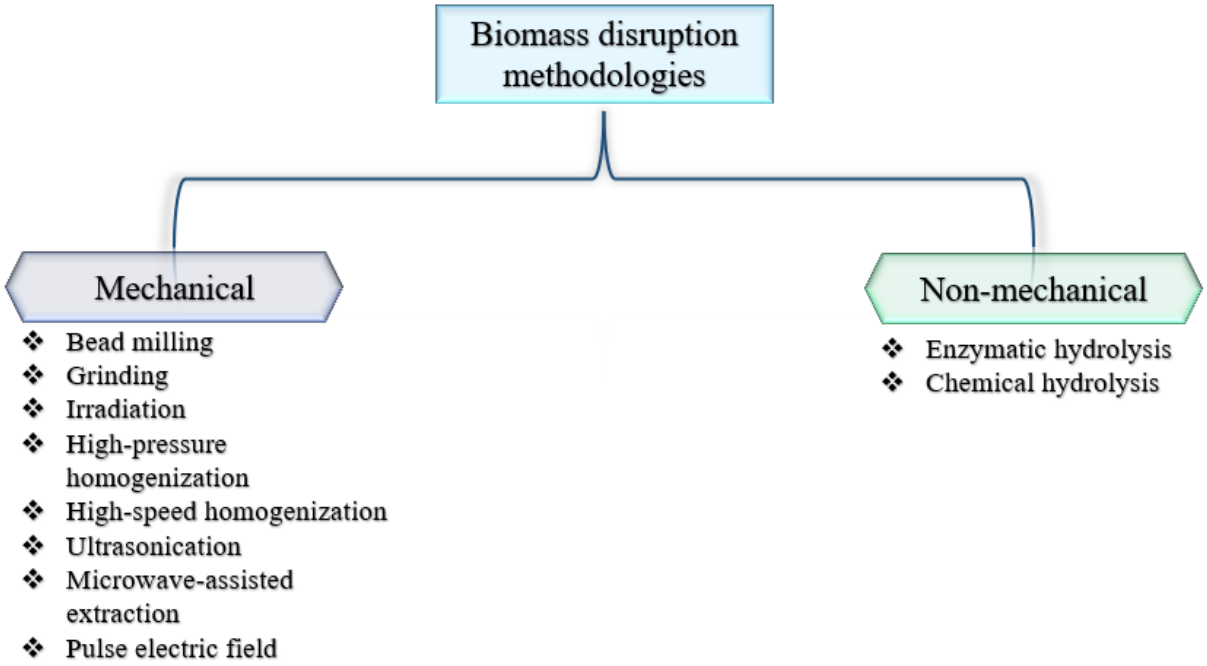

Figure 1.6: Examples of biomass disruption methodologies based on mechanical and non-mechanical treatments.

Among mechanical methodologies, HPH is widely adopted, due to its high disruption efficiency and ease of scalability from laboratory to industrial scale [45]. The process involves subjecting the cells to elevated pressure levels through single or multiple rotation cycles to induce fragmentation. The extent of biomass disruption is dependent on the rigidity of the cell walls, the pressure applied, and the number of times the biomass is subjected to this pressure (cycles) [45,46]. However, like any other mechanical method, HPH also presents certain limitations, including potential clogging, requiring extensive feedstock pre-treatment to reduce particle size, expensive equipment maintenance, and high energy consumption that may limit its scalability potential [47].

Within non-mechanical methods, enzymatic hydrolysis has the advantage over chemical extractions in biorefineries, due to its reduced toxicity, minimal equipment deterioration and corrosion, enhanced specificity, lower utility costs, diminished environmental damage and reduced ash content [48,49]. This methodology involves employing carefully selected specific enzymes to target molecules within the essential structures of the cells, facilitating permeabilization and

eventual cellular fragmentation [49]. However, enzymatic hydrolysis, like HPH and other approaches, also has drawbacks. These include extended reaction times, potentially higher costs to ensure optimum enzymatic activity conditions (e.g., pH, temperature, and agitation), and an in-depth knowledge of the biochemical composition of the cell wall to accurately determine the ideal enzymes to be employed [50,51].

It is worth noting that sometimes, due to the complexity of some microalgal cell walls, the most effective approach in disrupting microalgal biomass often involves a combination of disruption methodologies, carefully selected and applied to enhance cellular disruption efficiency [52,53]. One study found that combining a sonication treatment with an enzymatic hydrolysis processing step resulted in a 4-fold yield increase of the total reducing sugar content harvested from *Chlamydomonas mexicana* [52]. Another study found that a hydroxyl radical-aided thermal treatment of microalgal biomass could convert the cellulose present in the cell wall into easily fermentable sugars, thus enhancing the following enzymatic hydrolysis digestibility of the microalgal biomasses, achieving more than 80% of total enzymatic digestibility [53]. It is important to underline however that, while combining disruption methodologies might enhance the cellular disruption, a thorough economic analysis of the approach should be carefully performed to ensure the additional costs associated with increasing the number of steps and complexity of the pipeline do not worsen the economical and practical viability of the process as a whole [43].

1.5. Fractionation

Following biomass disruption, the subsequent fundamental stage in biorefineries is fractionation. This is a crucial step that significantly influences the quality of the final product and typically represents a substantial portion of the monetary investment, ranging from 40% to 90%, in industrial facilities [54]. It is defined as a process or combination of processes where the biomass is split into different fractions based on the chemical compositions of the compounds [54,55]. A diverse range of methodologies within fractionation that can be selected based on the specific chemical characteristics of the target compounds, and they play a vital role in the effective separation and purification of the desired components (**Figure 1.7**). These include: dephlegmation (separates vapors by differences in boiling and condensation points), fractional distillation (separates liquids and vapors by differences in boiling points), fractional crystallization/freezing (separates liquids by differences in freezing points), fractional melting (separates liquids by

differences in melting points), isotope fractionation (separates isotopes by differences in densities during phase transition), centrifugation (separates substances in solution by differences in

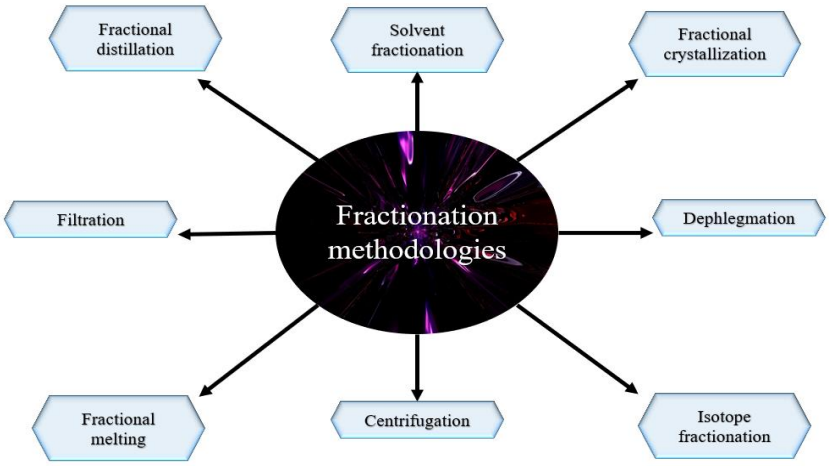

Figure 1.7: Example of fractionation methodologies. These take advantage of the unique chemical properties of the targeted compounds to separate them from other undesired compounds.

sedimentation speeds), filtration (separates substances in solution by differences in particle size, using porous physical barriers) and solvent fractionation (separates substances based on molecular polarity), among others [54,56,57].

Despite the availability of multiple approaches for fractionating disrupted biomass, this step encounters significant limitations in its applications. These arise from the need for expensive equipment and solvents, as well as extensive knowledge regarding the chemical composition of the disrupted biomass [58]. Among the currently available methods, membrane filtration is often more energy efficient. It offers a higher yield potential, ensuring superior product quality, minimizing usage of additional solvents, and facilitating an easier scalability while maintaining operational simplicity. However this is only true when the compounds have different molecular sizes [56]. This approach is based on implementing selectively permeable membranes in conjunction with an applied physical pressure, concentration, or chemically driven gradient, to separate the compounds in solution [59,60]. Depending on the molecular weight cutoff or pore size of the membrane, the filtration process can be classified into one of three types: microfiltration (0.1 to 10 µm), ultrafiltration (0.01 to 0.05 µm) and nanofiltration (<0.001 µm) [61]. However, membrane filtration is not exempt from certain limitations, such as the considerable expense associated with acquiring and replacing membranes, and the relatively sluggish filtration rates. A particular problem

associated with membrane technology is the fouling associated with frequent equipment usage, leading to decreased permeate flow rates and decreased compound fractionation efficiency [62]. Additionally, the fractionation capabilities of this method may be constrained by the availability and compatibility of suitable membranes to the desired target compounds [60].

An additional complementary fractionation method that can be performed separately or integrated with membrane filtration is organic solvent extractions, which employ an organic solvent to recover hydrophobic/apolar molecules, including oils and pigments [63–65]. While the use of organic solvents can enhance the filtration and recovery of specific compounds, this approach is not without limitations either, such as costs associated with acquiring organic solvents, the inherent toxicity of some organic solvents, a lack of environmentally friendly "green" solvents, and the fact that this method when integrated with membranes requires a distinct membrane setup capable of accommodating organic instead of aqueous solvents [63,66]. Although no effective solutions have been found to address the cost implications of organic solvents and the requirement for alternative membrane setups, the utilization of food-grade organic solvents, such as ethanol, offers a viable approach for extracting the desired compounds with minimal additional toxicity to the fraction, which enables the usage of these fractions in health and food related industrial sectors [67].

1.6. Stabilization

After the thorough disruption and fractionation of the biomass, subsequent stabilization steps are commonly implemented to ensure that the desirable properties are maintained over a commercially viable period, thus optimizing the preservation and stability of the final product [68]. Several methodologies have been developed to achieve this objective (**Figure 1.8**), including drying techniques (freeze-, spray- and solar-drying), antioxidant addition, pasteurization, freezing, and irradiation [69–72].

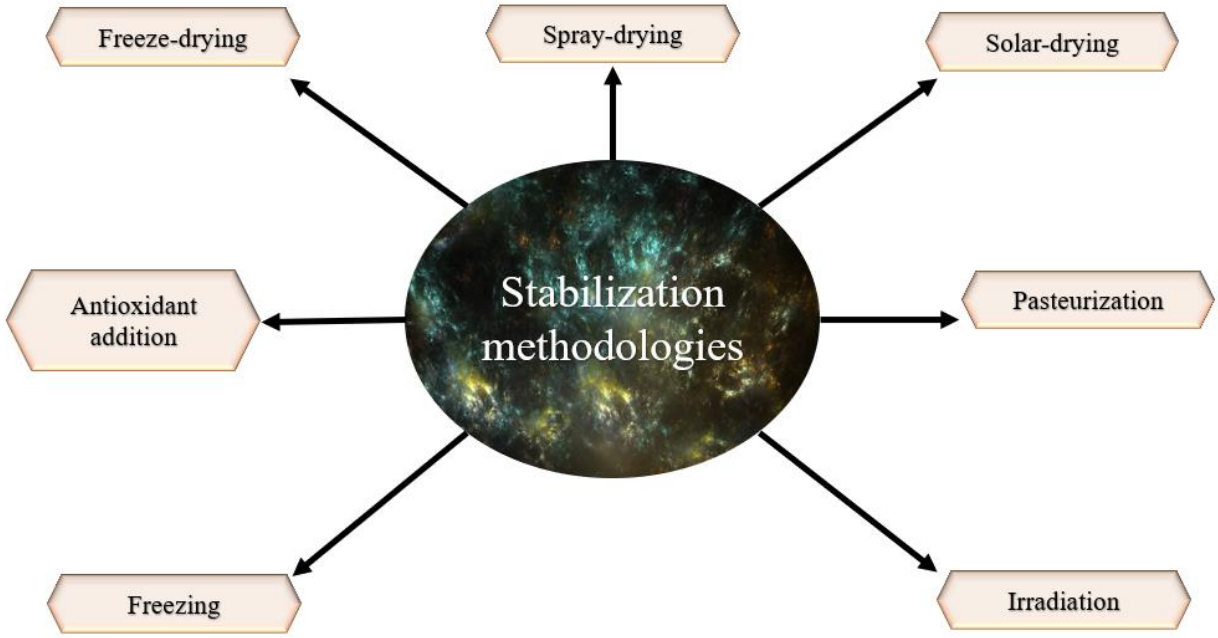

Figure 1.8: Example of stabilization methodologies employed to prevent the degradation or microbial proliferation that could compromise the quality of the end-product.

One of the preferred methods employed in the downstream extraction process is drying, based on the effective removal of the moisture and humidity content from the end-product, to mitigate the risk of potential bioproduct degradation or microbial proliferation that could compromise its quality [70]. Among drying techniques, spray-drying is the faster, more energy-efficient, and cost-effective alternative, as it quickly evaporates the water content of the products through elevated temperatures [73]. However, it has drawbacks, as the high temperatures used to achieve total dehydration often lead to substantial thermal degradation of heat-sensitive substances [73,74]. Freeze-drying, also known as lyophilization, is often used to overcome this challenge, through a sublimation process based on the removal of most water content at low temperatures under vacuum-like conditions [75]. Despite its ability to deliver superior quality yields while minimizing compound degradation, this alternative method is characterized by higher costs and limited working volume capacities. It is thus primarily employed in scenarios where the extraction targets include high-value compounds [68,74,75].

1.7. Processed microalgal biomass applications

By extensively processing microalgal biomass, a product rich in target compounds can be obtained. Depending on the harvested compounds, the potential microalgal biomass applications will vary according to the needs of each industrial sector (**Table 1.1**).

Table 1.1: Practical microalgal biomass application examples in various industrial sectors.

Area of application	Method Type	Methodology Description
Agricultural industry	Nitrogen mineral fertilization replacement for lettuce production	*Chlorella vulgaris* suspensions were found to provide significantly higher lettuce fresh matter yield [76]
Biofuel industry	Bioethanol production	Organo-solvent treatment coupled with simultaneous saccharification and fermentation of *Scenedesmus dimorphus* biomass had a bioethanol yield above 90% [77]
Cosmetic industry	Skin moisturizer production	Polysaccharides extracted from *Saccharina japonica* demonstrated potential as moisturizing agents [78]
Feed industry	Diet inclusion in pacific white shrimp	The inclusion of *Nannochloropsis* spp. in the diet of the pacific white shrimp was found to increase its resistance to thermal shock while stimulating the immune defense [79]
Food industry	Natural source of vitamin D_3	*Nannochloropsis oceannica* exposed to artificial ultraviolet-B was able to produce significant amounts of vitamin D_3 [80]
Health industry	Subunit vaccine production	*Chlamydomonas reinhardtii* transformed with the HPV16 E7 protein gene allowed

		the expression of E7GGG protein for therapeutic vaccines [24]
Wastewater treatment	Biomass cultivation in hydroponic effluents	*Tetraselmis* sp. grown in hydroponic effluents managed to significantly reduce concentrations of nitrogen and phosphorous compounds [81]

Among the various industrial sectors that microalgae can be applied to, the one being researched in this thesis is aquaculture. This industry is one of several approaches to minimize humanity's ecological footprint, offering a less resource-intensive alternative for seafood production, and contributing to sustainable practices in the food sector [82,83]. In addition, this industrial sector helps alleviate the ever-increasing food needs as the world population increases [84]. Nevertheless, aquaculture is not exempt from encountering its unique set of obstacles and bottlenecks, primarily revolving around the need for meticulous monitoring and maintenance of a controlled environment. These critical requirements will ensure optimal growth, well-being, and survivability of the produced aquatic animals [85]. To achieve these requirements, several tasks must be followed thoroughly, including the adequate usage of feed and complementary supplements, but with the exacerbation of climate changes and the expansion of aquaculture system to deal with food needs, these tasks are becoming ever more difficult to be accomplished [84,85]. A potential solution to tackle this is the research and application of microalgae as replacements for less sustainable ingredients in feed and supplements (e.g., as alternative protein sources), and as a source of bioactive compounds, which when paired with complementary systems, such as wastewater treatment facilities, contribute to a more sustainable aquaculture [86–88].

However, to determine if the processed microalgae biomass can be utilized as feed or supplements in aquacultures, in-depth studies must be performed to assess their influence in the fish's immunocompetence, robustness and overall health [89,90]. This is because fish are vulnerable to several stress factors that can very easily disrupt their health, resulting in debilitated health and potentially mortality episodes, lowering the quality of the aquaculture produce [85]. Thus, if the biomass is to be utilized as a supplement to boost the fish's health and survivability, particular attention should be given to the effects of biomass on the immune system, gut epithelial

stability, and stress markers such as corticosteroids levels [91–93]. One way to assess this is through dietary incorporations of previously processed biomass fractions, in either *in-vivo* or *ex-vivo* assays, to evaluate the bioactivity of these ingredients [94–96]. The intestine is the organ where most nutrients and related high-value compounds are absorbed, which is a major component in investigating this response [97] . As such, to evaluate the intestinal response, genetic or biochemical biomarkers must be carefully selected to ascertain the type of influence the ingredients have [98]. However, as it is frequent to obtain multiple fractions from a processing pipeline of biomass, fast screening trials are essential to first estimate which fractions hold key potential bioactive compounds, before a more in-depth study is developed, to minimize animal experimentation. This can be achieved through *ex-vivo* intestinal explant cultures, in which the ingredient is in direct contact with the epithelial cells, promoting a stronger response from the desired biomarkers as the samples did not need to go through the digestive tract to reach the intestine [94–96,98]. In this thesis, the epithelial stability, immunostimulation, and antioxidant capacity of fractions enriched in bioactive compounds were chosen for evaluation. To evaluate the epithelial stability potential, the transcriptional response of genes that contribute to its integrity such as *OCL* and *TJP2* can be utilized as biomarkers to assess the effectiveness of the fractions [89]. Meanwhile, the immunostimulating potential of the fractions is normally studied by evaluating the immune innate response, typically correlated with an increase in cytokines and other pro-inflammatory signaling compounds (e.g., *IL1B*, *IL8*, *COX2*) [99]. With regards to the antioxidant capacity, the transcriptional response of genes coding for antioxidant proteins is normally evaluated (e.g., *GPx*, *CAT*) [100].

In this thesis, a processing pipeline was developed, with the intention of extracting high-value and bioactive compounds, to produce several types of fractions, in order to enhance the fish's health. We also investigated and discussed the correlation between the biochemical composition of these fractions and the effect they had in the intestinal response, by evaluating, via an *ex-vivo* intestinal explant assay, the transcriptional response regarding epithelial stability (*OCL*; *TJP2*), antioxidant capacity (*GPx*; *CAT*) and immunostimulation (*Il1B*; *COX2*).

2.Objectives

The aquaculture field is struggling with the increase in demand for production of aquatic organisms. One of its limiting factors is the health of the species being produced, as a deterioration in their health directly influences the quantity and quality of the product. As a result, there has been an increase in the development of novel feed and supplements to ameliorate these challenges.

Raphidonema monicae is a poorly researched microalgal species, even though it has been found to possess a rich biochemical profile in LC-PUFA, specific carotenoids, and other high-value compounds, which could potentially have bioactive properties. Therefore, this species could possibly be harnessed in the production of functional ingredients holding key value in improving fish health.

Based on that, this study aimed to research in more detail the biochemical composition of *R. monicae*, and if a processing pipeline could be developed to harness its high-value compounds with potentially bioactive properties into products with potential application in aquafeeds as functional ingredients. To achieve this, 3 objectives were set for this thesis:

1. Biochemical characterization of *R. monicae* biomass;
2. Development and optimization of a processing pipeline combining disruption, fractionation and stabilization methodologies;
3. Assessment of the influence of the fraction in gilt-head sea bream (*Sparus aurata*) health through *ex-vivo* intestinal explant culture trials by measuring the intestinal mucosal response.

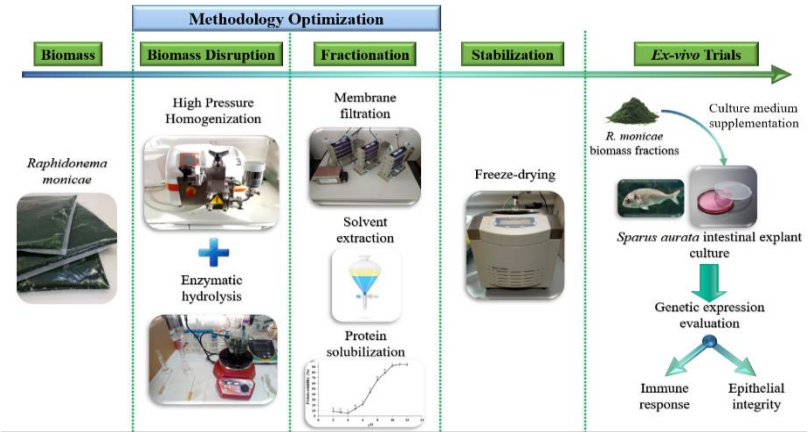

Figure 2.9 Flowchart of the methodology performed in this thesis to obtain different compound-rich fractions of *Raphidonema monicae*.

3.Materials and methods

3.1. Microalgae biomass

The biomass of *Raphidonema monicae* used for this work was produced in March 2022, by the microalgae production company Necton S.A. (Olhão, Portugal). This strain was grown in an industrial 19 m^3 tubular photobioreactor for 18 days, using hydroponic drain water provided by Hubel Group as a culture medium, within the ALGACYCLE project to provide nutrients to the culture. The biomass was harvested once it reached concentrations of 1.6 g/L dry weight, concentrated by centrifugation, and the concentrated paste was stored at -20 ºC until further use.

3.2. Optimization of cell disruption

The biomass was processed using two cell disruption methodologies: enzymatic hydrolysis (EH) and high-pressure homogenization (HPH).

3.2.1. Optimization of cell disruption using high pressure homogenization (HPH)

To maximize the biomass disruption, a lab-scale high-pressure homogenizer (PandaPLUS 2000, GEA, Germany) (**Figure 3.10**) was used and optimized for pressure (bars), biomass concentration (g/L) and one cycle of HPH. At this stage, a multi-factor, central composite design (CCD) was implemented using the software Design Expert v. 11 (StatEase, USA). The resulting experimental plan had 13 runs with different factor levels combinations of biomass concentration and pressure (**Supplementary Data 1**). The response factor chosen for this assay was the disruption efficiency (%). Once the biomass had been processed using the defined HPH conditions, a sample was collected, and the disruption efficiency was determined, as described in Spiden *et al.* [46], by measuring the turbidity of the samples and using **Equation 3.1**. The response factor was analyzed with the Design Expert software through response surface methodology (RSM), to select the best processing conditions.

Figure 3.10: Experimental high pressure homogenization setup utilized to perform the HPH optimization assay.

Equation 3.1

$$Disruption\ efficiency\ (\%) = 100 - (\frac{Treated\ sample}{Non\ treated\ sample} * 100)$$

3.2.2. Optimization of biomass disruption using enzymatic hydrolysis (EH)

3.2.2.1. Enzymatic hydrolysis screening

A preliminary enzymatic hydrolysis assay was carried out in 12-well microplates to identify the enzymes with the most potential for cell disruption. The selected enzymes were alcalase (from *Bacillus licheniformis*, ≥0.75 Anson units/mL, Sigma-Aldrich), cellulase (from *Trichoderma reesei*, ≥700 units/g, Sigma-Aldrich), mannanase (Mannaway, Novozymes), viscozyme (Viscozyme® L, cellulolytic enzyme mixture, ≥100 FBGU/g, Sigma-Aldrich), and pectinase (Pectinex® Ultra SP-L, Novozymes). Both the enzymes and their concentrations (8.5% w/w) were chosen based on previous studies [49,112,113]. To conduct this assay, the wells were arranged according to **Figure 3.11**, with the 6 wells in the most central columns selected for the enzymatic hydrolysis assay (treatment wells). The 6 wells in the outer columns contained only water to decrease the evaporation in the treatment wells. Afterwards, 1 mL of *R. monicae* biomass at 70 g/L was added to the treatment wells. To ensure the enzymatic reactions would occur at the optimal pH value for the enzymes tested, 1.75 mL of either citrate buffer (pH 4 and 6) or phosphate buffer (pH 8) at 100 mM was added to the treatment wells. Then, 5 microliters of each enzyme were added to

their respective wells. After, the microplates were placed in incubated shakers (ISS-4075R, Jeio Tech, Korea) and incubated at 50ºC, with agitation, for 16 hours. At the end of the assay, the samples in the treatment wells were transferred into 15 mL falcon tubes, and the disruption efficiency was evaluated.

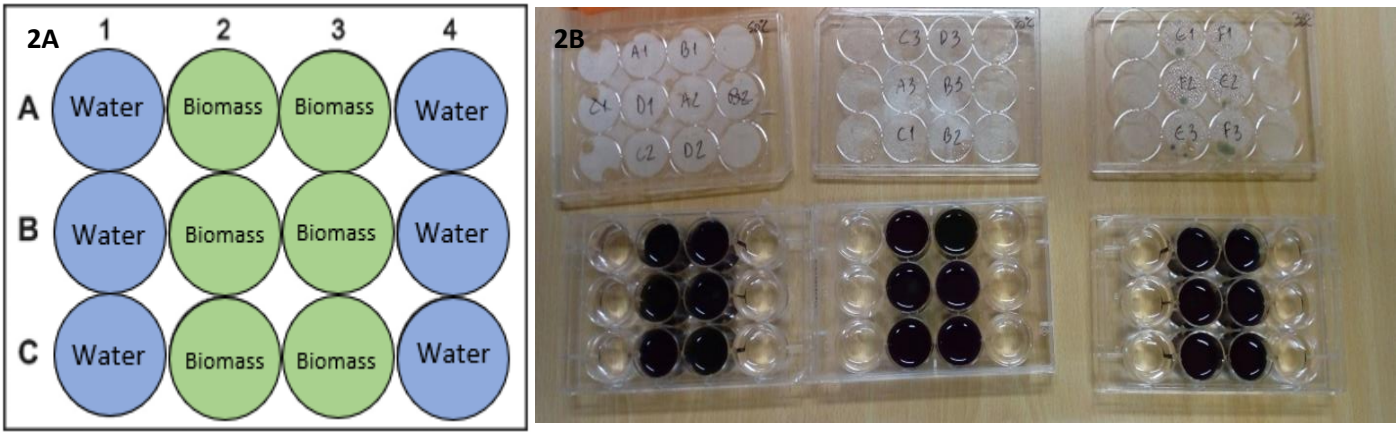

Figure 3.11: Schematic representation of the samples and water distribution in a 12-well plate (2A). Practical representation of the 12-well plates at the end of the incubation period of the enzymatic hydrolysis screening assay (2B).

3.2.2.2. Enzymatic hydrolysis optimization

After selecting the most effective enzymes, a second enzymatic hydrolysis assay was carried out to identify the best reaction conditions with optimal biomass concentration (g/L), enzyme concentration % (w/w), and pH to conduct the enzymatic hydrolysis. This was performed in 50 mL Erlenmeyer's flasks in an incubated shaker (ISS-4075R, Jeio Tech, Korea), at 50 ºC, with agitation, for 21 hours. To this end, a multi-factor CCD was implemented using the software Design Expert v. 11 (StatEase, USA). The resulting experimental plan had 30 runs with different factor levels combinations of biomass concentration, enzyme concentration, and pH (**Supplementary Data 2**). The response factor chosen for this assay was the disruption efficiency (%). The pH was maintained by adding 15mL of either citrate buffer (pH 6) or phosphate buffers (pH 7 and 8) at 100 mM, to the reaction mixes. At the end of this period, each sample was recovered, and the disruption efficiency was determined. The response factor was analyzed with the Design Expert software, through RSM, to select the best reaction conditions.

3.2.2.3. Enzymatic hydrolysis validation

A final third enzymatic hydrolysis assay was carried out to compare the biomass disruption potential of the best enzymatic hydrolysis conditions, against a previously developed methodology. That methodology used a sequential enzymatic hydrolysis treatment at 50 ºC, which included, in order, the addition of viscozyme, flavourzyme (Protease from *Aspergillus oryzae*, ≥500 U/g, Sigma-Aldrich), and alcalase, at 4% w/w, at a pH of 6.5, 7.0 and 8.0, and with an incubation time of 30, 60 and 120 minutes, respectively [49]. To compare the effectiveness of the methodologies, the enzymatic hydrolysis was performed in 250 mL reactors (**Figure 3.12**), with a working volume of 200 mL. The pH was closely monitored using a pH meter (pH 700, Eutech instruments, Singapore) and manually adjusted by adding 1 M NaOH and 1 M HCl. The temperature was maintained at 50 ºC, with a mixing speed of approximately 550 rpm, and an incubation time of 3.5 hours. Throughout the assay, samples were collected before and after the addition of each enzyme, and the degree of cellular disruption of each sample was then quantified by evaluating the disruption efficiency.

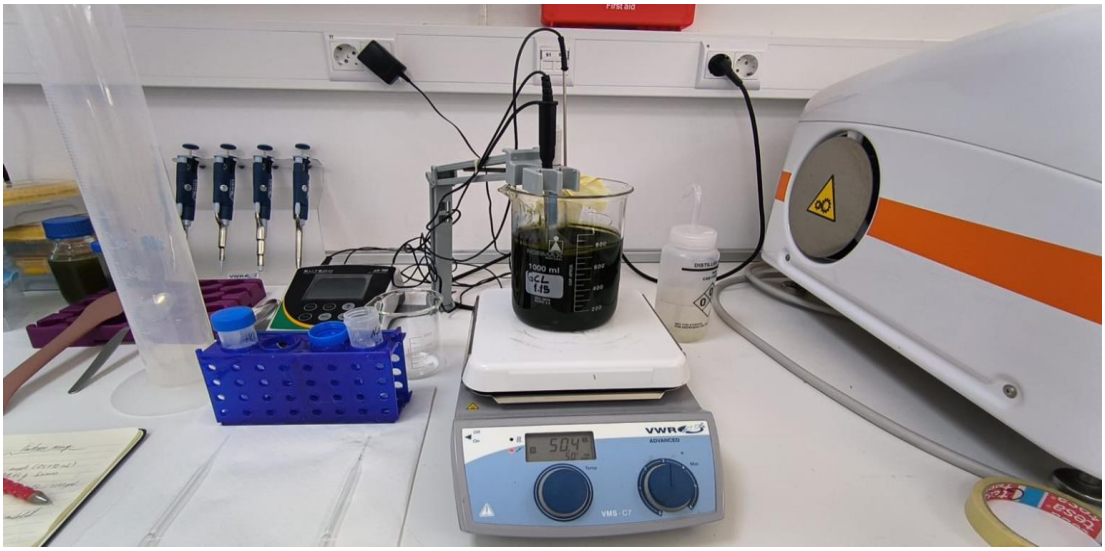

Figure 3.12: Experimental reactor setup utilized to perform the enzymatic hydrolysis validation assay.

3.2.3. Cell disruption pipeline optimization assay

Once the optimal HPH and EH conditions for biomass disruption were determined, a combination of both was carried out to evaluate the most efficient methodology in disrupting the biomass, firstly by subjecting the biomass to HPH, followed by EH. The methodologies were followed as described in sections 3.2.1 and 3.2.2.3. Samples were recovered from each condition at the end of the methodology, where one was left untouched (total biomass sample) while the other

was centrifuged (Centrifuge 5430, Eppendorf, Germany) at 5000 g for 5 minutes, and its supernatant and pellet were separated (supernatant sample and pellet sample) (**Figure 3.13**). The total biomass and pellet samples were freeze-dried, and the supernatant samples were stored at -20 ^{o}C.

At the end of the assay, the EH, HPH, and mixing conditions were compared regarding their cell disruption and target metabolite release capacity. To evaluate biomass disruption, the disruption efficiency was determined. Further detailed analysis assessed the release of free amino acids, reducing sugars, soluble proteins, soluble carbohydrates, and total lipids.

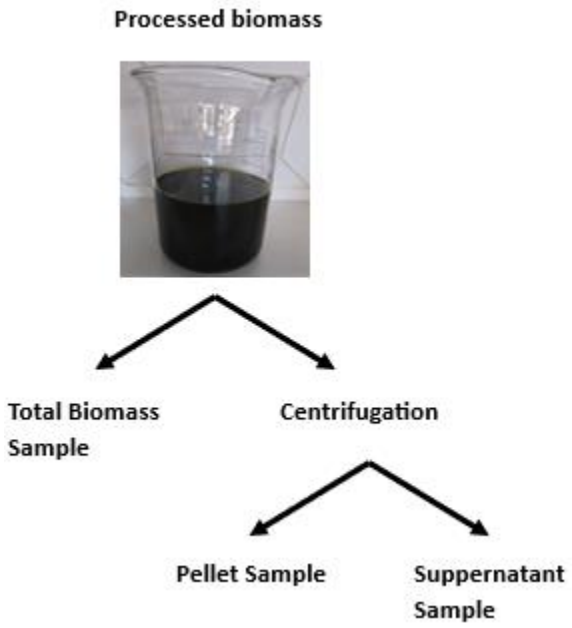

Figure 3.13: Schematic representation of how the three different sample types were obtained.

3.3. Fractionation

After disruption, different fractionation methodologies were used to produce bioactive fractions with different biochemical compositions.

3.3.1. pH Shifting

With the goal of increasing protein solubility and extractability, pH of the processed samples was increased to alkaline values, between 8 and 12. This was done by adding 2 M NaOH, with agitation, while controlling the pH with a pH meter (pH 700, Eutech Instruments, Singapore). Initially, two samples (total biomass and centrifugation samples) were taken at each unit of pH tested (8, 9, 10, 11, and 12) (**Figure 3.14**). The centrifugation sample was centrifuged (Centrifuge 5430, Eppendorf, Germany) at 5000 *g* for 5 minutes at 4 ºC. This process resulted in 3 final samples per pH value (pellet, supernatant and total biomass). The collected samples from each process were stored at -20 ºC. Small aliquots of the total biomass and pellet samples were taken, freeze-dried, and then stored at room temperature until further biochemical analysis.

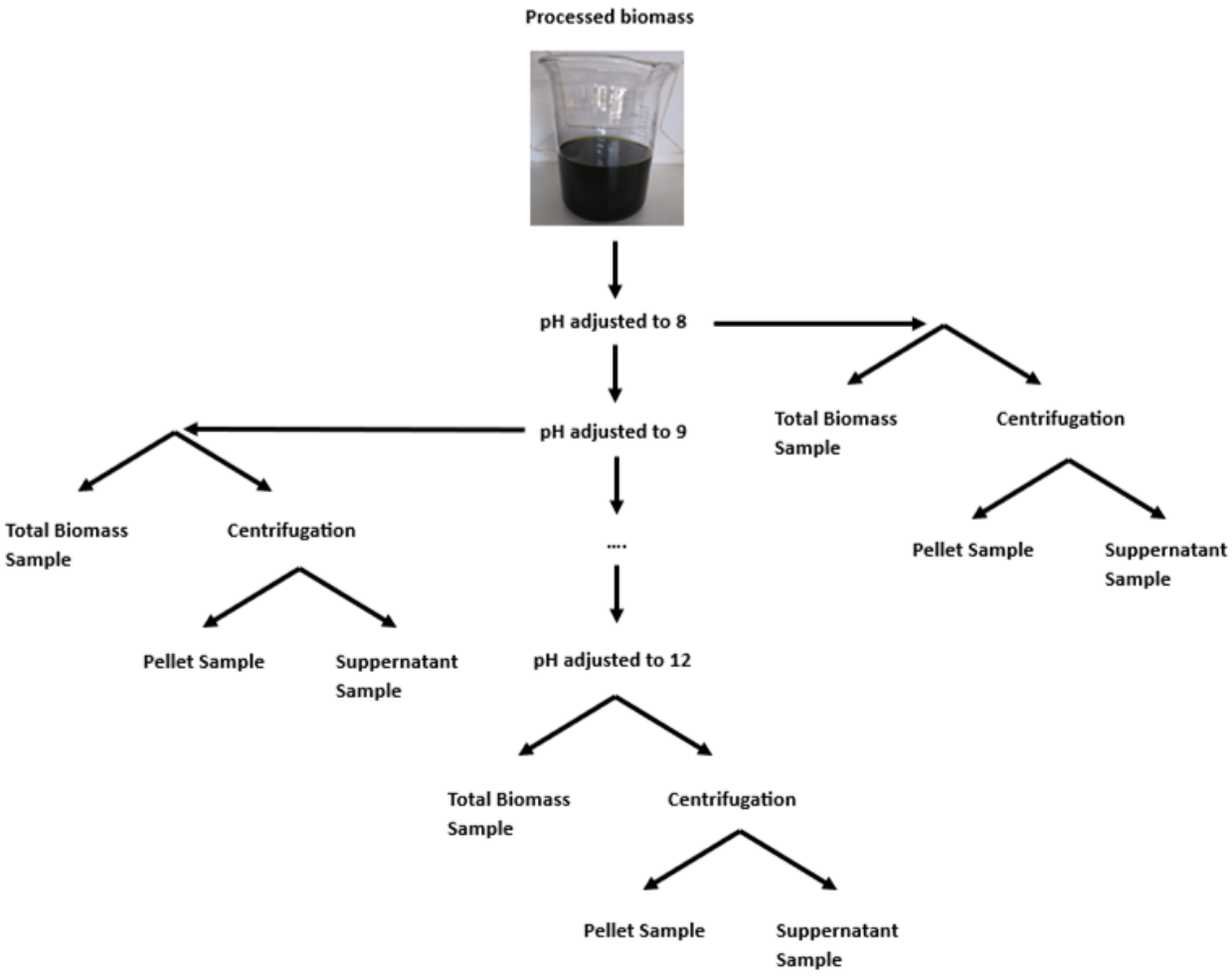

Figure 3.14: Schematic representation of how the three different sample types were obtained for the pH shifting assay.

3.3.2. Membrane filtration

Another methodology used to fractionate the processed biomass was membrane filtration. The system used was the Vibro-Lab3500 (SaniMembranes, Denmark) (**Figure 3.16**), and two different processing set-ups were tested (**Figure 3.15**), with samples taken from both the permeate and retentate fractions: 1) microfiltration using a 0.2 µm pore size membrane (V0.2 PVDF 0.2µm, Synder Filtration, USA); and 2) ultrafiltration using a 100 kDa membrane (LY MAX PES 100,000Da, Synder Filtration, USA). The collected fractions from each process were stored at -20 ºC, and small aliquots of the retentates were taken, freeze-dried, and then stored at room temperature for future biochemical analysis.

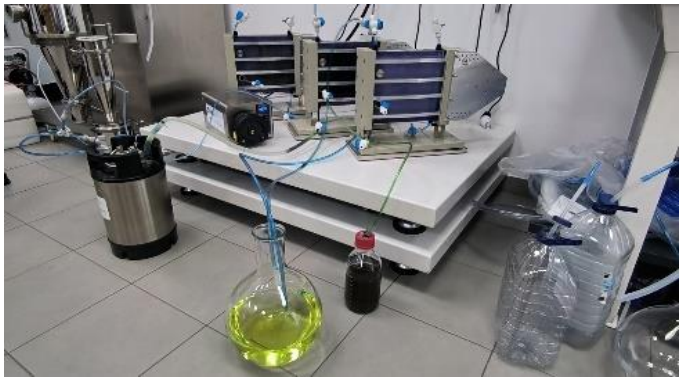

Figure 3.16: Experimental setup utilized for the membrane filtration fractionation assay.

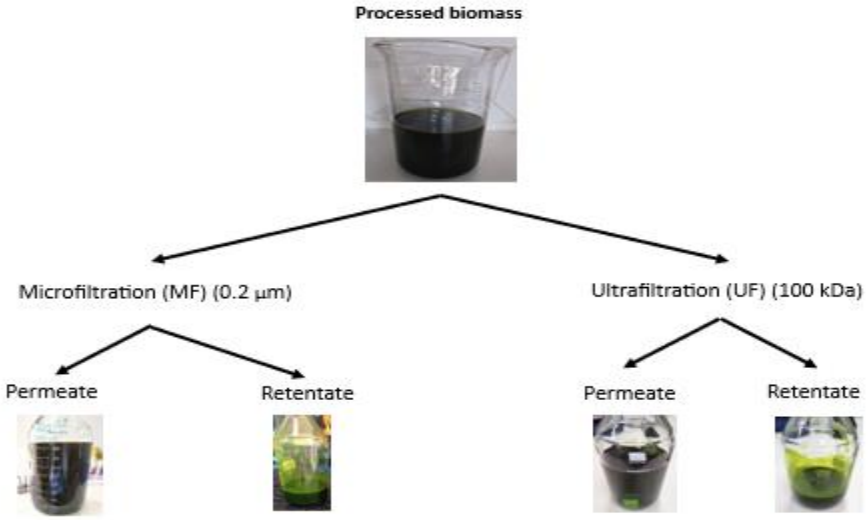

Figure 3.15: Schematic representation of how the membrane filtration fractionation assay was performed.

3.3.3. Ethanolic extraction

The final fractionation methodology was performed using an ethanolic extraction-based approach. In this step, the retentate fractions from 3.3.2 were used, where 80 mL of each retentate fraction was placed in a 100 mL flask and mixed with 20 mL of ethanol (99.9%) (4:1). The mixtures were left mixing overnight, at room temperature. Afterwards, they were recovered to two 50 mL falcon tubes each, and centrifuged (Centrifuge 5430, Eppendorf, Germany) at 5000 *g*, for 5 minutes at 5 ºC. The supernatant was recovered into new 50 mL falcon tubes, and the ethanol was evaporated with a gentle nitrogen flow. The supernatant and pellet extracts were then freeze-dried. The dried samples were kept in moisture-free bags at room temperature until biochemical analysis.

3.4. Biochemical analysis

3.4.1. Reducing sugars

To quantify the presence of reducing sugars, an adapted microplate methodology was utilized based on the original dinitrosalicylic acid (DNS) protocol [114]. First, a standard dilution curve of glucose was prepared, between 0 and 15 g/L. The reaction was performed directly in a 96-well plate, where 25 µL of each sample was mixed with 25 µL of the DNS reagent. Subsequently, the plate was incubated for 10 minutes at approximately 105 ºC, and then cooled in ice for 5 minutes. 250 µL of distilled water were added to each well, for a final volume of 300 µL. Immediately after, the absorbance at 540 nm was measured using a microplate reader (Synergy 4, BioTek, USA). The quantification of reducing sugars was then calculated using the previously established calibration curve.

3.4.2. Free amino acids

For the determination of free amino acids, an adapted methodology based on the original o-Phthaldialdehyde (OPA) method was used [115]. A standard curve of serine was prepared, between 0 and 100 mg/L. Subsequently, 1.5 mL of the OPA reagent was mixed with 200 µL of each sample directly in plastic cuvettes and incubated for 2 minutes at room temperature. For the quantification of free amino acids in solution, the cuvettes with the reaction mixture were read at 340 nm in a spectrophotometer (UH5300, Hitachi, Japan). The quantification of free amino acids was then calculated using the previously established calibration curve.

3.4.3. Soluble proteins

To quantify soluble proteins, an adapted methodology of the Lowry protocol was used [116]. Initially, a standard curve of bovine serum albumin (BSA) was prepared, between 0 and 400 mg/L. The necessary solutions were prepared for the procedure: Solution A, composed of 5% sodium carbonate in distilled H_2O; Solution B, by mixing 1% potassium tartrate and 0.5% copper sulfate pentahydrate in distilled H_2O; Solution C, by combining solutions A and B at a ratio of 25:1 (v/v); and solution D by diluting a stock solution of the Folin-Ciocalteu reagent from 2 M to 1 M.

The samples were prepared to a final concentration between 0.5 and 1 g/L, by dilution with distilled water. Then, 0.5 mL of each sample (including the BSA standard) were added to glass tubes, in duplicates. An alkaline hydrolysis was performed through the addition of 0.5 mL of 1 M NaOH to each sample, followed by vortex agitation, and a subsequent water bath incubation at 100 ºC for 5 minutes. Subsequently, the reaction mixtures were then cooled on ice for 10 minutes until room temperature was reached. Then, 2.5 mL of solution C was added to each tube, mixed, and incubated at room temperature for 10 minutes. Lastly, 0.5 mL of solution D was added to each reaction mixture and incubated in the dark at room temperature, for 30 minutes. At the end, the samples were read at 750 nm in a spectrophotometer (UH5300, Hitachi, Japan). The quantification of soluble proteins was then calculated using the previously established calibration curve.

3.4.4. Soluble carbohydrates

To assess the soluble carbohydrates in solution, an adapted methodology of the Dubois protocol was used [117]. Firstly, a standard glucose curve was prepared, between 0 and 240 mg/L. Afterwards, 1 mL of each sample was placed in glass tubes, in duplicates. Then, 1 mL of a 5% phenol solution was added to each sample, followed by agitation in a vortex. Subsequently, 5 mL of 96% sulfuric acid was added to every tube, which was then vortexed and incubated at room temperature for 10 minutes. The tubes were placed on ice for 20 minutes, and at the end, the samples were read at 488 nm in a spectrophotometer (UH5300, Hitachi, Japan). The quantification of soluble carbohydrates was then calculated using the previously established calibration curve.

3.4.5. Total lipids

An adapted gravimetry methodology [118] was utilized to quantify the total lipids present in the extracts, based on the Bligh & Dyer method [119]. Approximately 30 mg of dried biomass

was weighed (Sample weight) into 2 mL Eppendorf tubes with glass beads. After adding 0.5 mL of methanol and 0.2 mL of chloroform to each tube, the tubes were homogenized using a mixer mill (HM400, Retsch, Germany) for 3 minutes at 30 Hz. The samples were then transferred into glass centrifuge tubes and 1.5 mL of methanol and 0.75 mL of chloroform were added. The tubes were then homogenized using a vortex. Following this, 1 mL of chloroform was added to each glass tube and mixed using a vortex. Subsequently, 1 mL of distilled water was added, and the mixture was homogenized with a vortex. After centrifugation (Centrifuge 5430, Eppendorf, Germany), 2500 *g*, for 10 minutes, the organic phase (chloroform) was extracted into new tubes.

In the following step, 700 µL of the chloroform extract (Evaporated volume of chloroform) were transferred into pre-weighed microtubes (initial weight) and placed to dry in a 60 ºC dry bath. Once the chloroform had evaporated, the microtubes were placed in a desiccator for 3 hours. At the end, the dried microtubes were re-weighed (Final weight). To quantify the total lipids, **Equation 3.2** was used.

Equation 3.2

$$Total\ lipid\ content\ \left(\%\frac{w}{w}\right) = \frac{\frac{(Final\ Weight - Initial\ Weight) * Total\ volume\ of\ chloroform}{Evaporated\ volume\ of\ chloroform}}{Sample\ weight} * 100$$

3.4.6. Total protein

To evaluate the total protein content of the samples, the total nitrogen content was first quantified using an elemental analyzer (Vario EL III, Elementar, Germany), following the manufacturer's procedure. Accordingly, approximately 1 mg of each dry sample was weighed into small aluminum capsules, before being placed in the elemental analyzer. The total nitrogen content was converted into total protein content using the nitrogen-to-protein conversion factor (4.97) as described in Templeton *et al.* [120].

3.4.7. Fatty acids profile

Fatty acids profile was determined using a modified method of Lepage & Roy (1984), as described in Pereira *et al.* [121].

Initially, between 20 and 40 mg of dry biomass was weighed into 2 mL Eppendorf tubes with glass beads. Then, 1.5 mL of methanol/acetyl chloride (20:1 v/v) were added, followed by homogenization in a mixer mill (MM400, Retsch, Germany), at 25 Hz, for 1 minute, thrice. The

reaction mixtures were subsequently transferred to derivatization tubes together with 1 mL of *n*-hexane. The derivatization tubes were placed in a water bath at 70 ºC for 60 minutes. Afterwards, the tubes were cooled in ice for 15 minutes, and 1 mL of distilled water and 4 mL of *n*-hexane were added to the samples. The centrifuge tubes were then vortexed at max speed in two cycles of 30 seconds, before being centrifuged (Centrifuge 5430, Eppendorf, Germany) at 2000 *g* for 5 minutes at room temperature. The *n*-hexane fraction was recovered to new glass tubes, and the centrifugation step with hexane was repeated until the hexane fraction was colorless. All the resulting *n*-hexane fractions were pooled together, and anhydrous sodium sulfate was added in excess to remove any water that could be present in the fractions, being later filtered with 0.22 µm PTFE filters. An internal standard (Nonanoic acid, C9:0) was added to each sample, and the hexane was evaporated under a gentle nitrogen flow. The dried fractions were resuspended in 500 µL of HPLC-grade hexane and transferred to small vials.

The fatty acid profile was quantified using an Agilent GC-MS (Agilent Technologies 6890 Network GC System, 5973 Inert Mass Selective Detector), containing a DB5-MS capillary column (25 m x 0.25 mm internal diameter, 0.25 µm film thickness, Agilent Tech), using helium as a carrier gas. The temperature profile of the program was: 60 ºC for 1 min, 30 ºC/min to 120 ºC, 5ºC/min to 250 ºC, and 20 ºC/min to 300 ºC for 2 minutes. Regarding the fatty acid identification and quantification, a Supelco® 37 component FAME Mix (Sigma-Aldrich, St. Louis, Missouri) was used, with five different dilutions (1:10, 1:25, 1:50, 1:72 and 1:100), as a standard. The calibration curves were prepared for each of the 37 FAME present in the commercial standard.

3.4.8. Pigment profile

To quantify and evaluate the pigment profile, an adapted methodology of the total carotenoid and chlorophyll quantification protocol was used [122]. Firstly, 5 to 10 mg of dried samples were weighed into 2 mL Eppendorf tubes with glass and tungsten beads. Subsequently, 1 mL of methanol containing 0.03% butylhydroxytoluene (BHT) was added, followed by disruption in a mixer mill (MM400, Retsch, Germany), at 20 Hz, for 1 minute, thrice. The tubes were then centrifuged (Centrifuge 5430, Eppendorf, Germany) at 12000 *g* for 6 minutes, and the supernatant was recovered into new glass vials. The extraction step was repeated until both the pellet and supernatant were colorless. The carotenoids were determined using **Equation 3.3**.and the pigment profile was assessed via a GC analyzer (Chromaster HPLC system, Hitachi, Japan).

Equation 3.3

$$Total\ carotenoids = \frac{1000 * Abs_{470} - 2.86 * Chl\ a - 129.2 * Chl\ b}{245}$$

The pigment profile was determined by HPLC (Chromaster, Hitachi, VWR) with a Diode array detector (5430 DAD, Hitachi, VWR), based on Schüler et al. [123] and Couso et al. [124], with a Purospher® STAR RP-18 endcapped (Merck) (250 x 2.1 mm, 5 µm) chromatographic column at 20 °C, in a flow rate of 1 ml/min for 40 min. The injection volume was set to 50 µL. Compounds were identified at 450 nm by comparing with standards and their concentration was calculated based on the respective calibration curve.

3.5. *Sparus aurata* intestinal explants trials

Out of all the fractions that were produced and dried (**Figure 3.17**), 9 were chosen as potential bioactive fractions to be evaluated in a *Sparus aurata* (Gilthead sea bream) explant trial. This trial was performed to assess the functional properties of these potential new ingredients. This was achieved by measuring the transcriptional modulation properties of these ingredients in certain genes correlated with immunostimulation, antioxidant capacity and epithelial integrity, found in intestinal gut cells of *Sparus aurata*.

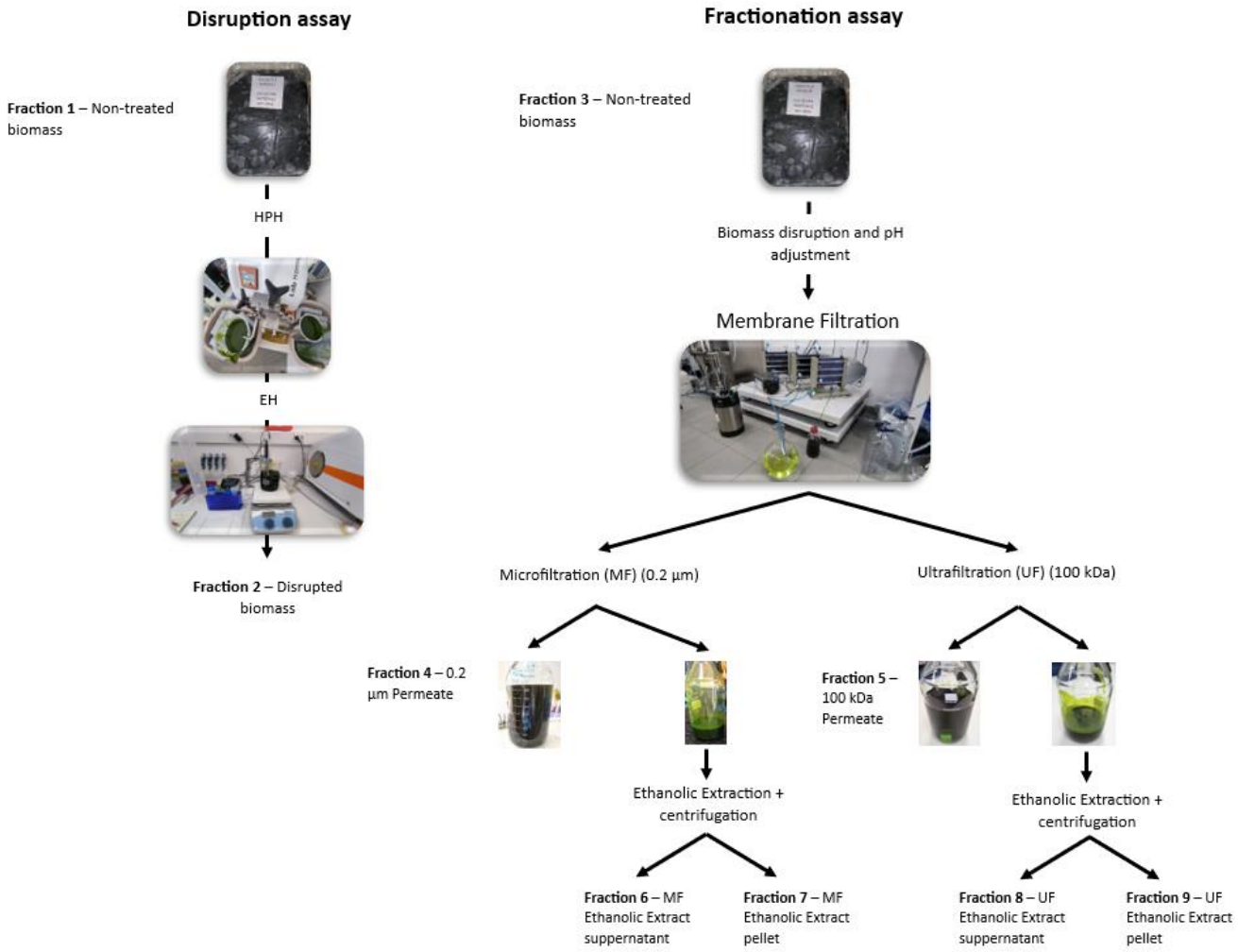

Figure 3.17: Schematic representation of the disruption and fractionation assay performed to obtain the 9 selected fractions for genetic expression evaluation. The first 2 fractions were obtained during the disruption assay, while the remaining 7 fractions were obtained during the fractionation assay.

3.5.1. *Sparus aurata* tissue culture

Two concentrations of each product were tested: 100 µL of the dried fractions resuspended in two different concentrations (5 and 20 mg in 1 mL of Iscove's Modified Dulbecco's Medium (IMDM, HyClone, Utah)), and 50 and 100 µL for the liquid permeate fractions. Juvenile gilthead sea bream fish were obtained from Ramalhete, Station of CCMAR, and the explant trial was prepared as follows. Fish were retrieved from the tank and placed in a bucket with a lethal dosage of anesthesia (2-Phenoxyethanol). Meanwhile, a biologically compatible and innocuous adhesive was placed in 48-well plates where the tissue culture would take place. Anesthetized fish were

dissected, and the anterior intestine excised. The extracted intestine was then perpendicularly cut into multiple pieces. These pieces were opened through a transverse cut that exposed the lumen. The tissues were then placed in the wells, with the lumen side facing upwards, and 1 mL of culture medium was added.

Subsequently, each sample (i.e., ingredient suspension or solution) was added to its respective well, in triplicates. The 48-well plates were then incubated for 5 hours at room temperature. At the end, the tissue of each well was recovered and placed into 1 mL of RNALater for RNA stabilization. The samples were kept at -80 ºC until RNA extraction.

3.5.2. RNA extraction

Before RNA extraction, the samples were retrieved from storage and thawed in ice. In the meantime, 1 mL of Nzyol (NZYTech, Portugal) and 1 ceramic bead were added to 2 mL Eppendorf tubes, on ice. Once the samples had thawed, the tissues were cut with a sterile scalpel in a glass plate placed on top of ice and transferred to the previously prepared tubes. The samples were then mixed in a mixer mill (MM400, Retsch, Germany) for 5 minutes, at 30 hertz, twice, and cooled on ice for 1 minute per grinding session. Following tissue grinding, the samples were incubated at room temperature for 5 minutes, before being centrifuged (Centrifuge 5430, Eppendorf, Germany) at 12000 *g* for 5 minutes at 4 ºC. After centrifugation, the supernatant (approximately 900 µL) was transferred into new 1.5 mL Eppendorf tubes, on ice. Then, 200 µL of chloroform were added to each tube, followed by agitation for approximately 15 seconds and incubation for 2 minutes at room temperature. The new tubes were then centrifuged at 14000 *g*, for 15 minutes at 4 ºC, after which three phases were visible, and the upper aqueous phase, containing the RNA, was transferred into new ice-cold tubes (approximately 600 µL), followed by the addition of 500 µL of ice-cold isopropanol, on ice. The tubes were gently mixed by inversion and incubated for 10 minutes. Subsequently, the tubes were centrifuged at 12000 *g* for 10 minutes, 4º C. The supernatant was discarded, and the RNA pellet was washed twice with 75% ethanol, followed by centrifugation at 7500 *g* for 5 minutes at 4 ºC. At the final washing step, the remaining ethanol drops were removed with a 200 µL pipette, and the pellet was then resuspended in 30 µL of molecular grade H_2O. The extracted RNA samples were stored at -80 ºC until further analysis.

3.5.3. cDNA synthesis

A RevertAid H Minus First Strand cDNA Synthesis Kit (Molecular Biology, Thermo Fisher Scientific, USA) was used for the cDNA synthesis procedure, as described by the manufacturers. Initially, the extracted RNA samples were thawed on ice and diluted to a concentration of 1000 µg/µL, before preparing the master mix solution. Once the samples had been thawed and diluted, 1 µL of each sample and 19 µL of master mix solution was placed in each well of a 96-well plate. The plate was sealed with a sealing film and incubated in a thermal cycler (MiniAmp^{TM} Plus, Thermo Fisher Scientific, USA) (**Table 3.2**).

Table 3.2: Amplification program used for cDNA synthesis. RT – Reverse transcription.

Steps	T (°C)	Time (minutes)	Cycles
Priming	25	5	1
Reverse transcription	42	60	
RT inactivation	70	42	

To determine if the cDNA synthesis was successful, a PCR amplification of the gene coding for the elongation factor 1 of sea bream (*EF1a*) (**Table 3.3**) was carried out using a GoTaq G2 Flexi DNA Polymerase kit (Promega, USA), as described by the manufacturers. First, a PCR master mix solution was prepared. Then, 19 µL of the PCR master mix solution and 1 µL of each cDNA sample was placed in a 96-well plate. The plate was then incubated in a thermal cycler (MiniAmp^{TM} Plus, Thermo Fisher, USA) using the conditions specified below (**Table 3.4**). While the plate was incubating, the cDNA samples were stored at -20 ºC. The amplification was then evaluated through electrophoresis, in 1.5% agarose gel with 1x TAE buffer (1.5g of agarose per 100 mL of 1x TAE). Before loading the PCR samples into the gel, they were first prepared by mixing 1 µL of PCR sample with 1 µL of 5X Green GoTaq Flexi Buffer with gel red 1:500 (2:1 v/v). A GeneRuler 50 bp DNA ladder was also used in the gel run, in a similar proportion to the samples. Once the samples and ladder had been placed in the wells, the electrophoresis run began, at 110 volts, for 30 minutes. The gel was then observed under UV-light with a gel documentation workstation (NuGenius, Syngene, India).

Table 3.3: EF1a gene characteristics.

Gene	Gene name	Accession number	Forward Primer Sequence	Reverse Primer sequence	Amplicon size	Annealing temperature (°C)	Amplification efficiency (%)
EF1a	Elongation factor 1 alpha	AF184170	GGAGATGC ACCACGAG TCTC	GCGTTGAA GTTGTCAG CTCC	150	59	114

Table 3.4 Amplification program used for thePCR confirmation protocol.

Steps	T (°C)	Time (minutes)	Cycles
Denaturation	95	5.0	1
Denaturation	95	0.5	35
Annealing	59	0.5	
Extension	72	1.0	
Extension	72	5.0	1

3.5.4. Evaluation of gene expression evaluation via qPCR

First, the cDNA samples stored at -20 ºC were thawed in ice and diluted 1:3. In the meanwhile, the master mix for each gene (**Table 3.5**) was prepared (**Table 3.6**). Afterwards, 2 µL of each sample, in duplicates, and 8 µL of the master mix were transferred, to the wells of a 384-well microplate. The microplate was then covered with optical film (Axygen Ultra Clear Sealing Film), and placed in a real-time qPCR system (QuantStudio™, Thermo Fisher, USA) to begin the incubation and analysis of the genetic expression (**Table 3.7**). At the end, the genetic expression results were analyzed digitally through the Thermo Fisher Connect™ program.

To calculate the mRNA relative expression rate, the *Pfaffl* formula [125] was utilized (**Equation 3.6**), which uses the amplification/primer efficiency, and ΔCt values of the sample correlating to the reference gene (*18S*) (found in a preliminary test to be the most stable) and the tested gene (Either *COX2*, *OCL*, *GPx*, *TJP2*, *Il1B*, or *CAT*). To do that, first, the primer efficiency (%) was converted (**Equation 3.4**), and then, the ΔCt values of the samples were calculated, based on the average the treatment and control samples (**Equation 3.5**).

Table 3.5: Characteristics of the genes selected for genetic expression evaluation.

Gene	Name	Accession number	Forward Primer Sequence	Reverse Primer sequence	Amplicon size	Annealing temperature (ºC)	Amplification efficiency
18S	18S ribosomal RNA	AM490061	TGCAGAA TCCTCGC CAGTAC	GGTGAGC CCGGATC TTCTTC	150	59	115.0
COX2	Cyclooxyge nase 2	AM296029	GACATCA TCAACAC TGCCTCC	GATATCA CTGCCGC CTGAGT	150	59	123.0
OCL	Occludin	JQ692876	TACGGTG GAATCGG AGGGAA	CTGGTGA GACACGA CGATGA	120	55	82.3
GPx	Glutathion Peroxidase	KC201352	TTTACGC CCTGACA GCCAAT	AGTAACG ACTGTGG AGCTCG	150	59	113.0
TJP	Tight Junction Protein ZO2	XM_03041 7304.1	CTGCTGG ATGTGAC ACCCAA	GGCGATC CTCTGTC TCAAGG	120	59	97.0
IL1B	Interleukin 1 Beta	AJ277166	TCCAAGC TTGCATC TGGAGG	GCTGAAG GGAACAG ACACGA	139	55	82.9
CAT	Catalase	JQ308823	CGACATG GTGTGGG ACTTCT	CGCTCAC CATTGGC ATTGAC	150	55	121.0

Table 3.6: Chemical composition of the master mix utilized during the evaluation of the genetic expression through real time qPCR.

Reagent	Volume (1 Reaction) µL
SyberGreen	5.000
Forward Primer	0.625
Reverse Primer	0.625
Water	1.750
Total	**10.000**

Table 3.7: Amplification program used for qPCR genetic expression evaluation.

Steps	T (°C)	Time (minutes)	Cycles
UDG activation	50	2	1
Denaturation	95	5	
Denaturation	95	0.25	40
Annealing	Annealing temperature*	0.25	
Extension	72	1	

Will depend on the gene being analyzed (refer to **Table 3.5)*

Equation 3.4

$$Converted\ primer\ efficiency = \left(\frac{Primer\ efficiency\ (\%)}{100}\right) + 1$$

Equation 3.5

$$\Delta Ct\ (per\ sample) = Control\ Average - Treatment\ average$$

Equation 3.6

$$Gene\ expression\ ratio\ (per\ sample) = \frac{Tested\ gene\ primer\ efficiency^{\Delta Ct\ treatment\ sample}}{Reference\ gene\ primer\ efficiency^{\Delta Ct\ control\ sample}}$$

3.6. Statistical analysis

Statistical analyses were performed using Jamovi v. 2.3 (Computer software, jamovi project). A descriptive analysis was performed to assess the parametric assumptions. Results outside a normal distribution were transformed using a Box-Cox transformation. Statistical differences were then estimated via either One-Way or Two-Way ANOVA, depending on the data, followed by post hoc Tuckey comparison tests (for a significant level of $p<0.05$).

Regarding experimental design analysis and response surface methodology, including statistical analysis the correlated data, were done using Design Expert software v. 11 (StatEase, USA).

4.Results and Discussion

4.1. Biomass Disruption

4.1.1. High pressure homogenization

To optimize the high-pressure homogenization of *R. monicae*, biomass concentration (60 – 150 g/L), and pressure (300 – 1200 bars) were the chosen parameters considered for process optimization with just 1 cycle. These were selected considering the equipment processing limitations, including the exponential increase in power consumption and equipment wearability, with the rise in pressure.

Within the input parameter range values, 13 runs were suggested in the experimental plan formulated by the software Design Expert (**Supplementary Data 1**). Each run was performed once, with disruption efficiency (%) based on turbidity chosen as the response factor. The software Design Expert evaluated and correlated the response factor with the treatment parameters, and a 3D graphic detailing the correlation between disruption efficiency, pressure and biomass concentration was obtained, using response surface methodology (**Figure 4.18**). An additional ANOVA statistical analysis was performed on the response factor (**Table 4.8**)

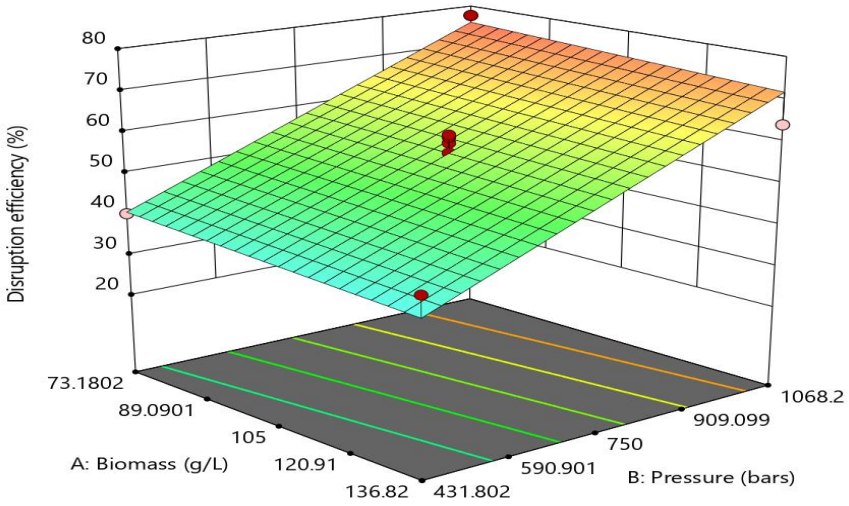

Figure 4.18: 3D surface graphic obtained using the Design Expert software coupled with response surface methodology. The graphic details the correlation between pressure (bars) and biomass (g/L) in their influence on disruption efficiency (%).

Table 4.8: Results of an ANOVA linear model of cell disruption efficiency.

Source	Sum of Squares	df	Mean Square	*F*-value	*p*-value	Observations
Model	2505.29	2	1252.64	45.03	< 0.0001	significant
A-Biomass	33.12	1	33.12	1.19	0.3008	not significant
B-Pressure	2472.17	1	2472.17	88.87	< 0.0001	significant
Residual	278.17	10	27.82			
Lack of Fit	235.90	6	39.32	3.72	0.1121	not significant
Pure Error	42.28	4	10.57			
Cor Total	2783.46	12				
Std. Dev.	5.27	R^2	0.9001			
Mean	43.82	Adjusted R^2	0.8801			
C.V. %	12.04	Predicted R^2	0.7992			
		Adeq Precision	19.6242			

Table 4.8 showcases that the linear model F-value for disruption efficiency was 45.03, implying that this model was significant, as there was only a 0.01% chance the F-value this large could have occurred due to noise. A *p*-value below 0.05 indicates that the model terms were significant. In this situation, the model term B (pressure) was deemed as significant. The value of R^2 was 0.9001 (above 0.80 implies a good fit of a model [126]), which was close to 1. Meanwhile the value of Adeq. Precision of the model was 19.6242 which means the signal of the model was sufficient and it could be used for the prediction algorithm.

By analyzing **Figure 4.18**, it was found that the disruption efficiency achieved with the HPH methodology in this study varied between 36.57% and 75.79%. A closer look at the data revealed that the lowest efficiency was achieved at a biomass concentration of 136 g/L and at a working pressure of 432 bars. Meanwhile, the highest disruption efficiency of 75.79% was reached with a biomass concentration of 73 g/L and a working pressure of 1068 bars. These values correlate with those obtained in Spiden *et al.* (2013) and Bernaerts *et al.* (2019), where an increase in disruption in function of higher pressures was found when analyzing the data. Spiden *et al.* (2013) managed to achieve a disruption efficiency of approximately 60% at 1500 bars, while Bernaerts *et al.* (2019) reached a disruption efficiency of 58% at 2700 bars [45,46]. As expected as well, the disruption efficiency would vary according to the type of microalgae as they possess different cell

walls compositions, and consequentially different resistances to mechanical disruption via HPH [33,40].

A closer look at the results found in **Figure 4.18**, and through the statistical analysis in **Table 4.8**, it was found that the pressure parameter significantly influenced the disruption efficiency, while the biomass concentration parameter did not. Looking closer at the influence of pressure on biomass disruption efficiency, it was observed that by increasing the pressure the biomass was subjected to during HPH, disruption efficiency also increased, achieving a maximum disruption efficiency of 75.79% at 1068 bars. This was within expectations, as higher pressures are more efficient in disrupting cells [127]. On the other hand, biomass concentration was found to have no significant impact on the disruption efficiency (p=0.3008), implying it was possible to work under higher biomass concentrations, minimizing the volume of biomass need to process and thus the time and energy spent during the disruption assay. However, as any solution is known to become more viscous as the solute concentration increases, working with higher biomass concentrations risks potentially clogging the homogenizer, which could in turn damage the equipment. As such, the pressure parameter was given higher relevance when selecting the most efficient HPH conditions in disrupting *Raphidonema monicae* cells. It is worth noting that the biomass temperature during the processing was not controlled, with a tendency to increase 1 ºC per 100 bars. This means that there was the possibility that the hotter temperatures at higher pressures could have somewhat influenced the disruption efficiency detected when evaluating the turbidity of the samples processed at higher pressures. However, temperature increase can be easily solved by using a heat exchanger, which efficiently cools down the biomass preventing it from overheating and potentially degrading important biochemical compounds.

At the end of the assay, the Design Expert software was also used to extrapolate three different parameter combinations based on: 1) maximizing disruption efficiency; 2) maximizing disruption efficiency and biomass concentration; and 3) maximizing disruption efficiency while minimizing pressure (**Table 4.9**).

Table 4.9: High pressure homogenization optimized methodologies suggested by the Design Expert software after choosing the tendency of each parameter.

HPH optimized methodology	Methodology ID	[Biomass] (g/L)	Pressure (bars)	Predicted disruption efficiency (%)
Maximizing disruption efficiency	**H1**	73	1068	75.79
Maximizing disruption efficiency and biomass concentration	**H2**	136	1068	71.63
Maximizing disruption efficiency while minimizing pressure	**H3**	73	573	48.40

In H1, by maximizing the disruption efficiency, the objective was to select the condition that offers the most effective biomass disruption methodology. In H2, by maximizing the disruption efficiency and biomass concentration, the goal was to identify the conditions that offer a procedure capable of effectively disrupting as much biomass as possible within the imposed limits of the equipment, while decreasing processed volume and time, and energy used. In H3, by maximizing the disruption efficiency while minimizing the pressure, the purpose was to identify the condition that offers a methodology with a reasonably efficient biomass disruption, while reducing the wearability of the equipment. These 3 methodologies were thus selected to be evaluated in the trial which compares the high-pressure homogenization and enzymatic hydrolysis methodologies.

4.1.2. Enzymatic hydrolysis

4.1.2.1. Enzymatic hydrolysis screening assay

As *R. monicae* has been poorly researched regarding cell disruption, there is a lack of literature data to compare against the experimental data obtained in this work. Therefore, it was important to perform a screening assay, to see which enzymes would affect the integrity of *R. monicae* cells. An initial enzymatic hydrolysis screening assay was thus carried out, comparing the effect of several enzymes (mannanase, pectinase, cellulase, viscozyme and alcalase) in disrupting microalgal cells. Mannanase, pectinase, cellulase and viscozyme, known carbohydrases, were

selected based on previous research indicating them as potential enhancers for lipid and carbohydrate extraction [112,128,129]. Meanwhile, the endoprotease alcalase, was chosen due to previous research on this enzyme highlighting its potential in producing bioactive peptides by hydrolyzing proteins [130]. Five controls were included in the assay, one containing non-treated biomass, essential for the determination of the disruption efficiency, a second one corresponding to temperature control, to evaluate if the temperature (50 º C) had any influence in the disruption efficiency, and the remaining three for controlling the pH influence on the disruption efficiency were set at pH 4, 6 and 8 respectively (**Table 4.10**). The disruption efficiency was used to evaluate the enzymatic hydrolysis efficiency (**Figure 4.19**).

Table 4.10: Enzymatic hydrolysis screening conditions tested and respective disruption efficiency±standard deviation (n=2) (%). Different letters correspond to different significance levels (p<0.05). C1 – Temperature Control; C2 – pH 4 control; C3 – pH 6 control; C4 – pH 8 control; n.d. – Not determined.

Sample name	[Biomass] (g/L)	pH	Enzyme	[Enzyme] % (w/w)	Disruption efficiency (%)
C1	20	n.d.	-	-	29.37 ± 0.32^{bc}
C2	20	4	-	-	18.91 ± 4.20^{d}
Mannanase	20	4	Mannanase	8	20.18 ± 1.76^{d}
Pectinase	20	4	Pectinase	8	37.50 ± 0.24^{ce}
C3	20	6	-	-	26.52 ± 1.27^{bd}
Cellulase	20	6	Cellulase	8	38.34 ± 2.47^{e}
Viscozyme	20	6	Viscozyme	8	35.97 ± 4.80^{ce}
C4	20	8	-	-	27.00 ± 4.53^{bd}
Alcalase	20	8	Alcalase	8	62.84 ± 2.14^{a}

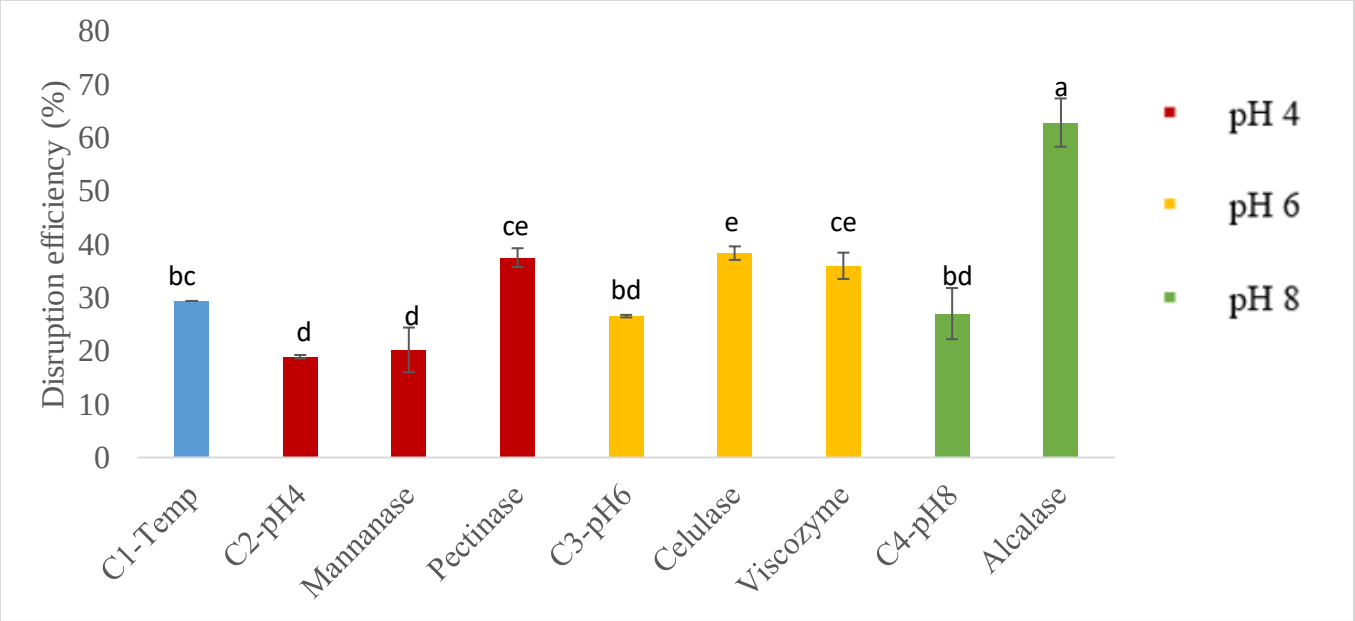

Figure 4.19: Disruption efficiency (%) of the enzymatic hydrolysis screening assay. The error bars correspond to the standard deviation of the biological replicates (n=2). Different letters correspond to different significance levels (p<0.05)

Before comparing the enzymatic treatments, it was necessary to evaluate if the reaction parameters (temperature and pH) contributed to the cell disruption. In **Figure 4.19**, it was possible to see that the temperature control had a disruption efficiency of 29.37±0.32%, and the controls of pH 4, 6 and 8 also presented a disruption efficiency of 18.91±4.20, 26.52±1.27 and 27.00±4.53%, respectively. These disruption efficiencies were all statistically significant when compared with the non-treated biomass, implying that the temperature and pH adjustments contributed to the cell disruption. However, significant differences between temperature and pH controls were only found between the temperature and pH 4 control, suggesting that only these influenced the cell disruption by themselves. In the case of the temperature parameter, it was expected that raising the temperature of the solution to 50 ºC would potentially damage the cells and partially hydrolyze their contents, hence the disruption efficiency of 29.37±0.32% [131]. However, the pH 4 control (C2), incubated to 50 ºC, had a lower disruption efficiency than the temperature control (C1). This could be related to the fact that the acidic pH in this situation affected the turbidity value during the reading of the samples at 750 nm, from which the biomass disruption efficiency values were derived. It is known that acidic pH values often trigger the aggregation and precipitation of molecules and particles, particularly of proteins, and in turn, could have contributed to the opaqueness of the sample, and thus a higher turbidity value than expected, lowering the estimated biomass disruption efficiency [132–134].

In relation to the enzymatic treatment with the hydrolytic enzymes, it was possible to assess that, depending on the hydrolytic enzyme the biomass was exposed to, the resulting biomass disruption efficiency would vary significantly. This was expected, as hydrolytic enzymes have been known to have a higher or lower potential in disrupting biomass depending on the biochemical composition of the microalga [135]. The maximum disruption efficiency achieved was 62.84±2.14%, with alcalase, and the lowest disruption efficiency achieved was 20.18±1.76%, with mannanase. Meanwhile, viscozyme, pectinase, and cellulase had similar non-significant disruption efficiencies, of 35.97±4.80, 37.50±0.24 and 38.34±2.47% respectively, between them. This disruption efficiency however, varied significantly when compared with other studies. In Soto-Sierra *et al.* (2021), they only achieved a 25% disruption efficiency with alcalase against *Nannochloropsis* sp. [136]. In Horst *et al.* (2012), they also only found a disruption efficiency of 20% with viscozyme against *Nannochloropsis occulta* [137]. It's worth noting that these articles used different methods to estimate the disruption efficiency, including peptide bond hydrolysis quantification (Soto-Sierra *et al.*) and lipid release (Horst *et al.*), which in itself could produce significantly different results, as turbidity in itself was found to exacerbate the real disruption efficiency obtained from the disruption methodology [46,136,137].

Based on the results obtained in this assay, alcalase was selected as the main enzyme for cell disruption. However, while this protease could potentially produce bioactive peptides, it was also possible that it could synergistically interact with a carbohydrase, enhancing the disruption efficiency even further. As such, a carbohydrase was also selected to complement the enzymatic activity of alcalase in biomass disruption. Mannanase was immediately discarded among the 4 tested carbohydrases, as it demonstrated the lowest disruption efficiency (20.18±1.76%). As the 3 remaining carbohydrases had no significant differences, the decision was made based on the operating pH parameter and composition of the enzymatic solution instead. Among the 3, pectinase and viscozyme had the closest working pH value (pH 6) compared to that of alcalase (pH 8). Additionally, viscozyme was the carbohydrase with the most non-specific enzymatic activity, due to being a cocktail of carbohydrases [137], and thus could hydrolyze a broader group of target molecules. Therefore, alcalase and viscozyme were thus selected for the enzymatic hydrolysis optimization assay.

4.1.2.2. Enzymatic hydrolysis optimization

To further optimize the enzymatic hydrolysis, a design of experiment was carried out based on 4 parameters: Biomass concentration, between 20 and 60 g/L; pH, between 6 and 8; alcalase concentration, between 0 and 6 % (w/w); and viscozyme concentration, between 0 and 6 % (w/w).

Accounting for those factors and range values, the Design Expert software suggested an assay with 30 runs (**Supplementary Data 2**). Each run was carried out once, with disruption efficiency as the chosen response factor. The software Design Expert evaluated and correlated the response factor with the treatment parameters, and a 3D graphic detailing the correlation between disruption efficiency, biomass concentration, pH, and enzyme concentration, was formed using response surface methodology (**Figure 4.20**). An additional ANOVA statistical analysis was performed on the response factor (

Table 4.11).

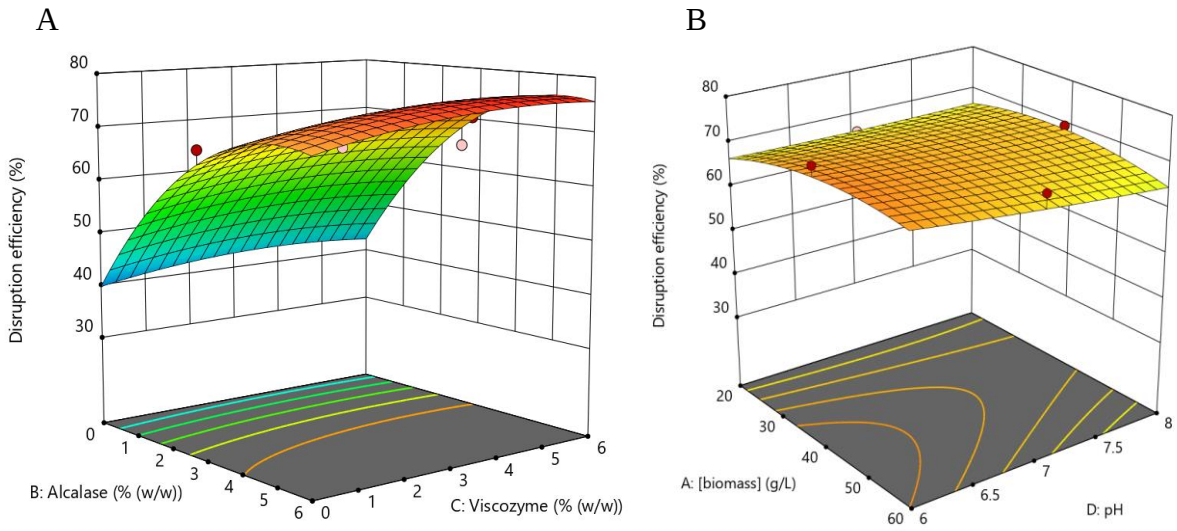

Figure 4.20: 3D graphic obtained using the Design Expert software coupled with response surface methodology. The graphic details the correlation between disruption efficiency (%), alcalase concentration % (w/w) and viscozyme concentration % (w/w) (A), and between disruption efficiency (%), biomass concentration (g/L) and pH (B).

Table 4.11: Results of an ANOVA based quadratic model of disruption efficiency, upon enzymatic hydrolysis.

Source	Sum of Squares	df	Mean Square	*F*-value	*p*-value	Observations
Model	6318.77	14	451.34	35.52	< 0.0001	significant
A-[biomass]	7.08	1	7.08	0.5573	0.4669	not significant
B-Alcalase	4566.83	1	4566.83	359.43	< 0.0001	significant
C-Viscozyme	69.81	1	69.81	5.49	0.0333	significant
D-pH	39.40	1	39.40	3.10	0.0986	not significant
AB	1.98	1	1.98	0.1560	0.6984	
AC	11.93	1	11.93	0.9389	0.3479	
AD	36.55	1	36.55	2.88	0.1105	
BC	6.89	1	6.89	0.5423	0.4728	
BD	3.57	1	3.57	0.2806	0.6041	
CD	56.65	1	56.65	4.46	0.0519	
Residual	190.59	15	12.71			
Lack of Fit	186.78	10	18.68	24.51	0.0013	significant
Pure Error	3.81	5	0.7620			
Cor Total	6509.36	29				
Std. Dev.	3.56		R^2	0.9707		
Mean	60.52		Adjusted R^2	0.9434		
C.V. %	5.89		Predicted R^2	0.8542		
			Adeq Precision	17.7664		

Table 4.11 showcased that the quadratic model *F*-value for disruption efficiency was 35.52, suggesting that this model was significant, as there was only a 0.01% chance the *F*-value this large could have occurred due to noise. The *p*-value below 0.05 of the model also indicates that the model terms were significant. In this situation, the model terms B (alcalase) and C (viscozyme) were significant. The value of R^2 was 0.9707 (above 0.80 implies a good fit of a model [126]), which was close to 1. Meanwhile the value of Adeq. Precision of the model was 17.7664 which means that the model's signal was good and could be used for the prediction algorithm.

In **Figure 4.20-A**, it was possible to observe that both alcalase and viscozyme influenced the disruption of the biomass. However, this influence was much more significant with alcalase (p-value<0.0001) than with viscozyme (p-value=0.0333). A closer look at alcalase influence on disruption efficiency revealed that its activity peaked around a concentration of 6% (w/w), with a

disruption efficiency of 70.94%. In relation to viscozyme, its effect was much less noticeable than with alcalase, reaching only 46.55% disruption efficiency with a concentration of 5.81% (w/w).

In relation to biomass concentration and pH influence on disruption efficiency (**Figure 4.20-B**), it was found that neither had a significant influence (

Table 4.11). As neither factor is hydrolytic in nature, these results were to be expected, and as such, neither were considered relevant for the optimization of the enzymatic hydrolysis assay.

The results from this assay were used in the Design Expert software through the predictive model obtained, to predict three methodologies with different objectives in optimizing the enzymatic hydrolysis assay: 1) maximizing disruption efficiency; 2) maximizing disruption efficiency and biomass concentration; and 3) maximizing disruption efficiency while minimizing viscozyme concentration % (w/w) (**Table 4.12**).

Table 4.12: Optimized enzymatic hydrolysis by using the predictive model obtained, while favoring the levels and weights of the independent variables.

HPH optimized methodology	Methodology ID	[Biomass] (g/L)	[Alcalase] (% w/w)	[Viscozyme] (% w/w)	pH	Predicted disruption efficiency (%)
Maximizing disruption efficiency	**E1**	47.0	5.43	3.70	6.31	78.05
Maximizing disruption efficiency and biomass concentration	**E2**	60.0	6.00	6.00	6.00	79.35
Maximizing disruption efficiency while minimizing viscozyme concentration	**E3**	33.5	5.00	-	8.00	71.99

In E1, by maximizing the disruption efficiency, the aim was to select the condition that offers the most effective biomass disruption methodology, using just enzymatic hydrolysis. In E2, by maximizing both disruption efficiency and biomass concentration, the aim was to obtain conditions that would allow minimizing operating volumes while maintaining an efficient biomass disruption. In E3, the goal was to maximize the disruption efficiency while minimizing the

viscozyme concentration %, aiming to simplify the hydrolysis process and reduce the number of resources required to process the biomass.

4.1.2.3. Enzymatic hydrolysis validation assay

This assay aimed to compare the hydrolytic efficiency of E1, E2, and E3 with a previously established enzymatic hydrolysis methodology in García, *et al*. [49] (**Table 4.13**). One run of each assay was performed, and one sample was collected after the hydrolysis incubation period of each enzyme, for disruption efficiency quantification (**Figure 4.21**)

Table 4.13: Enzymatic hydrolysis screening assay conditions that were tested and respective disruption efficiency±standard deviation (n=2). The sequential assay (SA) refers to the hydrolytic methodology already established by Garcia *et al.* [49]. Different letters correspond to different significance levels (p<0.05). SA – Sequential assay; V – viscozyme; VA – viscozyme and alcalase; VAF – viscozyme, alcalase and flavourzyme.

Methodology ID	Sample name	[Biomass] (g/L)	[Viscozyme] % (w/w)	[Alcalase] % (w/w)	[Flavourzyme] % (w/w)	pH	Disruption efficiency (%)
Sequential assay (SA)	SA-V	60.0	4.00	-	-	6.50	10.30±4.72[b]
	SA-VA	60.0	4.00	4.00	-	8.00	52.92±0.63[a]
	SA-VAF	60.0	4.00	4.00	4.00	7.00	53.25±0.64[a]
E1	E1	47.0	3.70	5.43	-	6.31	52.51±1.36[a]
E2	E2	60.0	6.00	6.00	-	6.00	52.47±0.94[a]
E3	E3	33.5	-	5.00	-	8.00	49.04±0.39[a]

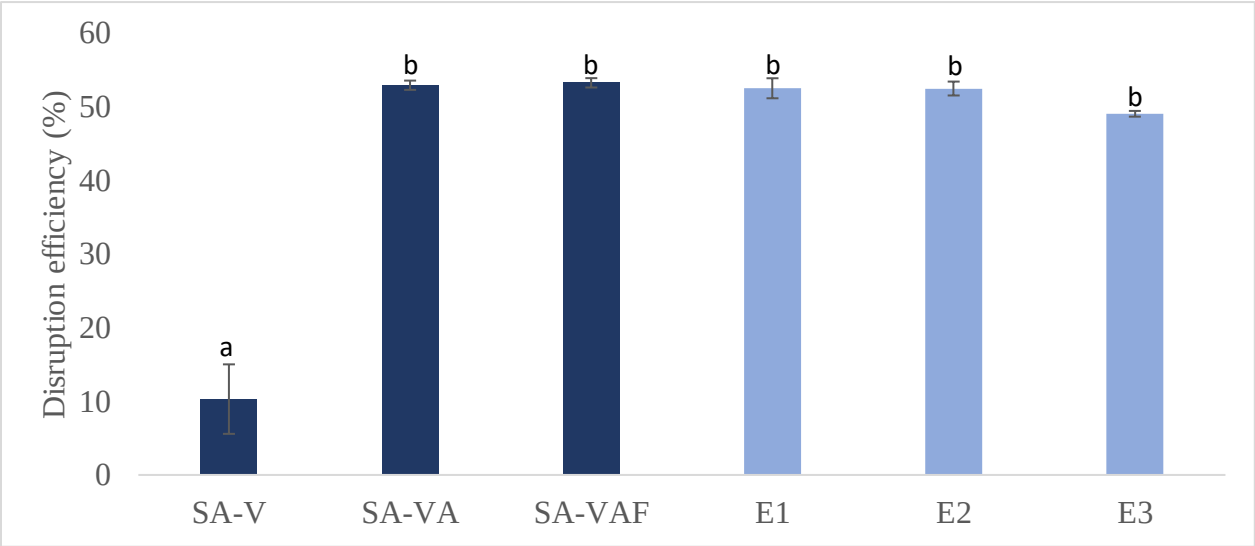

Figure 4.21: Disruption efficiency (%) of the enzymatic hydrolysis validation assay. The error bars refer to the standard deviation of the analytical replicates (n=2). Different letters correspond to different significance levels (p<0.05). SA – Sequential assay; V – viscozyme; VA – viscozyme and alcalase; VAF – viscozyme, alcalase and flavourzyme.

As could be observed in **Figure 4.21**, it was found that all enzymatic treatments had a significant influence on the disruption of *R. monicae* biomass. Concerning the sequential enzymatic assay, it was further identified that the impact of viscozyme to disrupt biomass was smaller when compared with alcalase, as previously observed in the enzymatic hydrolysis optimization assay. More specifically, when adding viscozyme first, the disruption efficiency was only 10.30±4.72%, while through the second enzymatic addition of alcalase, the disruption efficiency increased 5-fold (to 52.92±0.63%). Nevertheless, no statistical significance was found between the alcalase and flavourzyme treatment, implying that the addition of flavourzyme did not contribute to the biomass disruption.

When comparing the sequential enzymatic assay with the three enzymatic hydrolysis methodologies predicted in the optimization assay, it was found that neither E1, E2 or E3 had statistically significant variations of turbidity in comparison with the sequential assay, implying similar disruption efficiencies between all four methodologies.

Taking into consideration that the aim was to maximize the disruption efficiency while minimizing the complexity of the methodology, among the three enzymatic hydrolysis tested in this assay, E3 was selected to be tested in the final pipeline aimed at combining HPH and EH

methodologies to maximize the biomass disruption process. This choice was based on the fact that, as all enzymatic methodologies tested have a similar disruption efficiency, the ideal methodology to select would be the simplest and least resource-intensive methodology, which in this case was E3, as it discarded the usage of viscozyme and used only alcalase for the enzymatic hydrolysis.

4.1.3. Biomass disruption pipeline optimization assay

In order to carry out the assay to optimize the biomass disruption pipeline, the HPH and EH methodologies previously selected (H1, H2, H3, and E3), were tested, either alone or combined (Mix 1: H1+E3; Mix 2: H3+E3), to evaluate their potential in disrupting *R. monicae* biomass (**Table 4.14**). H2 was not tested in combination with E3 because during the assay it was found that its elevated biomass concentration significantly increased the chances of clogging the homogenizer. Nevertheless, it was still evaluated alongside the other treatments in the possibility it could have a significantly better extraction of compounds. Three types of samples were collected during this assay (**Figure 3.13**) to evaluate the efficiency of these methodologies, in terms of disruption efficiency (**Figure 4.22**), as well as the release of free amino acids (**Figure 4.23**), soluble proteins (**Figure 4.24**), soluble carbohydrates (**Figure 4.25**), and total lipids (**Figure 4.26**).

Table 4.14: Methodologies evaluated in the biomass disruption pipeline optimization assay. M1 and M2 methodologies first subjected the biomass to the selected HPH methodology, followed by the chosen enzymatic hydrolysis methodology. N.d – not determined.

Sample name	Methodology ID	[Biomass] (g/L)	pH	Alcalase % (w/w)	Pressure (bars)
E3	E3	33.5	8	5	-
H1	H1	73	n.d	-	1068
H2	H2	136	n.d	-	1068
H3	H3	73	n.d	-	573
M1	H1+E2	73 –> 33.5	8	5	1068
M2	H3+E2	73 –> 33.5	8	5	573

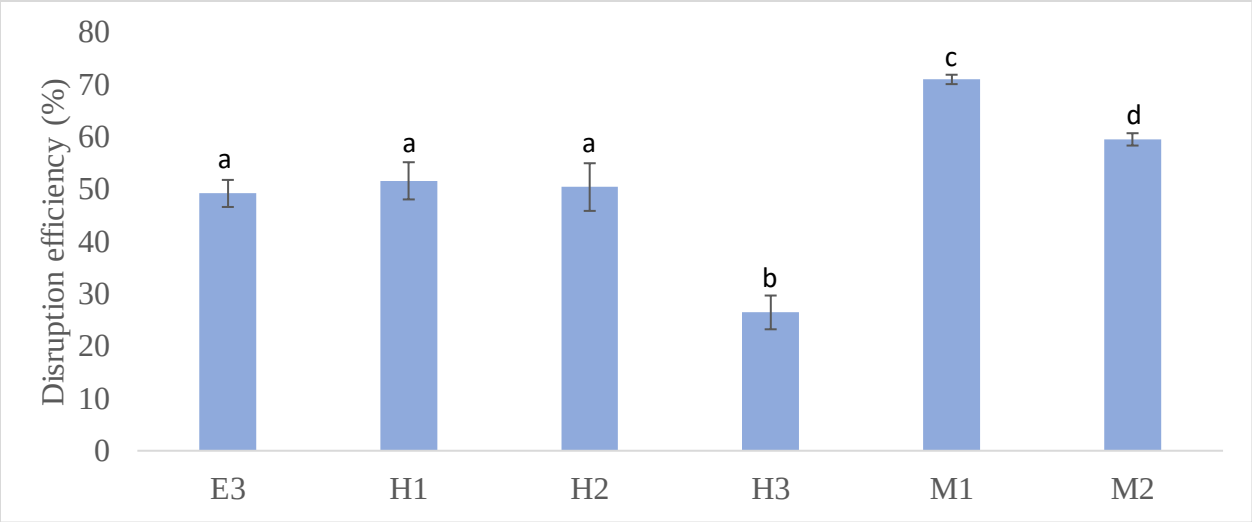

Figure 4.22: Disruption efficiency (%) of the biomass disruption optimization assay. The error bars refer to the standard deviation of the analytical replicates (n=2). Different letters correspond to different significance levels (p<0.05).

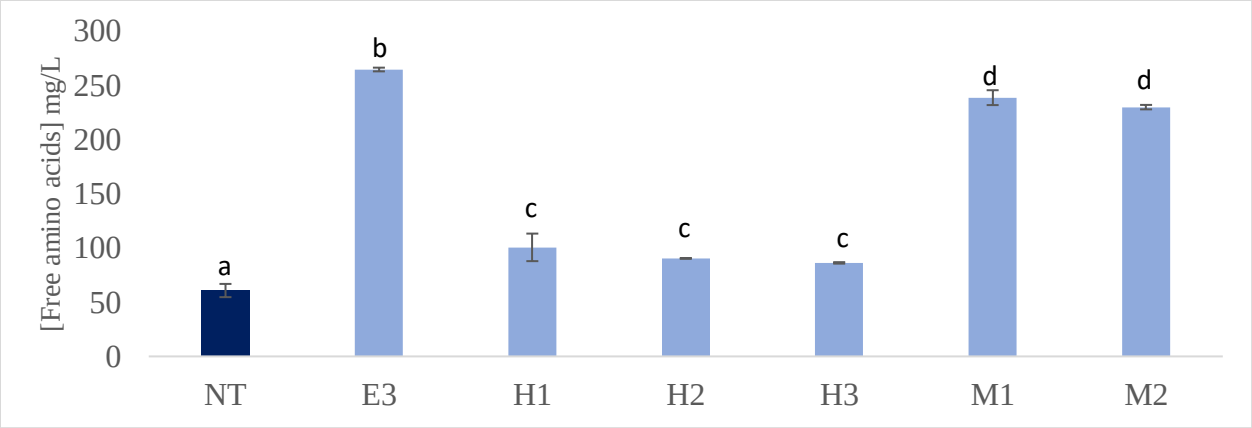

Figure 4.23: Free amino acids (mg/L) analysis of the supernatant samples obtained during the biomass disruption optimization assay. The error bars refer to the standard deviation of the analytical replicates (n=2). Different letters correspond to different significance levels (p<0.05). NT – Non-treated biomass.

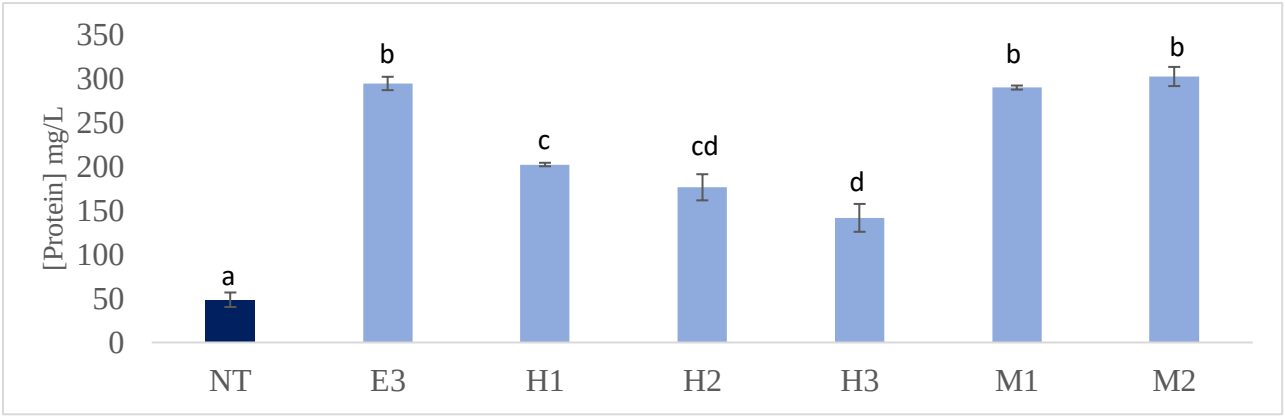

Figure 4.24: Soluble proteins (mg/L) analysis of the supernatant samples obtained during the biomass disruption optimization assay. The error bars refer to the standard deviation of the analytical replicates (n=2). Different letters correspond to different significance levels (p<0.05). NT – Non-treated biomass

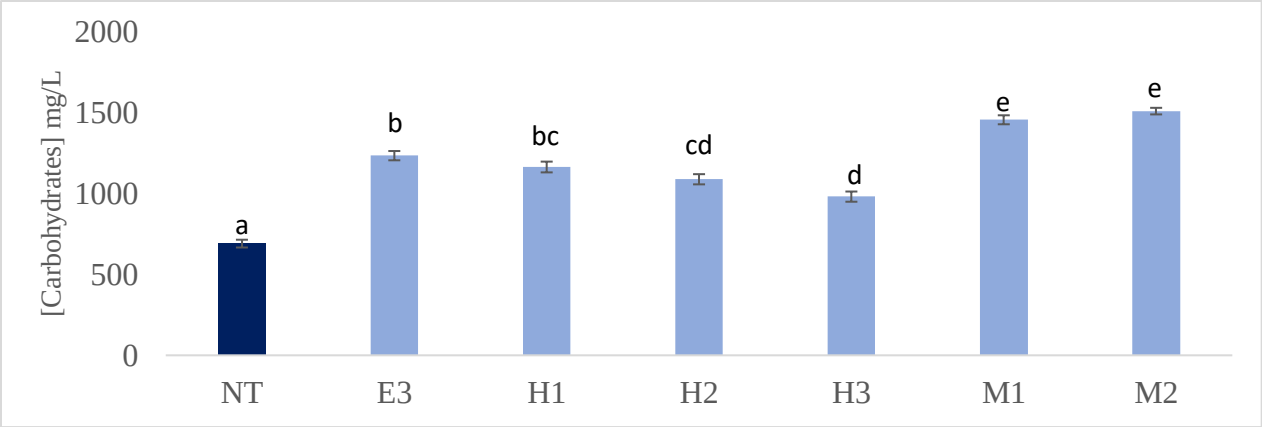

Figure 4.25: Soluble carbohydrates (mg/L) analysis of the supernatant samples obtained during the biomass disruption optimization assay. The error bars refer to the standard deviation of the analytical replicates (n=2). Different letters correspond to different significance levels (p<0.05). NT – Non-treated biomass.

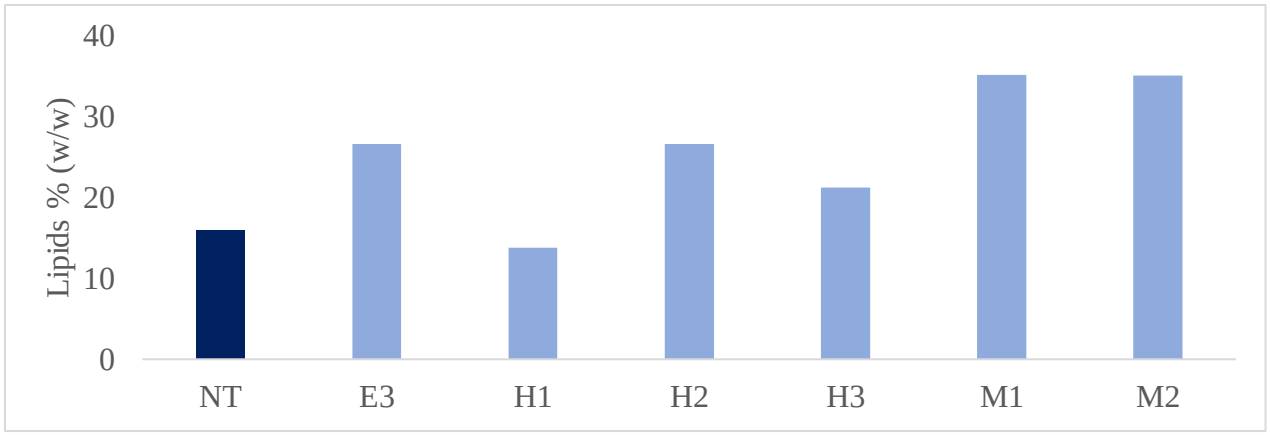

Figure 4.26: Total lipids % (w/w) analysis of the supernatant samples (n=1) obtained during the biomass disruption optimization assay. NT – Non-treated biomass.

In relation to the disruption efficiency (**Figure 4.22**), a significant decrease was observed in all treatments, as little as 26.43±3.23% (H3), and as high as 70.95±0.90% (M1). Considering these results, M1 proved to be significantly more efficient than all other treatments in disrupting the biomass. This was within the expected results, as treatment M1 combined the most aggressive EH and HPH treatment (E3 and H1). However, what was unexpected is that all three HPH treatments disruption efficiencies were significantly lower than predicted through the predictive algorithm. At the time, an older *R. monicae* biomass batch had been used, which could have facilitated the disruption and artificially increased the estimated disruption efficiency. Nevertheless, the goal was to identify the method that not only extensively disrupted the cells, but also, released the most compounds with potential bioactivity, including free amino acids, reducing

sugars, soluble proteins, soluble carbohydrates, and total lipids, since this is the main goal behind the disruption processes tested.

Regarding free amino acid release (**Figure 4.23**), it was found that treatment E3 was the most efficient in amino acids extraction, by increasing 3-fold their concentration in the supernatant (264.52±1.72 mg/L) when compared to the non-treated (NT) sample (60.73±6.10 mg/L). The mixed treatments M1 and M2 shared a similar 3-fold increase in the release of amino acids (238.56±6.86 and 229.83±2.06 mg/L, respectively), with no significant differences between them. Meanwhile, all three HPH treatments demonstrated the lowest increase in amino acid concentration, between 166 and 142%, with no significant differences between them (from 100.52±12.70, 90.33±0.34 and 86.21±0.67 mg/L, respectively). It was expected that the HPH treatments (H1, H2 and H3) would have the lowest release of amino acids, as they did not undergo enzymatic hydrolysis with alcalase, a known proteolytic enzyme. However, what was not expected was treatment E3 having a higher release of amino acids than the mixed treatments, although the difference was minimal. Given the variability within the samples, it was possible that with more biological replicates, this difference would potentially be found to be insignificant between E3 and M1 and M2. Another possible reason for E3 higher amino acid concentration could be correlated to the potential amino acid degradation that occurred as the biomass was exposed to an increase during HPH. However, this is unlikely, as most amino acids are known only to degrade at temperatures above 185 ºC [138,139].

Through the analysis of the soluble proteins (**Figure 4.24**), it was found that E3 (293.99±7.58 mg/L), M1 (289.34±2.31 mg/L) and M2 (301.91±10.87 mg/L) had the highest increase in protein concentration, of approximately 5-fold, when compared with the non-treated biomass (48.52±8.23 mg/L). However, no significant differences were found between these treatments. Meanwhile, the HPH treatments (H1, H2 and H3) had significantly lower protein concentrations in the supernatant samples, with only a 2 to 3-fold increase in released protein levels (201.99±1.97, 176.14±14.82 and 141.44±15.81 mg/L, respectively). As expected, the enzymatic and mixed treatments had the highest release potential of soluble proteins, due to the alcalase treatment. Most probably, this treatment not only denatured several proteins and exposed their peptides bonds, but also solubilized several insoluble proteins by degrading them into soluble peptides, which were subsequently quantified through the Lowry protocol.

In **Figure 4.25**, it was seen that the M1 (1457.17±27.78 mg/L) and M2 (1510.86±20.37 mg/L) treatments had the highest concentration of soluble carbohydrates, with an approximately 115% increase in these levels when compared to that of the non-treated biomass (691.04±24.08 mg/L), although no significant differences were found. This result suggests that the mixed treatments were both as efficient in extracting carbohydrates from the raw biomass. Meanwhile, the enzymatic and HPH treatments had a lower increase in soluble carbohydrates concentration, as high as 79% (E2, with 1235.19±28.71 mg/L) and as little as 42% (H3, with 981.78±31.49 mg/L). As expected, the mixed treatments demonstrated the highest potential to extract soluble carbohydrates from *R. monicae* biomass. This is most likely related to the fact that the mixed treatments were found to be the most efficient in disrupting the raw biomass, and since no carbohydrases were used, the soluble carbohydrates released would have to be already available intracellularly. Furthermore, the alcalase treatment could have contributed even further by hydrolyzing glycoproteins, increasing the soluble carbohydrate concentration.

Regarding the total lipid concentration (**Figure 4.26**), it was found that treatment M1 and M2 had the highest lipid concentration (35.22 and 35.11%, respectively), while the enzymatic and HPH treatments all demonstrated a smaller release in lipids, as high as 26.60% (E3 and H2) and as low as 13.82% (H1). These results were within expectation, as M1 and M2 treatments demonstrated the highest increase in lipid concentration since these treatments were identified in the disruption efficiency analysis (**Figure 4.22**) to have the most potential to disrupt biomass. This in turn, increases the available lipids in solution which can be detected by the lipid quantification protocol.

Bearing in mind the disruption efficiency and compound release analysis results, the treatment that stood out the most was the M1 treatment, with the highest disruption efficiency (71%), and a measurable release of soluble protein (496%), soluble carbohydrate (115%) and total lipids (35%). Interestingly, this treatment resulted in one of the highest amino acid release (239%).

4.2. Fractionation

As treatment M1 was chosen as the disruption methodology, the processed biomass using this method still had to be fractionated into multiple potentially bioactive fractions. Therefore, the processed biomass was subjected to pH shifting, membrane filtration and ethanol extraction.

4.2.1. pH shifting

The pH shifting aimed to identify the pH at which the most proteins could be extracted from the disrupted biomass, since protein solubility generally increases with pH [140]. The supernatant samples' soluble protein concentration (mg/L) was then measured through the Lowry protocol (**Figure 4.27**).

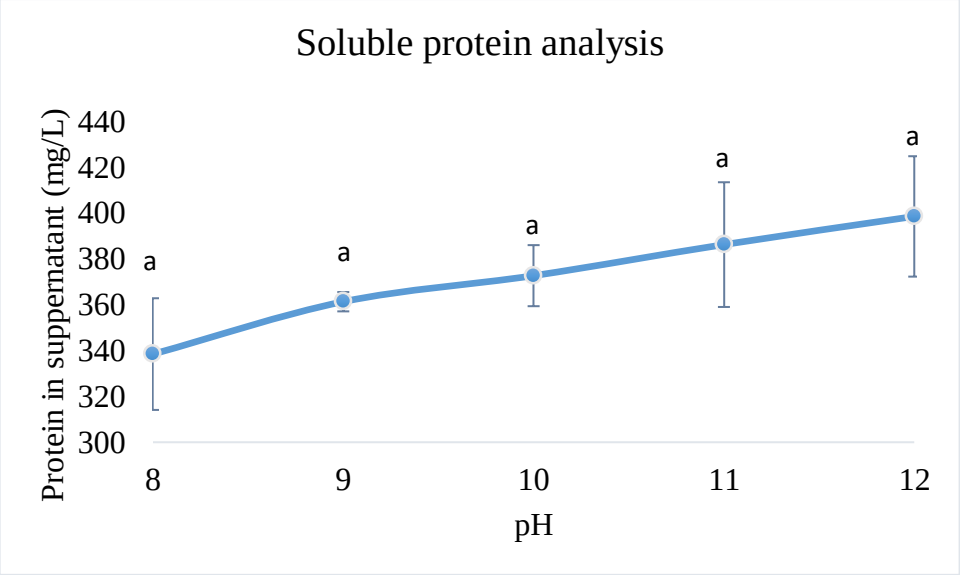

Figure 4.27: Soluble protein (mg/L) of the pH shifting assay. The supernatant samples were used for this analysis. The error bars correspond to the standard deviation of the biological replicates (n=3). Different letters correspond to different significance levels (p<0.05).

By analyzing the protein results in **Figure 4.27**, a trend was observed for an increase in protein solubility as the pH was increased, from 8 up to 12. However, a statistical analysis revealed that no significant differences were present between the 5 tested pH values, suggesting the increase in pH did not contribute significantly to the protein extraction. This was unexpected, as other studies found that more alkaline pH values used during protein extraction often achieved higher protein extraction rates [140,141]. For example, one study enhanced 3-fold the protein extraction from the seaweed *Saccharina latissimi* with an alkaline protein extraction at pH 12[140]. Another study reviewed the alkalinity influence on protein extraction of microalgal biomass and concluded that, although not as efficient as an enzymatic extraction, it still managed to enhance protein extraction [141]. Nonetheless, pH 10 was considered the ideal pH for membrane filtration and ethanol extraction. This was because pH 10 was the maximum tolerable alkaline pH the membrane filtration system could work with. Furthermore, while more alkaline pH values are associated with enhanced protein solubility, studies have also found that if the alkalinity is too high, it could

contribute to the degradation of proteins and peptides [142]. This is problematic, as this thesis aimed to develop an extraction methodology that both maximized the extraction of bioactive compounds while preserving their structural integrity, and bioactive properties.

4.2.2. Membrane filtration

Regarding membrane filtration, the processed biomass with pH adjusted to 10 was subjected to micro- and ultrafiltration, at pores size 0.2 µm and 100 kDa, respectively. Multiple analytical methods were performed to quantify the distribution of certain compounds between permeate and retentate, including free amino acids, soluble and total proteins, soluble carbohydrates, lipids, and total carotenoid content (**Figure 4.28**).

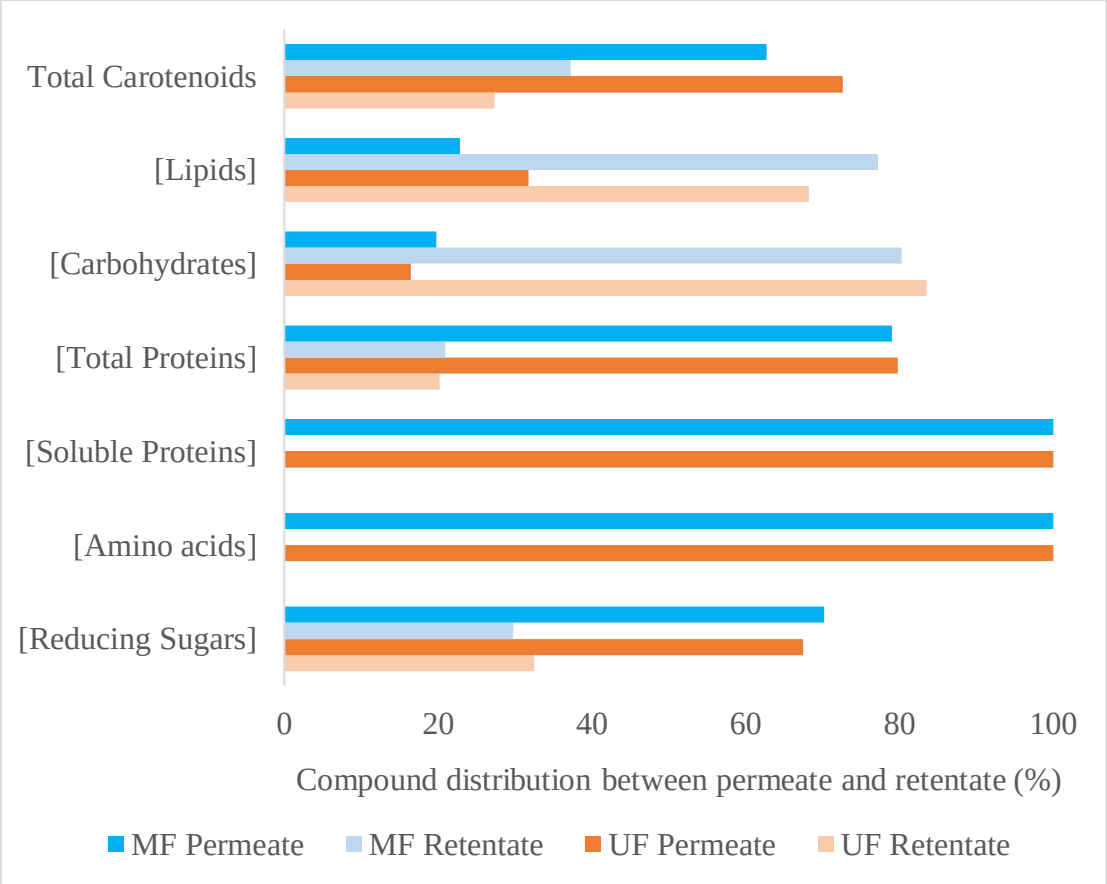

Figure 4.28: Biochemical analysis of the compound distribution between permeate and retentate samples obtained from microfiltration (MF) and ultrafiltration (UF).

Reducing sugars, amino acids, soluble proteins, total proteins, and total carotenoids were mostly found in the permeate, when the processed biomass was subjected to microfiltration (**Figure 4.28**), as they are smaller than the 0.2 µm pore size of the membrane [59]. In the lipidic fraction,

as most lipids are found within the cellular debris, which most do not pass through a 0.2 µm pore, a higher concentration of lipids was found in the retentate. As no carbohydrases were used, most carbohydrates accumulated in the retentate. This might be explained by the fact that a large portion of carbohydrates within the cells are either found intracellularly, acting as storage components, or in the cell wall, acting as structural components, and thus, during disruption, remained attached to the cellular debris or formed aggregates that were too large for the pore size used [143].

Similar outcomes were obtained when the processed biomass was subjected to ultrafiltration, where reducing sugars, amino acids, soluble and total proteins, and total carotenoids were mainly in the permeate. Furthermore, similarly to microfiltration, ultrafiltration also retained most lipids and carbohydrates in the retentate.

When comparing micro- and ultrafiltration permeates, it was found that the microfiltration permeate was richer in reducing sugars and carbohydrates. However, the ultrafiltration permeate was richer in total proteins, lipids and carotenoids. The inverse was expected and observed when comparing the micro- and ultrafiltration retentates. In this situation, the microfiltration retentate was richer in total proteins, lipids and carotenoids, while the ultrafiltration retentate was richer in reducing sugars and soluble carbohydrates.

Since the retentate samples were vastly richer in lipidic content, they were selected for an ethanolic extraction to extract and concentrate as many essential fatty acids as possible with potential bioactivity.

4.2.3. Ethanol extraction

The ethanolic extraction was performed on the retentate samples obtained from micro- and ultrafiltration. The ethanolic extract was then centrifuged and separated into a pellet and a supernatant sample, which were freeze-dried. These samples were then evaluated in terms of total protein (**Figure 4.29**), soluble carbohydrates (**Figure 4.30**), and total lipids (**Figure 4.31**), as well as pigment (**Figure 4.32**) and fatty acids (**Table 4.15**) profiles.

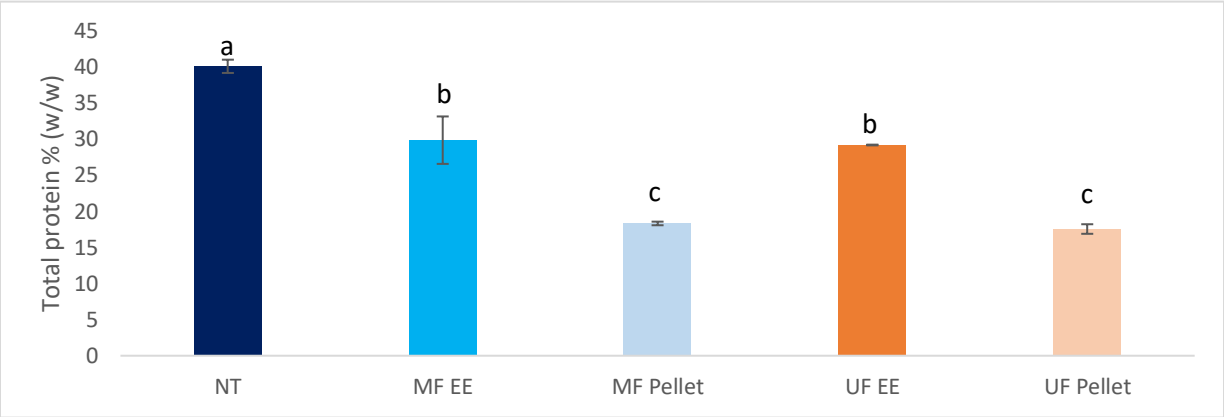

Figure 4.29: Total protein % (w/w) of the ethanolic extraction fractionation. The error bars correspond to the standard deviation of the analytical replicates (n=2). Different letters correspond to different significance levels (p<0.05). NT – Non-treated biomass; MF – Microfiltration; UF – Ultrafiltration; EE – Ethanolic Extract.

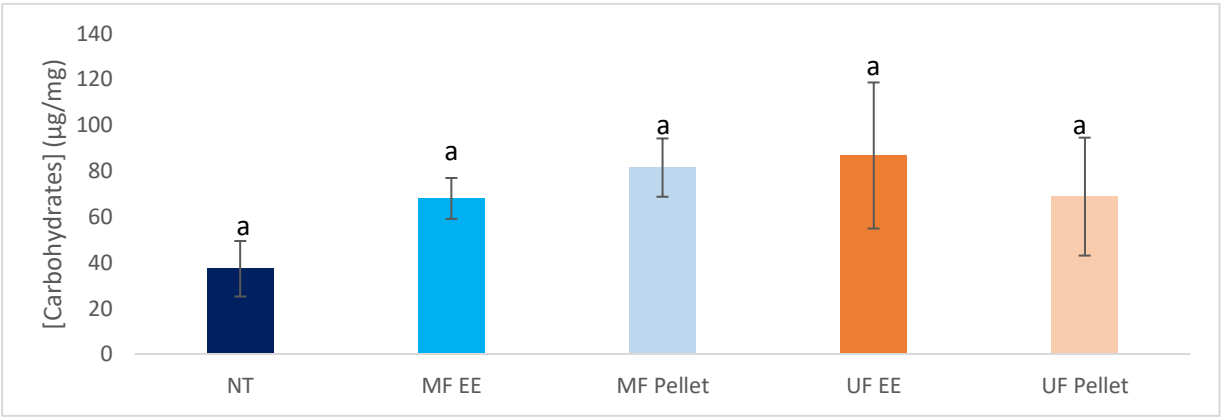

Figure 4.30: Soluble carbohydrates (mg/L) of the ethanolic extraction fractionation. The error bars correspond to the standard deviation of the analytical replicates (n=2). Different letters correspond to different significance levels (p<0.05). NT – Non-treated biomass; MF – Microfiltration; UF – Ultrafiltration; EE – Ethanolic Extract.

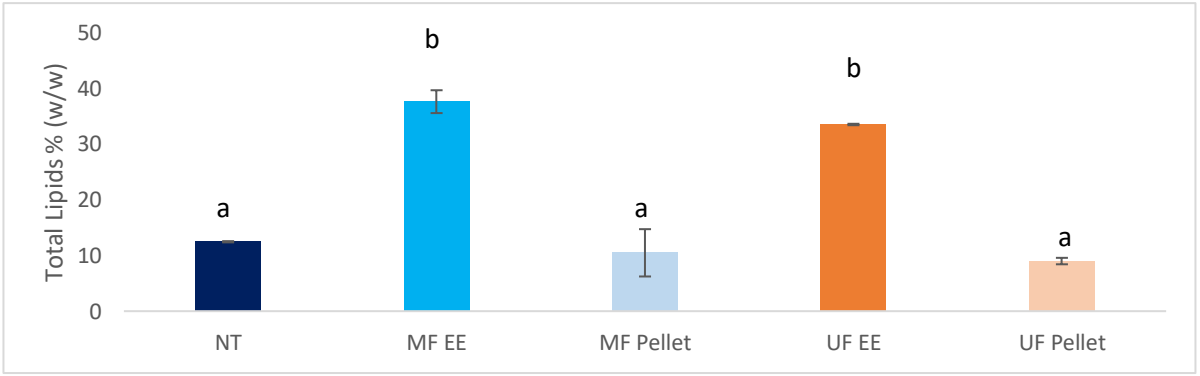

Figure 4.31: Total lipids % (w/w) of the ethanolic extraction fractionation. The error bars correspond to the standard deviation of the analytical replicates (n=2). Different letters correspond to different significance levels (p<0.05). NT – Non-treated biomass; MF – Microfiltration; UF – Ultrafiltration; EE – Ethanolic Extract.

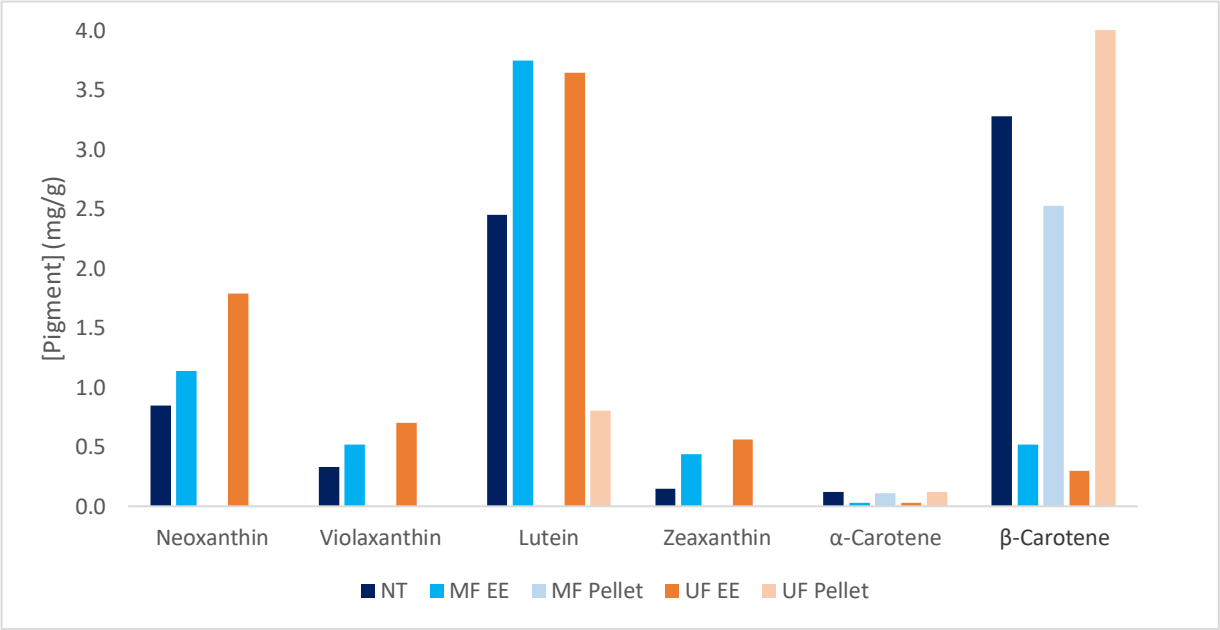

Figure 4.32: Pigment profile (mg/g) of the ethanolic extraction fractionation. NT – Non-treated biomass; MF – Microfiltration; UF – Ultrafiltration; EE – Ethanolic Extract.

Table 4.15: Fatty acid profile of *Raphidonema monicae*. Values indicated as total FAME percentage ± standard deviation (n=2). Different letters correspond to different significance levels (p<0.05). n.d. - not detected; NT – Non-Treated biomass; MF – Microfiltration; UF – Ultrafiltration; EE – Ethanolic Extract.

Fatty acid (%)	Fatty acid name	NT	MF EE	UF EE	MF Pellet	UF Pellet
C14:0	**Tetradecanoic**	1.56±0.01^{a}	1.69±0.01^{a}	1.64±0.05^{a}	1.22±0.00^{a}	1.24±0.57^{a}
C16:0	**Hexadecanoic**	14.44±0.18^{a}	14.51±0.30^{a}	14.76±0.43^{a}	12.61±0.06^{a}	16.34±5.53^{a}
C18:0	**Octadecanoic**	0.23±0.12^{a}	0.39±0.31^{a}	0.19±0.02^{a}	0.70±0.14^{a}	1.36±1.24^{a}
C24:0	**Tetracosanoic**	0.58±0.12^{a}	0.51±0.01^{a}	0.49±0.05^{a}	0.93±0.29^{a}	n.d.
∑ SFA		**16.81±0.42^{a}**	**17.10±0.64^{a}**	**17.08±0.55^{a}**	**15.46±0.50^{a}**	**18.93±7.34^{a}**
C16:1*n*-7	**Hexadecenoic**	0.19±0.01^{a}	0.82±0.00^{b}	0.81±0.02^{b}	0.17±0.01^{a}	0.38±0.03^{ab}
C18:1*n*-9c	**Octadecenoic**	1.29±0.02^{a}	1.18±0.00^{a}	1.17±0.04^{a}	1.15±0.03^{a}	1.11±0.10^{a}
C20:1*n*-9	**Eicosenoic**	1.02±0.01^{a}	1.06±0.01^{a}	1.06±0.03^{a}	1.06±0.01^{a}	1.07±0.01^{a}
C24:1*n*-9	**Tetracosenoic**	0.98±0.15^{ab}	1.02±0.11^{ab}	0.85±0.12^{a}	1.37±0.10^{b}	n.d.
∑ MUFA		**3.47±0.19^{ab}**	**4.09±0.12^{a}**	**3.90±0.20^{ab}**	**3.75±0.15^{ab}**	**2.55±0.44^{b}**
C16:2*n*-6	**Hexadecadienoate**	6.50±0.01^{a}	7.55±0.26^{b}	7.38±0.08^{b}	4.43±0.03^{c}	4.00±0.12^{c}
C16:3*n*-3	**Hexadecatrienoate**	4.78±0.32^{a}	4.96±0.13^{a}	4.90±0.05^{a}	3.52±0.04^{b}	3.10±0.18^{b}
C16:4*n*-3	**Hexadecatetraenoate**	13.60±0.03^{a}	13.29±0.29^{a}	13.33±0.17^{a}	11.65±0.40^{b}	10.81±0.06^{b}
C18:2*n*-6	**Octadecadienoic**	15.59±0.21^{ab}	16.27±0.25^{b}	16.23±0.18^{b}	14.48±0.52^{ab}	13.56±1.20^{b}
C18:3*n*-3*α*	**Octadecatrienoic**	14.59±0.17^{a}	14.30±0.15^{a}	14.34±0.31^{a}	13.56±0.64^{a}	13.49±1.25^{a}

C18:3*n*-6γ	**Octadecatrienoic**	1.07±0.02[a]	1.08±0.02[a]	1.08±0.04[a]	1.27±0.01[b]	1.09±0.06[a]
C18:4*n*-3	**Octadecatetraenoic**	3.48±0.04[ab]	3.38±0.06[b]	3.40±0.05[b]	4.12±0.03[c]	3.68±0.10[a]
C20:2*n*-6	**Eicosadinoic**	0.34±0.02[a]	0.36±0.06[a]	0.33±0.09[a]	0.41±0.10[a]	0.23±0.32[a]
C20:3*n*-6	**Eicosatrinoic**	1.20±0.02[a]	1.19±0.01[a]	1.20±0.02[a]	1.61±0.07[b]	1.53±0.04[b]
C20:4*n*-6	**Eicosatetranoic**	5.60±0.05[a]	5.10±0.02[a]	5.22±0.14[a]	7.98±0.51[b]	7.83±0.77[b]
C20:5*n*-3	**Eicosapentanoic**	12.86±0.01[ab]	11.34±0.08[b]	11.61±0.12[b]	17.76±0.79[ac]	19.20±3.26[c]
∑ PUFA		**79.71±0.90[a]**	**78.81±1.35[a]**	**79.03±1.26[a]**	**80.79±3.45[a]**	**78.51±7.38[a]**
∑n-3		**49.30±0.58[a]**	**47.27±0.72[a]**	**47.58±0.70[a]**	**50.61±1.90[a]**	**50.28±4.86[a]**
∑n-6		**30.41±0.32[a]**	**31.54±0.63[a]**	**31.45±0.56[a]**	**30.18±1.55[a]**	**28.23±2.52[a]**
∑n-6/∑n-3		**0.62**	**0.67**	**0.66**	**0.60**	**0.56**
MUFA/SFA		**0.21**	**0.24**	**0.23**	**0.24**	**0.13**
PUFA/SFA		**4.74**	**4.61**	**4.63**	**5.23**	**4.15**

Regarding protein content (**Figure 4.29**), a decrease was observed in the supernatant and pellet obtained from the ethanolic extraction. This was expected, as noticed earlier in the membrane fractionation, that most protein content was found in the permeate. Since the retentate used for the ethanolic extract was already poor in protein content, the fractions richer in protein were the permeates. Furthermore, no significant differences were found between ethanolic extractions or pellet samples of micro- or ultrafiltration. These results go in accordance with what was noticed in the membrane filtration biochemical analysis, where both micro- and ultrafiltration retentates had a similar protein content, and given the ethanolic extract was equal between both retentates, the total protein content of both pellet and supernatant was expected to be similar. However, studies have found that ethanol solubility differs in proteins, depending on their biochemical composition [144,145]. This could potentially explain why the protein distribution was slightly higher in the ethanolic extract samples.

In relation to the carbohydrate content (**Figure 4.30**), no significant differences were found between any of the samples in this biochemical analysis implying that the carbohydrate content did not significantly change between the original raw biomass and the ethanolic extract fractions produced from the micro- and ultrafiltration retentates. This was unexpected, as it is reported in literature that most carbohydrates often precipitate the higher the ethanol concentration in solution [146]. Nevertheless, other studies have also revealed that some carbohydrates are more soluble in ethanol [147,148].

As mentioned before, one of the main reasons for doing an ethanolic extraction in the retentate, was the higher content in total lipids compared to the permeate. The idea was that the ethanolic extraction would contribute to concentrating the lipid content in the supernatant samples of this extraction. As was expected, bearing in mind that most lipids are soluble in ethanol, both ethanolic extract (EE) samples obtained by micro- (MF) and ultrafiltration (UF) had an increase in total lipid content (**Figure 4.31**), in comparison with the non-treated biomass (NT). This increase was significant, with an increase in content from 12.45±0.11% (NT) to 37.59±2.05% and 33.49±0.13% (MF EE and UF EE respectively). However, no significant differences were found between the ethanolic extract of the samples processed by micro- and ultrafiltration. This was expected, as observed earlier in the membrane filtration biochemical analysis, since both retentates had a similar lipid content. Considering the ethanolic extraction method was equal between both retentates, since their lipid content was similar, the final separation between supernatant and pellet was conjectured to be similar. This was observed when analyzing the fatty acid profile (**Table 4.*15***), where the relative fatty acid distribution remained relatively unchanged between the non-treated and treated samples.

Within *R. monicae* biomass, 19 fatty acids were identified, including saturated (SFA), monounsaturated (MUFA) and polyunsaturated fatty acids (PUFA). Overall, the fatty acid profile was similar to that previously described for *R. monicae* [107], with the addition of 5 new fatty acids, including C16:2, C16:3, C16:4, C18:3*n*-3 and C18:4. Regarding SFA and MUFA, it was theorized that their presence in the fatty acid profile was disadvantageous for the purpose of these fractions, as both SFA and MUFA have been found in other studies to possess pro-inflammatory properties [149]. A higher content in MUFA is preferred over SFA as other studies have indicated that MUFA can replace SFA in diets, possessing significantly less pro-inflammatory properties [150]. Considering that, the fractions that contain the highest MUFA/SFA ratio would have considerably fewer negative effects if they were to be used as ingredients for feed. Concerning the fatty acid distribution ratio (**Table 4.15**), the micro- and ultrafiltration ethanolic extractions and microfiltration pellet would be ideal fractions (0.24, 0.23 and 0.24 respectively), when compared to the non-treated (0.20) and ultrafiltration pellet (0.11) samples. This implies that the ethanolic extracts were significantly less inflammatory properties than the original non-treated *R. monicae* biomass.

Nevertheless, the main focus was to extract PUFA, as these have been found in other studies to have several beneficial effects on animal health, particularly as inflammation modulators [121]. These include several *n*-3 fatty acids such as ALA (C18:3α), and EPA (C20:5), with the latter possessing extensive anti-inflammatory properties [151]. However, other studies have found that some PUFA, particularly *n*-6 fatty acids, were correlated with pro-inflammatory and pro-thrombotic properties, as well as promoting other cell harmful effects [152,153]. As such, and as recommended by WHO, the lower the ∑n-6/∑n-3 ratio, the more beneficial the fraction would be as food or feed [154,155]. Regarding *R. monicae* PUFA distribution ratio (**Table 4.15**), the fractions possessing the lowest ∑n-6/∑n-3 ratio were the micro- and ultrafiltration pellets, with a ratio of 0.60 and 0.56, respectively, significantly lower than the non-treated biomass, with a ratio of 0.62, implying the ethanolic extraction was successful in producing fractions substantially more beneficial in terms of dietary ingredients. On the other hand, the micro and ultrafiltration ethanolic extracts had a higher ratio than the non-treated biomass, of 0.67 and 0.66 respectively, suggesting that these fractions in terms of health benefits might be less beneficial than the original non-treated biomass.

A more detailed look at the PUFA profile of *R. monicae* (**Table 4.15**) revealed that it has a fatty acid profile composed of 79.71±0.90% PUFA, a value significantly higher than those found in other microalgae, including *Chlorella* sp. (55.52%), *Scenedesmus dimorphus* (39.03%), *Phaeodactylum tricornutum* (14.90%) [156]. Its profile was also found to remain similar, irrespective of the extraction, suggesting all extractions were just as efficient in recovering in equal amounts all fatty acids identified in the profile. However, while *R. monicae* was found to have a fatty acid profile enriched in PUFA, further studies are recommended to assess if this microalga has a sufficient concentration of fatty acids to valorize the biomass. Suzuki *et al.* (2019) found that this microalgae under stress can produce up to 271.9 mg/g (DW). This study would suggest that *R. monicae* would be a good source of PUFA, as its concentration is close to that of *Tisochrysis lutea*, a microalga known for its large abundance in fatty acids, up to 320 mg/g (DW) [102,157].

By further analyzing the PUFA profile of *R. monicae* (**Table 4.15**), the presence of a few rather influential fatty acids in animal health was found. These included two *n*-3 fatty acids, C18:3α (ALA) and C20:5 (EPA), and 3 *n*-6 fatty acids, C18:2 (LA), C18:3γ (GLA) and C20:4 (ARA). Regarding ALA, it is an essential PUFA, and is recognized for its health benefits, particularly as a

precursor for the biosynthesis of other high-value bioactive fatty acids, including EPA and DHA [158]. It was found to make up 14.59±0.17% of the total fatty acid profile of this microalga. Regarding EPA, this fatty acid is an essential PUFA known for its anti-inflammatory properties and plays a role in endothelium integrity [108]. This PUFA was quantified in large amounts in this microalga, making up 12.86±0.01% of the total fatty acid profile. LA, meanwhile, is an essential major fatty acid found in substantial amounts in plant oils, acting as an important precursor to other important long-chain PUFA, such as ARA [108]. It accounted for 15.69±0.21% of the total fatty acid profile. Regarding ARA, this LC-PUFA plays a role as a precursor of prostaglandins and many other eicosanoids, influences cellular membrane fluidity and flexibility, acts as a lipid secondary messenger in cell-to-cell signaling, and is an inflammatory mediator (pro-inflammatory) [108]. It made up to 5.60±0.05% of the total fatty acid profile. GLA is a PUFA frequently used as a nutritional supplement, known for its anti-inflammatory and anti-proliferative effects [108]. This PUFA was identified in *R. monicae* biomass at 1.07±0.02% of the total fatty acid profile. These results imply *R. monicae* is rich in EPA, ALA and LA, although other microalgae have been found to have similar or even higher EPA, ALA and/or LA contents, such as *Nannochloropsis* sp. with an EPA content of 34%, or *Phaeodactylum tricornutum* with an EPA content of 30% [159].

When reviewing **Figure 4.32**, it was found that the ethanolic extraction fractions produced from *R. monicae* biomass were significantly rich in neoxanthin (0.85 mg/g), violaxanthin (0.33 mg/g), lutein (2.45 mg/g), zeaxanthin (0.15 mg/g), α-carotene (0.12 mg/g) and β-carotene (3.28 mg/g). *Chlorella vulgaris*, a green microalga, was found in a study to have a pigment profile similar to *R. monicae*, containing neoxanthin, violaxanthin, lutein, zeaxanthin and β-carotene. However the concentrations were considerably lower (0.09, 0.04, 1.28, 0.01 and 0.28 mg/g, respectively) [160]. *Scenedesmus obliquus*, another green microalga, also had a pigment profile similar to *R. monicae*, containing neoxanthin, violaxanthin and lutein [161]. However, its concentrations were significantly lower than in *R. monicae* (approximately 0.20, 0.15, 1.10 and 0.30 mg/g, respectively) These findings suggest that while *R. monicae* biomass lacks certain bioactive pigments, its value could potentially be found in a highly concentrated, although limited, pigment profile.

Regarding the significance of these pigments, it is known that neoxanthin, zeaxanthin, lutein and β-carotene possess strong antioxidant properties [109,162,163]. As such, the aim was to extract as many of these pigments as possible through fractionation methodologies. **Figure 4.32**

highlighted that, through the ethanolic extraction fractionation methodology, it was possible to concentrate these pigments in the ethanolic extract samples that underwent either micro- or ultrafiltration. Neoxanthin and zeaxanthin were found in higher quantities in the ultrafiltration ethanolic extract (1.79 and 0.56 mg/g respectively). Meanwhile, lutein and β-carotene were found in higher amounts in the microfiltration ethanolic extract (3.75 and 0.52 mg/g, respectively). It was also found that this ethanolic extraction methodology could concentrate neoxanthin, violaxanthin, lutein and zeaxanthin in the ethanolic extracts, when compared with the non-treated biomass sample. However, β-carotene was found to be concentrated in higher amounts in the pellet fraction of the ethanolic extract for the ultrafiltration sample. β-carotene was found mainly in the pellet and not in the ethanolic extract because this pigment is only soluble in ethanol if degraded, and no treatments were used that specifically targeted that molecule [164].

Overall, *R. monicae* is enriched in multiple bioactive pigments, in potentially higher concentrations than other types of green microalgae, although it lacks the presence of other just as important pigments (e.g., fucoxanthin and astaxanthin). Nevertheless, through the pipeline optimized in this methodology, it was possible to extract and concentrate these compounds in multiple high-value fractions.

4.3. Intestinal response

In order to assess seabream's intestinal response to the produced algae fractions, an *ex-vivo* intestinal explant assay was carried out, while attempting to maintain the tissue's architecture to mimic *in-vivo* conditions. The transcriptional response regarding epithelial integrity, immunostimulation and antioxidant capacity was chosen to assess the intestinal response. Three controls were included in this assay, including a neutral control composed only of culture medium, and two positive controls, composed of either β-glucan or H_2O_2 in culture medium. Furthermore, the algae fractions were tested in two concentrations (low and high). The dried fractions low concentration consisted of 5 mg of fraction resuspended in 1 mL of culture medium and high concentration consisted of 20 mg of fraction resuspended in 1 mL of culture medium. The liquid fractions (permeates) low concentration consisted of 50 µL of the sample while high concentration consisted of 100 µL of the sample.

4.3.1. Epithelial integrity response

Regarding the evaluation of epithelial integrity, *OCL* and *TJP2* genes were selected for analysis. The *OCL* gene was selected for analysis due to its biological role in stabilizing the epithelial integrity of the intestinal epithelial cells [165]. It codes for occludin, a 65 kDa tetraspan integral membrane protein, which contributes to the stability of tight junctions and optimal barrier function [165]. Meanwhile, the *TJP2* gene was selected for analysis due to its biological role in intestinal epithelial integrity, coding for a MAGUK family member protein that participates as a tight junction adaptor and regulator of the adherens junctions [166]. The influence of the fractions on the transcriptional profile for *OCL* and *TJP2* can be found in **Figure 4.33** and **Figure 4.34**, respectively.

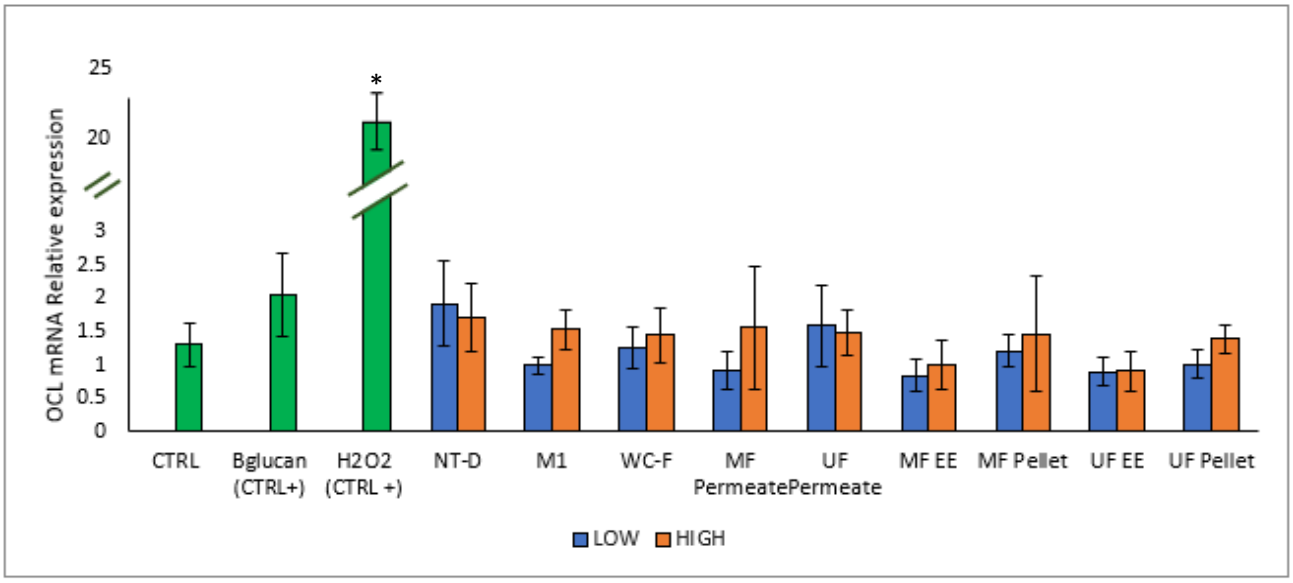

Figure 4.33: mRNA relative expression of the *OCL* gene. The error bars correspond to the standard error of the biological replicates (n=3). "*" indicates significant variation in comparison with CTRL (p<0.05). NT-D – Non-treated batch from disruption assay; NT-F – Non-treated batch from fractionation assay; MF – Microfiltration; UF – Ultrafiltration; EE – Ethanolic Extract.

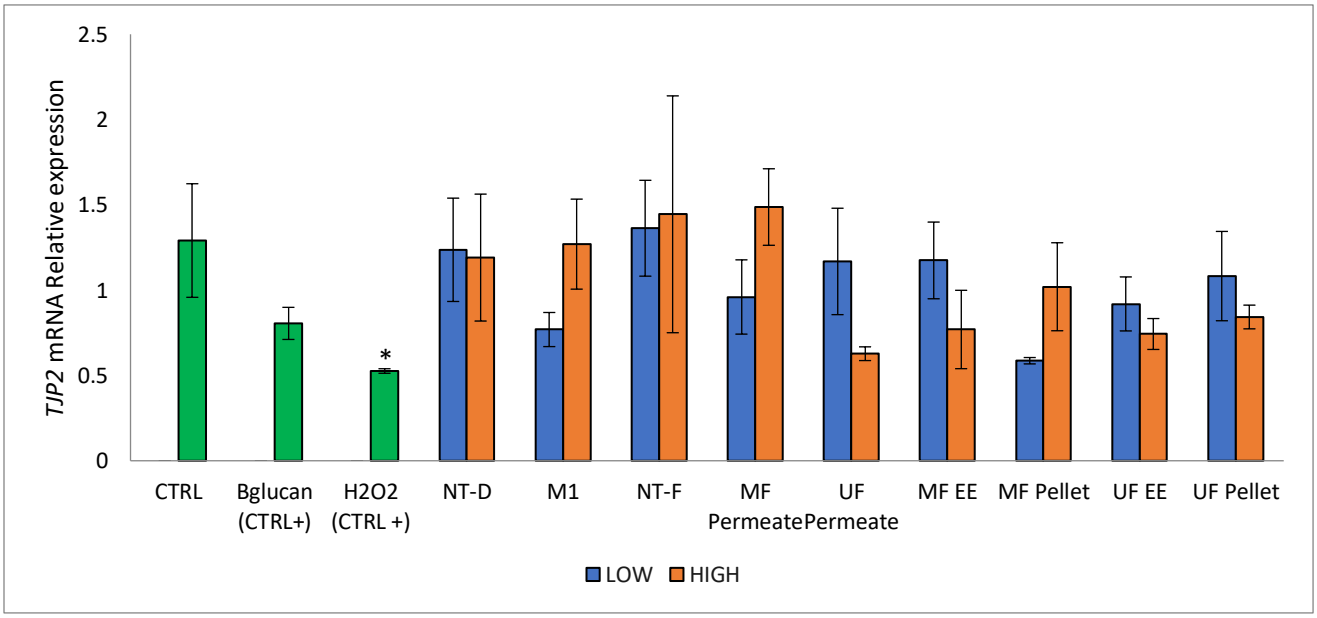

Figure 4.34: mRNA relative expression of the *TJP2* gene. The error bars correspond to the standard error of the biological replicates (n=3). "*" indicates significant variation in comparison with CTRL (p<0.05). NT-D – Non-treated batch from disruption assay; NT-F – Non-treated batch from fractionation assay; MF – Microfiltration; UF – Ultrafiltration; EE – Ethanolic Extract.

When analyzing the transcriptional response of *OCL* (**Figure 4.33**), it was found that none of the treatments, irrespective of the concentration, significantly influenced its expression. Similarly to the transcriptional response of *OCL* (**Figure 4.33**), *TJP2* (**Figure 4.34**) was found to have no significant differences in all treatments, irrespective of the concentration. It was also observed that for both genes, only one of the two positive controls (H_2O_2) significantly influenced their expression, reducing it.

4.3.2. Antioxidant response

Regarding the assessment of antioxidant response, the *GPx*, and *CAT* genes were selected for analysis. The *GPx* gene was selected as it plays a role in the defense against reactive oxygen species (ROS), coding for a protein, glutathione peroxidase, with known strong antioxidant properties, responsible for the removal of hydroperoxides formed in cells [167,168]. The *CAT* gene was selected, as it codes for catalase, a protein with strong antioxidant properties known to neutralize ROS, especially hydrogen peroxide [169]. The influence of the fractions on the transcriptional profile for *GPx*, and *CAT* can be found in **Figure 4.35** and **Figure 4.36**, respectively.

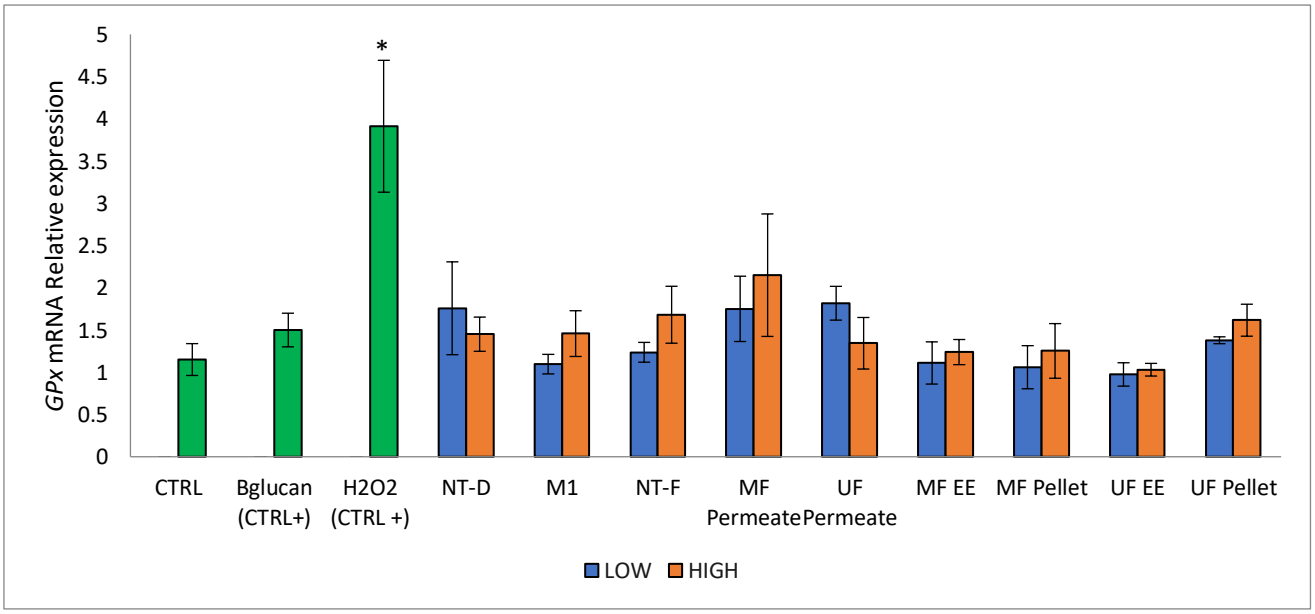

Figure 4.35: mRNA relative expression of the *GPx* gene. The error bars correspond to the standard error of the biological replicates (n=3). "*" indicates significant variation in comparison with CTRL (p<0.05). NT-D – Non-treated batch from disruption assay; NT-F – Non-treated batch from fractionation assay; MF – Microfiltration; UF – Ultrafiltration; EE – Ethanolic Extract.

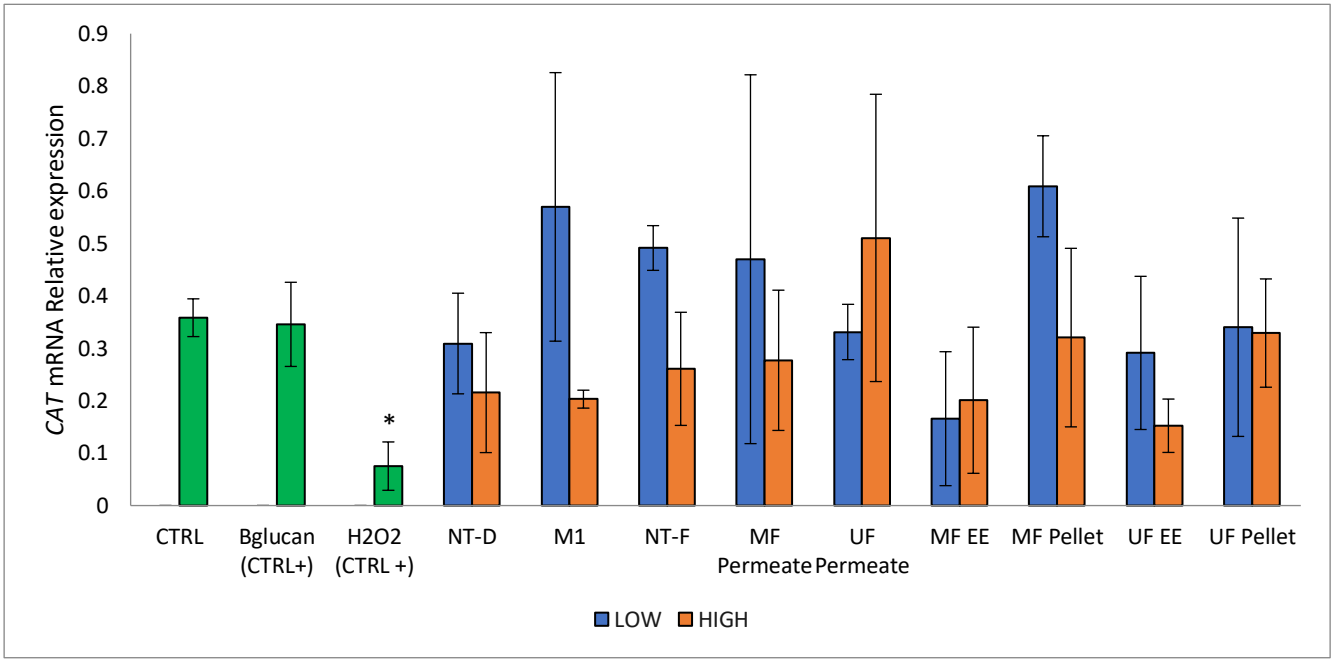

Figure 4.36: mRNA relative expression of the *CAT* gene. The error bars correspond to the standard error of the biological replicates (n=3). "*" indicates significant variation in comparison with CTRL (p<0.05). NT-D – Non-treated batch from disruption assay; NT-F – Non-treated batch from fractionation assay; MF – Microfiltration; UF – Ultrafiltration; EE – Ethanolic Extract.

In regards to the transcriptional response of *GPx* (**Figure 4.35**), a non-significant trend was observed suggesting that the treatments up-regulated the transcriptional response of this gene. This behavior was similarly observed in the transcriptional response of *CAT* (**Figure 4.36**), which also displayed a non-significant trend up-regulating the transcriptional response of this gene.

However, a more detailed analysis revealed that none of the treatments, irrespective of the concentration, significantly influenced their expression. It was also noticed that for the transcription response of both genes, only one of the positive controls (H_2O_2) significantly influenced the response, decreasing it.

4.3.3. Immunostimulation response

Regarding the assessment of immune defense, the *COX2*, *and Il1B* genes were selected for analysis. The gene *COX2* was selected for analysis due to its biological role as an inflammatory modulator agent, coding for an enzyme (cyclooxygenase 2) with pro-inflammatory properties, responsible for converting arachidonic acid to prostaglandins, which play a key role in the generation of the inflammatory response [170–172]. The *IL1B* gene was selected as it participates in immune-mediated responses, coding for interleukin-1, a cytokine with potent inflammatory

properties [173]. The influence of the fractions on the transcriptional profile for *COX2*, and *Il1B* can be found in **Figure 4.37** and **Figure 4.38** respectively.

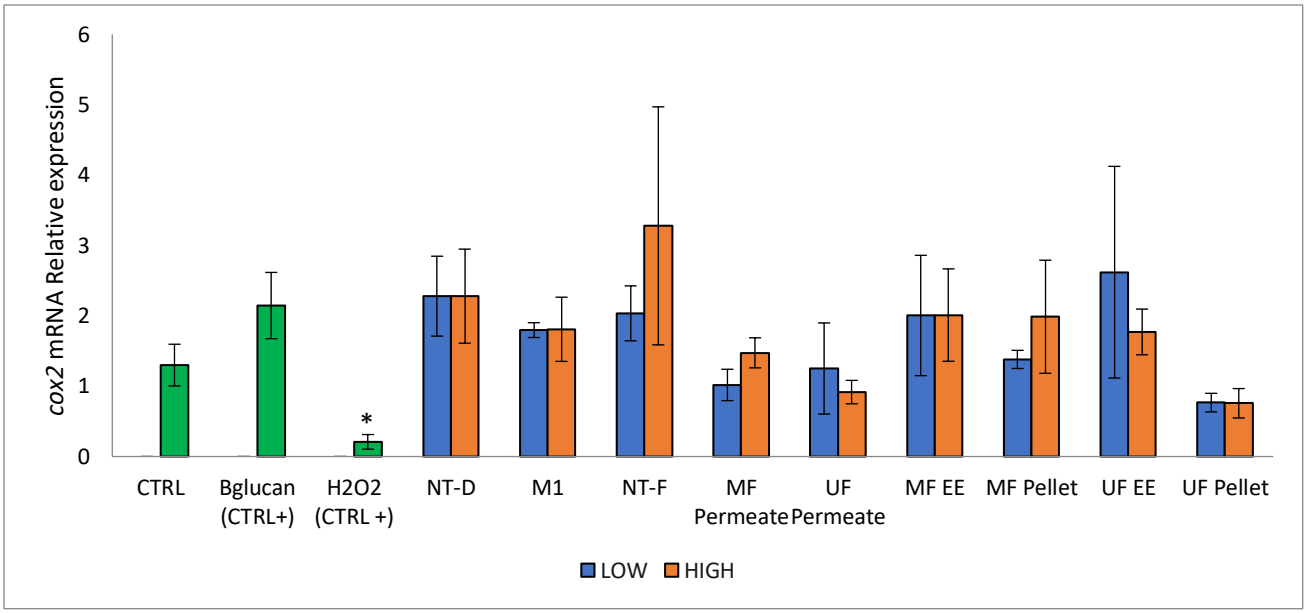

Figure 4.37: mRNA relative expression of the *COX2* gene. The error bars correspond to the standard error of the biological replicates (n=3). "*" indicates significant variation in comparison with CTRL (p<0.05). NT-D – Non-treated batch from disruption assay; NT-F – Non-treated batch from fractionation assay; MF – Microfiltration; UF – Ultrafiltration; EE – Ethanolic Extract.

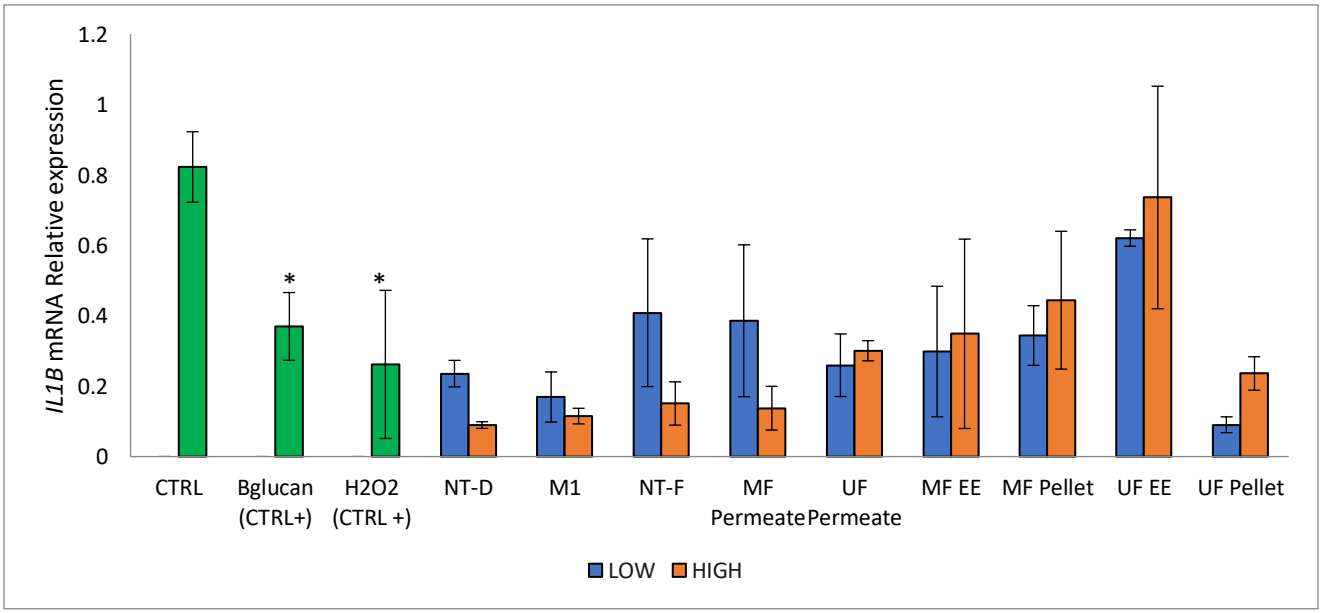

Figure 4.38: mRNA relative expression of the *IL1B* gene. The error bars correspond to the standard error of the biological replicates (n=3). "*" indicates significant variation in comparison with CTRL (p<0.05). NT-D – Non-treated batch from disruption assay; NT-F – Non-treated batch from fractionation assay; MF – Microfiltration; UF – Ultrafiltration; EE – Ethanolic Extract.

When analyzing the response of *IL1B* (**Figure 4.38**), and *COX2* (**Figure 4.37**), a trend was observed in IL1B, regarding the downregulation of the transcriptional response. However, a closer analysis of this response revealed that this trend was not significant, as none of the treatments, irrespective of the concentration, displayed a significant difference when compared with the control samples. Furthermore, only *IL1B* had a significant response for both positive controls, decreasing its expression. On the other hand, *COX2* demonstrated no significant responses or trends to the tested fractions, and only had a significant response to one of the positive controls (H_2O_2), which decreased its expression.

4.3.4. Intestinal explant response discussion

The results of this study indicate the fractions were unsuccessful in significantly up or downregulating the transcriptional response of genes related to epithelial integrity, antioxidant capacity and immunostimulation. While a clear answer as to why this happened would require further studies, given this is a preliminary trial, it was assumed that the high variability within samples of similar treatment was partially responsible for this.

A closer look to the epithelial integrity response revealed that the fractions produced in this study yielded no significant effect in the transcriptional response of genes correlated to the epithelial integrity. These results correlate with a previously reported study on epithelial integrity related genes, by Peñaranda *et al.* (2020). They found that by conducting an *ex-vivo* assay on *S. aurata* intestinal explant cultures, the exposure of the gut to an enrichened plant protein diet did not yield a significant transcriptional response for the *OCL* gene [98]. However, another study carried out by Cerezo-Ortega *et al.* (2021) observed that a diet fed to *S.* aurata with 5% of hydrolyzed *Nannochloropsis gaditana* yielded a significant change in *OCL* expression [174]. Given other studies report on the effect of ingredients on the transcriptional response of genes with a role in epithelial integrity, as this was a screening assay, further studies are required to better assess the influence of the produced fractions in epithelial stability.

In regard to the antioxidant response, it is often associated with the presence of reactive oxygen species (ROS) which induce the expression of genes coding for anti-oxidative proteins, or the presence of antioxidant molecules with regulatory capabilities [175]. In this study, both *GPx* and *CAT*, coding for proteins with a role in suppressing ROS, were observed to have a non-significant up-regulatory trend with all processed samples as compared to the respective controls.

This could potentially suggest the presence of antioxidant modulatory molecules. These results correlate to a study performed by Reis *et al.* (2021), which found that feeds enriched in *Phaeodactylum tricornutum*-derived β-glucans, upregulated the expression of *CAT* in juvenile gilthead seabream [176]. Other studies have found a correlation between the presence of bioactive ingredients with antioxidant roles and an enhanced transcriptional response of genes associated with the antioxidative response, including *CAT* and *GPx* [175,177–180]. These bioactive ingredients include certain types of carotenoids, such as β-carotene and lutein, which have been reportedly found to have ROS-scavenging and regulatory properties and can induce a stimulation in the antioxidative response of cells to oxidative stress [175,177,179,180]. Given that *Raphidonema monicae* was found possessing a carotenoid profile rich in Lutein and β-carotene, these results match the previously mentioned studies in suggesting that the fractions produced could potentially hold key bioactive ingredients with antioxidant modulatory capabilities.

In relation to the immunostimulation response, two pro-inflammatory biomarkers were monitored (*IL1B* and *COX2*). As these two genes code for pro-inflammatory proteins with a role in immunomodulation, the assessment of their transcriptional response directly correlates with the immunological status of the fish [181–183]. *IL1B* in particular demonstrated a down-regulatory non-significant trend regarding all the processed samples, when compared to the respective controls, correlating with the fatty acid profile of *R. monicae* which was found to be enriched in anti-inflammatory PUFA, such as EPA and ARA. In contradiction to this study, Carballo *et al.* (2019) observed that exposing Senegalese sole (*Solea senegalensis*) to microalgal polysaccharide-enriched extracts from *P. tricornutum* upregulated the expression of *Il1B*. In that study, it was theorized that the upregulation was due to the immunostimulant effect of the compounds found within the microalgal extracts [181]. However, another study, by Reis *et al.* (2021) found that other microalgal extracts obtained from *P. tricornutum* downregulated the expression of *Il1B*. In this study, it was thought that this was due to the immunomodulatory properties of the compounds which induced a local anti-inflammatory state in the intestinal cells, which led to a decrease in immune cell activation [176]. Given a non-significant down-regulatory trend was found in the *Il1B* transcription response analyzed in this thesis, it can be assumed that the fractions obtained from *R. monicae* could potentially hold key anti-inflammatory ingredients. With regards to the *COX2* transcriptional response, no trends were observed in the results, which would suggest that the fractions produced did not possess immunomodulating compounds that could influence the

expression of this gene in particular. However, Nayak *et al.* (2020) found that by exposing zebrafish for a month to a diet supplemented with omega-6 LC-PUFA rich *Lobosphaera incisa* biomass had an up-regulation in the expression of *COX2* [183]. Furthermore, Cerezuela *et al.* (2013) also observed that a 4-week diet supplemented with *Bacillus subtilis* biomass also up-regulated the expression of *COX2* in intestinal cells of *Sparus aurata* [182]. Given the results of these studies, it is assumed that the reason behind the absence in transcriptional response of *COX2* could be associated with the period of exposure of the intestinal explants to the fractions, which in this thesis was of 5 hours, and a longer exposure could potentially reveal the bioactivity of the produced fractions.

As these results, in general, only demonstrated non-significant trends, it was not possible to assess if the fractions had any influence in the health of the fish. As this was just a screening assay, with only 5 hours of exposure to the produced fractions, the presence of these trends, even though they were not significant, suggested that the fractions obtained from *R. monicae* could potentially modulate the health of *Sparus aurata*. However, in order to extensively assess this response, further studies are needed. It's worth noting that these *ex-vivo* trials are, however, limited in their potential to research the bioactivity of the fractions, as they presume the ingredients were not degraded while passing through the digestive tract. Therefore, further *in-vivo* studies are eventually needed once the fractions with the most bioactivity have been detected in *ex-vivo* assays [98].

5.Conclusions and future perspectives

By aiming to develop a resource-friendly and simplified optimized disruption methodology, a methodology that combined high pressure homogenization and enzymatic hydrolysis techniques was determined. This combination of methodologies achieved 71% disruption efficiency by initially exposing the biomass to 1 cycle of HPH at 1068 bars, followed by a 90-minute enzymatic hydrolysis with alcalase at pH 8, 50 ºC. This optimized methodology increased the soluble carbohydrate and total lipid content by 2-fold and the free amino acid and soluble proteins by 5-fold. To simplify this process, the usage of carbohydrases was discarded, which could have impacted the disruption efficiency, but through the enzymatic hydrolysis optimization assay, it was found that the absence of carbohydrases did not significantly influence cell disruption, as a treatment with only alcalase or with alcalase and viscozyme produced similar disruption efficiencies, of approximately 50%.

By further fractionating the disrupted biomass through pH shifting, micro- and ultrafiltration, and ethanolic extraction, it was possible to produce 6 fractions enriched in several high-value compounds. Regarding pigment content, it was possible to extract neoxanthin, lutein, zeaxanthin α-carotene and β-carotene up to 1.79, 3.75, 0.56, 0.12 and 9.84 mg/g, respectively. This is an interesting result, as these carotenoids are known for their health benefits. Furthermore, these values were found to be higher than in the original non-treated biomass, implying that it was possible to concentrate the pigments through the fractionation methodology. Regarding PUFA content, it was possible to extract and maintain the fatty acid profile relative abundance, especially of EPA, ALA, LA, ARA and GLA. Overall, fractions enriched in several compounds known for their beneficial bioactive properties in literature were obtained. It was also found that, as had been theoretically predicted, *R. monicae* is significantly enriched in certain bioactive compounds including PUFA and some pigments. However, further analysis would have to be done to determine if that reason stemmed from the environmental conditions in which this microalga is known to grow in.

Regarding the intestinal mucosal response, it was not possible to assess if the fractions had any influence in the health of the fish, as the variability within the same treatments was found to be exacerbated. However, as there was clearly a trend in the results, given this was just a

preliminary study, the potential remains for the usage of this microalga as feed ingredients in the improvement of fish health.

In conclusion, the results produced in this thesis suggest that *R. monicae* is a microalga enriched in high-value compounds. As they showed a trend to improve the fish health via a transcriptional response evaluation assay, this microalga remains a potential candidate for biomass incorporation in food and feed as well as being a source of certain high-value compounds, particularly of PUFA and bioactive pigments, through a simplified processing pipeline. Nevertheless, further *ex-vivo* and *in-vivo* studies are needed to assess if these fractions are valuable to be used as feed ingredients, as they demonstrate the potential to improve fish health.

References

[1] Khan, M.I., Shin, J.H. and Kim, J.D. (2018) The promising future of microalgae: Current status, challenges, and optimization of a sustainable and renewable industry for biofuels, feed, and other products. *Microbial Cell Factories*, BioMed Central Ltd. **17**. https://doi.org/10.1186/s12934-018-0879-x

[2] Lehmuskero, A., Skogen Chauton, M. and Boström, T. (2018) Light and photosynthetic microalgae: A review of cellular- and molecular-scale optical processes. *Progress in Oceanography*, Pergamon. **168**, 43–56. https://doi.org/10.1016/J.POCEAN.2018.09.002

[3] Baslam, M., Mitsui, T., Hodges, M., Priesack, E., Herritt, M.T., Aranjuelo, I. et al. (2020) Photosynthesis in a Changing Global Climate: Scaling Up and Scaling Down in Crops. Front Plant Sci. Frontiers Media S.A. https://doi.org/10.3389/fpls.2020.00882

[4] Kukwa, D.T. and Chetty, M. (2021) Microalgae: The Multifaceted Biomass of the 21st Century. *IntechOpen*, IntechOpen. https://doi.org/10.5772/intechopen.94090

[5] Ampofo, J. and Abbey, Lord. (2022) Microalgae: Bioactive Composition, Health Benefits, Safety and Prospects as Potential High-Value Ingredients for the Functional Food Industry. Foods. MDPI. https://doi.org/10.3390/foods11121744

[6] Show, P.L. (2022) Global market and economic analysis of microalgae technology: Status and perspectives. *Bioresource Technology*, Elsevier. **357**, 127–329. https://doi.org/10.1016/J.BIORTECH.2022.127329

[7] Lucakova, S., Branyikova, I. and Hayes, M. (2022) Microalgal Proteins and Bioactives for Food, Feed, and Other Applications. Applied Sciences. MDPI. https://doi.org/10.3390/app12094402

[8] Barka, A. and Blecker, C. (2016) Microalgae as a potential source of single-cell proteins. A review. *Biotechnology, Agronomy and Society and Environment*, **20**, 427–36. https://doi.org/10.25518/1780-4507.13132

[9] Udayan, A., Pandey, A.K., Sirohi, R., Sreekumar, N., Sang, B.I., Sim, S.J. et al. (2022) Production of microalgae with high lipid content and their potential as sources of nutraceuticals. *Phytochemistry Reviews*, Springer Science and Business Media B.V. https://doi.org/10.1007/s11101-021-09784-y

[10] Schulze, C., Strehle, A., Merdivan, S. and Mundt, S. (2017) Carbohydrates in microalgae: Comparative determination by TLC, LC-MS without derivatization, and the photometric thymol-sulfuric acid method. *Algal Research*, Elsevier B.V. **25**, 372–80. https://doi.org/10.1016/j.algal.2017.05.001

[11] Chen, C.Y., Lee, P.J., Tan, C.H., Lo, Y.C., Huang, C.C., Show, P.L. et al. (2015) Improving protein production of indigenous microalga Chlorella vulgaris FSP-E by photobioreactor design and cultivation strategies. *Biotechnology Journal*, Wiley-VCH Verlag. **10**, 905–14. https://doi.org/10.1002/biot.201400594

[12] Sun, X.M., Ren, L.J., Zhao, Q.Y., Ji, X.J. and Huang, H. (2018) Microalgae for the production of lipid and carotenoids: A review with focus on stress regulation and adaptation. Biotechnol Biofuels. BioMed Central Ltd. https://doi.org/10.1186/s13068-018-1275-9

[13] Cheng, D., Li, D., Yuan, Y., Zhou, L., Li, X., Wu, T. et al. (2017) Improving carbohydrate and starch accumulation in Chlorella sp. AE10 by a novel two-stage process with cell dilution. *Biotechnology for Biofuels*, BioMed Central Ltd. **10**. https://doi.org/10.1186/s13068-017-0753-9

[14] Papapolymerou, G., Karapanagiotidis, I.T., Katsoulas, N. and Metsoviti, M.N. (2019) Current and Potential Applications of Microalgae: A Mini Review. *Oceanography & Fisheries*, Juniper Publishers. **11**. https://doi.org/10.19080/ofoaj.2019.11.555811

[15] Plöhn, M., Spain, O., Sirin, S., Silva, M., Escudero-Oñate, C., Ferrando-Climent, L. et al. (2021) Wastewater treatment by microalgae. *Physiologia Plantarum*, John Wiley and Sons Inc. **173**, 568–78. https://doi.org/10.1111/ppl.13427

[16] Benedetti, M., Vecchi, V., Barera, S. and Dall'Osto, L. (2018) Biomass from microalgae: The potential of domestication towards sustainable biofactories. *Microbial Cell Factories*, BioMed Central Ltd. **17**. https://doi.org/10.1186/s12934-018-1019-3

[17] Kusmayadi, A., Leong, Y.K., Yen, H.W., Huang, C.Y. and Chang, J.S. (2021) Microalgae as sustainable food and feed sources for animals and humans – Biotechnological and environmental aspects. *Chemosphere*, Pergamon. **271**, 129800. https://doi.org/10.1016/J.CHEMOSPHERE.2021.129800

[18] Oliveira, A.P.F. and Bragotto, A.P.A. (2022) Microalgae-based products: Food and public health. *Future Foods*, Elsevier. **6**, 100–57. https://doi.org/10.1016/J.FUFO.2022.100157

[19] Yarkent, Ç., Gürlek, C. and Oncel, S.S. (2020) Potential of microalgal compounds in trending natural cosmetics: A review. *Sustainable Chemistry and Pharmacy*, Elsevier. **17**, 100–304. https://doi.org/10.1016/J.SCP.2020.100304

[20] Nicoletti, M. (2016) Microalgae nutraceuticals. *Foods*, MDPI AG. **5**, 1–13. https://doi.org/10.3390/foods5030054

[21] Osorio-Reyes, J.G., Valenzuela-Amaro, H.M., Pizaña-Aranda, J.J.P., Ramírez-Gamboa, D., Meléndez-Sánchez, E.R., López-Arellanes, M.E. et al. (2023) Microalgae-Based Biotechnology as Alternative Biofertilizers for Soil Enhancement and Carbon Footprint Reduction: Advantages and Implications. *Marine Drugs*, MDPI. **21**. https://doi.org/10.3390/md21020093

[22] Wijffels, R.H. and Barbosa, M.J. (2010) An outlook on microalgal biofuels. *Science*, **329**, 796–9. https://doi.org/10.1126/science.1189003

[23] Moreno Osorio, J.H., Pollio, A., Frunzo, L., Lens, P.N.L. and Esposito, G. (2021) A Review of Microalgal Biofilm Technologies: Definition, Applications, Settings and Analysis. *Frontiers in Chemical Engineering*, Frontiers Media SA. **3**. https://doi.org/10.3389/fceng.2021.737710

[24] Khavari, F., Saidijam, M., Taheri, M. and Nouri, F. (2021) Microalgae: therapeutic potentials and applications. *Molecular Biology Reports*, Springer Science and Business Media B.V. **48**, 4757–65. https://doi.org/10.1007/s11033-021-06422-w

[25] Cinar, S.O., Chong, Z.K., Kucuker, M.A., Wieczorek, N., Cengiz, U. and Kuchta, K. (2020) Bioplastic production from microalgae: A review. *International Journal of Environmental Research and Public Health*, MDPI AG. **17**. https://doi.org/10.3390/ijerph17113842

[26] Mildner, S.-A., Lauster, G. and Wodni, W. (2011) Scarcity and Abundance Revisited: A Literature Review on Natural Resources and Conflict. *International Journal of Conflict and Violence*, **5**, 155–72.

[27] Henly-Shepard, S., K. Iwashita, D., Caddell, R., Miller, K., Lepczyk, C.A., Bergstrom, R. et al. (2013) A Review of Solutions and Challenges to Addressing Human Population Growth and Global Climate Change. *The International Journal of Climate Change: Impacts and Responses*, Common Ground Research Networks. **4**, 147–72. https://doi.org/10.18848/1835-7156/cgp/v04i03/37178

[28] Abbass, K., Qasim, M.Z., Song, H., Murshed, M., Mahmood, H. and Younis, I. (2022) A review of the global climate change impacts, adaptation, and sustainable mitigation measures. *Environmental Science and Pollution Research*, Springer Science and Business Media Deutschland GmbH. **29**, 42539–59. https://doi.org/10.1007/s11356-022-19718-6

[29] Araújo, R., Calderón, F.V., López, J.S., Azevedo, I.C., Bruhn, A., Fluch, S. et al. (2021) Current Status of the Algae Production Industry in Europe: An Emerging Sector of the Blue Bioeconomy. *Frontiers in Marine Science*, Frontiers Media S.A. **7**. https://doi.org/10.3389/fmars.2020.626389

[30] Reis, A. and Silva, T.L. (2016) Scale-up Problems for the Large Scale Production of Algae. *Algal Biorefinery: An Integrated Approach*, Springer International Publishing. p. 125–49. https://doi.org/10.1007/978-3-319-22813-6_6

[31] Nur, M.M.A. and Buma, A.G.J. (2019) Opportunities and Challenges of Microalgal Cultivation on Wastewater, with Special Focus on Palm Oil Mill Effluent and the Production of High Value Compounds. *Waste and Biomass Valorization*, Springer Netherlands. **10**, 2079–97. https://doi.org/10.1007/s12649-018-0256-3

[32] Gerken, H.G., Donohoe, B. and Knoshaug, E.P. (2013) Enzymatic cell wall degradation of Chlorella vulgaris and other microalgae for biofuels production. *Planta*, **237**, 239–53. https://doi.org/10.1007/s00425-012-1765-0

[33] Carvalho, J.C., Magalhães, A.I., Pereira, G.V.M., Medeiros, A.B.P., Sydney, E.B., Rodrigues, C. et al. (2020) Microalgal biomass pretreatment for integrated processing into biofuels, food, and feed. *Bioresource Technology*, Elsevier. **300**, 122–719. https://doi.org/10.1016/J.BIORTECH.2019.122719

[34] Calvo-Flores, F.G. and Martin-Martinez, F.J. (2022) Biorefineries: Achievements and challenges for a bio-based economy. *Frontiers in Chemistry*, Frontiers Media S.A. **10**. https://doi.org/10.3389/fchem.2022.973417

[35] Ng, D.K.S., Ng, K.S. and Ng, R.T.L. (2017) Integrated Biorefineries. *Encyclopedia of Sustainable Technologies*, Elsevier. 299–314. https://doi.org/10.1016/B978-0-12-409548-9.10138-1

[36] Saini, J.K., Gupta, R., Hemansi, Verma, A., Gaur, P., Saini, R. et al. (2019) Integrated Lignocellulosic Biorefinery for Sustainable Bio-Based Economy. *Sustainable Approaches for Biofuels Production Technologies*, p. 25–46. https://doi.org/10.1007/978-3-319-94797-6_2

[37] Buck, V., Polanska, M. and Impe, J. Van. (2020) Modeling Biowaste Biorefineries: A Review. *Frontiers in Sustainable Food Systems*, Frontiers Media S.A. **4**. https://doi.org/10.3389/fsufs.2020.00011

[38] Bhatia, L., Bachheti, R.K., Garlapati, V.K. and Chandel, A.K. (2022) Third-generation biorefineries: a sustainable platform for food, clean energy, and nutraceuticals production. *Biomass Conversion and Biorefinery*, Springer Science and Business Media Deutschland GmbH. **12**, 4215–30. https://doi.org/10.1007/s13399-020-00843-6

[39] Monlau, F., Suarez-Alvarez, S., Lallement, A., Vaca-Medina, G., Giacinti, G., Munarriz, M. et al. (2021) A cascade biorefinery for the valorization of microalgal biomass: biodiesel, biogas, fertilizers and high valuable compounds. *Algal Research*, Elsevier. **59**, 102–433. https://doi.org/10.1016/J.ALGAL.2021.102433

[40] Lari, Z., Ahmadzadeh, H. and Hosseini, M. (2019) Cell Wall Disruption: A Critical Upstream Process for Biofuel Production. In: Hosseini J, editor. *Advances in Feedstock Conversion Technologies for Alternative Fuels and Bioproducts: New Technologies, Challenges and Opportunities*, Woodhead Publishing. p. 21–35. https://doi.org/10.1016/B978-0-12-817937-6.00002-3

[41] Wagle, A., Angove, M.J., Mahara, A., Wagle, A., Mainali, B., Martins, M. et al. (2022) Multi-stage pre-treatment of lignocellulosic biomass for multi-product biorefinery: A review. *Sustainable Energy Technologies and Assessments*, Elsevier. **49**, 101–702. https://doi.org/10.1016/J.SETA.2021.101702

[42] Günerken, E., D'Hondt, E., Eppink, M.H.M., Garcia-Gonzalez, L., Elst, K. and Wijffels, R.H. (2015) Cell disruption for microalgae biorefineries. *Biotechnology Advances*, Elsevier Inc. **33**, 243–60. https://doi.org/10.1016/j.biotechadv.2015.01.008

[43] Galbe, M. and Wallberg, O. (2019) Pretreatment for biorefineries: A review of common methods for efficient utilisation of lignocellulosic materials. *Biotechnology for Biofuels*, BioMed Central Ltd. **12**. https://doi.org/10.1186/s13068-019-1634-1

[44] Bleakley, S. and Hayes, M. (2017) Algal proteins: Extraction, application, and challenges concerning production. *Foods*, MDPI AG. **6**, 1–34. https://doi.org/10.3390/foods6050033

[45] Bernaerts, T.M.M., Gheysen, L., Foubert, I., Hendrickx, M.E. and Loey, A.M. Van. (2019) Evaluating microalgal cell disruption upon ultra high pressure homogenization. *Algal Research*, Elsevier B.V. **42**, 101–616. https://doi.org/10.1016/j.algal.2019.101616

[46] Spiden, E.M., Yap, B.H.J., Hill, D.R.A., Kentish, S.E., Scales, P.J. and Martin, G.J.O. (2013) Quantitative evaluation of the ease of rupture of industrially promising microalgae

by high pressure homogenization. *Bioresource Technology*, Elsevier Ltd. **140**, 165–71. https://doi.org/10.1016/j.biortech.2013.04.074

[47] Yurdacan, H.M. and Sari, M.M. (2021) Functional green-based nanomaterials towards sustainable carbon capture and sequestration. *Sustainable Materials for Transitional and Alternative Energy*, Gulf Professional Publishing. p. 125–77. https://doi.org/10.1016/B978-0-12-824379-4.00004-5

[48] Wang, T. and Lü, X. (2021) Overcome saccharification barrier: Advances in hydrolysis technology. *Advances in 2nd Generation of Bioethanol Production*, Woodhead Publishing. p. 137–59. https://doi.org/10.1016/B978-0-12-818862-0.00005-4

[49] García, J.M.R., Fernández, F.G.A. and Sevilla, J.M.F. (2012) Development of a process for the production of l-amino-acids concentrates from microalgae by enzymatic hydrolysis. *Bioresource Technology*, **112**, 164–70. https://doi.org/10.1016/j.biortech.2012.02.094

[50] Yin, X.B., Wu, P., Li, Y. and Yan, X.P. (2012) Mercury Speciation and Binding to Biomacromolecules. *Comprehensive Sampling and Sample Preparation*, Academic Press. **3**, 435–60. https://doi.org/10.1016/B978-0-12-381373-2.00094-6

[51] Branco, R.H.R., Serafim, L.S. and Xavier, A.M.R.B. (2019) Second generation bioethanol production: On the use of pulp and paper industry wastes as feedstock. *Fermentation*, MDPI AG. **5**. https://doi.org/10.3390/fermentation5010004

[52] Eldalatony, M.M., Kabra, A.N., Hwang, J.H., Govindwar, S.P., Kim, K.H., Kim, H. et al. (2016) Pretreatment of microalgal biomass for enhanced recovery/extraction of reducing sugars and proteins. *Bioprocess and Biosystems Engineering*, Springer Verlag. **39**, 95–103. https://doi.org/10.1007/s00449-015-1493-5

[53] Gao, L., Li, D., Gao, F., Liu, Z., Hou, Y., Chen, S. et al. (2015) Hydroxyl radical-aided thermal pretreatment of algal biomass for enhanced biodegradability. *Biotechnology for Biofuels*, BioMed Central Ltd. **8**. https://doi.org/10.1186/s13068-015-0372-2

[54] Ibrahim, H.A. (2019) Introductory Chapter: Fractionation. *Fractionation*, IntechOpen. https://doi.org/10.5772/intechopen.78050

[55] Justino, C.I.L., Duarte, K., Freitas, A.C., Duarte, A.C. and Rocha-Santos, T. (2014) Classical Methodologies for Preparation of Extracts and Fractions. *Comprehensive Analytical Chemistry*, Elsevier. p. 35–57. https://doi.org/10.1016/B978-0-444-63359-0.00003-3

[56] Strathmann, H., Giorno, L. and Drioli, E. (2006) An Introduction to Membrane Science and Technology. Consiglio Nazionale Delle Ricerche.

[57] Safi, C., Olivieri, G., Campos, R.P., Engelen-Smit, N., Mulder, W.J., Broek, L.A.M.V. et al. (2017) Biorefinery of microalgal soluble proteins by sequential processing and membrane filtration. *Bioresource Technology*, Elsevier Ltd. **225**, 151–8. https://doi.org/10.1016/j.biortech.2016.11.068

[58] N, Y.K., M, M.U.T., S, K., Sachdeva, S., Thakur, S., S, A.K. et al. (2023) Lignocellulosic Biorefinery Technologies: A Perception into Recent Advances in Biomass Fractionation, Biorefineries, Economic Hurdles and Market Outlook. *Fermentation*, MDPI AG. **9**. https://doi.org/10.3390/fermentation9030238

[59] Gerardo, M.L., Oatley-Radcliffe, D.L. and Lovitt, R.W. (2014) Integration of membrane technology in microalgae biorefineries. *Journal of Membrane Science*, Elsevier. **464**, 86–99. https://doi.org/10.1016/j.memsci.2014.04.010

[60] Qin, Z., Liu, H.M., Ma, Y.X. and Wang, X. De. (2021) Developments in extraction, purification, and structural elucidation of proanthocyanidins (2000–2019). *Studies in Natural Products Chemistry*, Elsevier. p. 347–91. https://doi.org/10.1016/B978-0-12-819485-0.00008-6

[61] Koyuncu, I., Sengur, R., Turken, T., Guclu, S. and Pasaoglu, M.E. (2015) Advances in water treatment by microfiltration, ultrafiltration, and nanofiltration. *Advances in Membrane Technologies for Water Treatment*, Woodhead Publishing. p. 83–128. https://doi.org/10.1016/B978-1-78242-121-4.00003-4

[62] Guo, W., Ngo, H.H. and Li, J. (2012) A mini-review on membrane fouling. *Bioresource Technology*, **122**, 27–34. https://doi.org/10.1016/j.biortech.2012.04.089

[63] Leeper, S.A. and Tsao, G.T. (1987) Membrane separations in ethanol recovery: an analysis of two applications of hyperfiltration. *Journal of Membrane Science*, Elsevier. **30**, 289–312. https://doi.org/10.1016/S0376-7388(00)80124-6

[64] Hu, X., Tanaka, A. and Tanaka, R. (2013) Simple extraction methods that prevent the artifactual conversion of chlorophyll to chlorophyllide during pigment isolation from leaf samples. *Plant Methods*, **9**. https://doi.org/10.1186/1746-4811-9-19

[65] Baümler, E.R., Carrín, M.E. and Carelli, A.A. (2016) Extraction of sunflower oil using ethanol as solvent. *Journal of Food Engineering*, Elsevier. **178**, 190–7. https://doi.org/10.1016/J.JFOODENG.2016.01.020

[66] Ajila, C.M., Brar, S.K., Verma, M., Tyagi, R.D., Godbout, S. and Valéro, J.R. (2011) Extraction and Analysis of Polyphenols: Recent trends. *Critical Reviews in Biotechnology*, **31**, 227–49. https://doi.org/10.3109/07388551.2010.513677

[67] Hikmawanti, N.P.E., Fatmawati, S. and Asri, A.W. (2021) The effect of ethanol concentrations as the extraction solvent on antioxidant activity of Katuk (Sauropus androgynus (L.) Merr.) leaves extracts. *IOP Conference Series: Earth and Environmental Science*, IOP Publishing Ltd. https://doi.org/10.1088/1755-1315/755/1/012060

[68] Aljabri, H., Cherif, M., Siddiqui, S.A., Bounnit, T. and Saadaoui, I. (2023) Evidence of the drying technique's impact on the biomass quality of Tetraselmis subcordiformis (Chlorophyceae). *Biotechnology for Biofuels and Bioproducts*, **16**, 85. https://doi.org/10.1186/s13068-023-02335-x

[69] Ryckebosch, E., Muylaert, K., Eeckhout, M., Ruyssen, T. and Foubert, I. (2011) Influence of drying and storage on lipid and carotenoid stability of the Microalga Phaeodactylum tricornutum. *Journal of Agricultural and Food Chemistry*, **59**, 11063–9. https://doi.org/10.1021/jf2025456

[70] Barbosa de Lima, A.G., Da Silva, J. V., Pereira, E.M.A., Dos Santos, I.B. and Barbosa de Lima, W.M.P. (2015) Drying of bioproducts: Quality and energy aspects. *Drying and*

Energy Technologies, Springer International Publishing. p. 1–18. https://doi.org/10.1007/978-3-319-19767-8_1

[71] Schmid, B., Navalho, S., Schulze, P.S.C., Van De Walle, S., Van Royen, G., Schüler, L.M. et al. (2022) Drying Microalgae Using an Industrial Solar Dryer: A Biomass Quality Assessment. *Foods*, MDPI. **11**. https://doi.org/10.3390/foods11131873

[72] Zhang, H., Gong, T., Li, J., Pan, B., Hu, Q., Duan, M. et al. (2022) Study on the Effect of Spray Drying Process on the Quality of Microalgal Biomass: a Comprehensive Biocomposition Analysis of Spray-Dried S. acuminatus Biomass. *Bioenergy Research*, Springer. **15**, 320–33. https://doi.org/10.1007/s12155-021-10343-8

[73] Sosnik, A. and Seremeta, K.P. (2015) Advantages and challenges of the spray-drying technology for the production of pure drug particles and drug-loaded polymeric carriers. *Advances in Colloid and Interface Science*, Elsevier B.V. **223**, 40–54. https://doi.org/10.1016/j.cis.2015.05.003

[74] Chen, W., Chiu, H.T., Feng, Z., Maes, E. and Serventi, L. (2021) Effect of Spray-Drying and Freeze-Drying on the Composition, Physical Properties, and Sensory Quality of Pea Processing Water (Liluva). *Foods*, MDPI AG. **10**. https://doi.org/10.3390/foods10061401

[75] Nowak, D. and Jakubczyk, E. (2020) The freeze-drying of foods-the characteristic of the process course and the effect of its parameters on the physical properties of food materials. *Foods*, MDPI AG. **9**. https://doi.org/10.3390/foods9101488

[76] Alvarenga, P., Martins, M., Ribeiro, H., Mota, M., Guerra, I., Cardoso, H. et al. (2023) Evaluation of the fertilizer potential of Chlorella vulgaris and Scenedesmus obliquus grown in agricultural drainage water from maize fields. *Science of the Total Environment*, Elsevier B.V. **861**. https://doi.org/10.1016/j.scitotenv.2022.160670

[77] Chng, L.M., Lee, K.T. and Chan, D.J.C. (2017) Synergistic effect of pretreatment and fermentation process on carbohydrate-rich Scenedesmus dimorphus for bioethanol production. *Energy Conversion and Management*, Elsevier Ltd. **141**, 410–9. https://doi.org/10.1016/j.enconman.2016.10.026

[78] Wang, H.M.D., Chen, C.C., Huynh, P. and Chang, J.S. (2015) Exploring the potential of using algae in cosmetics. *Bioresource Technology*, Elsevier Ltd. **184**, 355–62. https://doi.org/10.1016/j.biortech.2014.12.001

[79] Guimarães, A.M., Guertler, C., Pereira, G.D.V., Coelho, J. da R., Rezende, P.C., Nóbrega, R.O. et al. (2021) Nannochloropsis spp. as feed additive for the pacific white shrimp: Effect on midgut microbiology, thermal shock resistance and immunology. *Animals*, MDPI. **11**, 1–16. https://doi.org/10.3390/ani11010150

[80] Ljubic, A., Jacobsen, C., Holdt, S.L. and Jakobsen, J. (2020) Microalgae Nannochloropsis oceanica as a future new natural source of vitamin D3. *Food Chemistry*, Elsevier Ltd. **320**. https://doi.org/10.1016/j.foodchem.2020.126627

[81] Khatoon, H., Penz, K.P., Banerjee, S., Rahman, M.R., Mahmud Minhaz, T., Islam, Z. et al. (2021) Immobilized Tetraselmis sp. for reducing nitrogenous and phosphorous compounds

from aquaculture wastewater. *Bioresource Technology*, Elsevier Ltd. **338**. https://doi.org/10.1016/j.biortech.2021.125529

[82] Oddsson, G.V. (2020) A definition of aquaculture intensity based on production functions-the aquaculture production intensity scale (APIS). *Water*, MDPI AG. **12**. https://doi.org/10.3390/w12030765

[83] Troell, M., Kautsky, N., Beveridge, M., Henriksson, P., Primavera, J., Rönnbäck, P. et al. (2017) Aquaculture. *Reference Module in Life Sciences*, Elsevier. https://doi.org/10.1016/B978-0-12-809633-8.02007-0

[84] Sadigov, R. (2022) Rapid Growth of the World Population and Its Socioeconomic Results. *Scientific World Journal*, Hindawi Limited. **2022**. https://doi.org/10.1155/2022/8110229

[85] Martos-Sitcha, J.A., Mancera, J.M., Prunet, P. and Magnoni, L.J. (2020) Editorial: Welfare and Stressors in Fish: Challenges Facing Aquaculture. *Frontiers in Physiology*, Frontiers Media S.A. **11**. https://doi.org/10.3389/fphys.2020.00162

[86] Han, P., Lu, Q., Fan, L. and Zhou, W. (2019) A review on the use of microalgae for sustainable aquaculture. *Applied Sciences*, MDPI AG. **9**. https://doi.org/10.3390/app9112377

[87] Geng, B., Li, Y., Liu, X., Ye, J. and Guo, W. (2022) Effective treatment of aquaculture wastewater with mussel/microalgae/bacteria complex ecosystem: a pilot study. *Scientific Reports*, Nature Research. **12**. https://doi.org/10.1038/s41598-021-04499-8

[88] Eilam, Y., Khattib, H., Pintel, N. and Avni, D. (2023) Microalgae—Sustainable Source for Alternative Proteins and Functional Ingredients Promoting Gut and Liver Health. *Global Challenges*, John Wiley and Sons Inc. **7**. https://doi.org/10.1002/gch2.202200177

[89] Firmino, J.P., Vallejos-Vidal, E., Balebona, M.C., Ramayo-Caldas, Y., Cerezo, I.M., Salomón, R. et al. (2021) Diet, Immunity, and Microbiota Interactions: An Integrative Analysis of the Intestine Transcriptional Response and Microbiota Modulation in Gilthead Seabream (Sparus aurata) Fed an Essential Oils-Based Functional Diet. *Frontiers in Immunology*, Frontiers Media S.A. **12**. https://doi.org/10.3389/fimmu.2021.625297

[90] Pankhurst, N.W. (2011) The endocrinology of stress in fish: An environmental perspective. *General and Comparative Endocrinology*, Academic Press Inc. **170**, 265–75. https://doi.org/10.1016/j.ygcen.2010.07.017

[91] Barton, B.A. and Zwama, G.K. (1991) Physiological changes in fish from stress in aquaculture with emphasis on the response and effects of corticosteroids. *Annual Review of Fish Diseases*, **1**, 3–26. https://doi.org/10.1016/0959-8030(91)90019-G

[92] Alves, R.N., Cordeiro, O., Silva, T.S., Richard, N., de Vareilles, M., Marino, G. et al. (2010) Metabolic molecular indicators of chronic stress in gilthead seabream (Sparus aurata) using comparative proteomics. *Aquaculture*, **299**, 57–66. https://doi.org/10.1016/j.aquaculture.2009.11.014

[93] Guardiola, F.A., Cuesta, A. and Esteban, M.Á. (2016) Using skin mucus to evaluate stress in gilthead seabream (Sparus aurata L.). *Fish and Shellfish Immunology*, Academic Press. **59**, 323–30. https://doi.org/10.1016/j.fsi.2016.11.005

[94] Sitjà-Bobadilla, A., Peña-Llopis, S., Gómez-Requeni, P., Médale, F., Kaushik, S. and Pérez-Sánchez, J. (2005) Effect of fish meal replacement by plant protein sources on non-specific defence mechanisms and oxidative stress in gilthead sea bream (Sparus aurata). *Aquaculture*, Elsevier. **249**, 387–400. https://doi.org/10.1016/J.AQUACULTURE.2005.03.031

[95] Kokou, F., Sarropoulou, E., Cotou, E., Kentouri, M., Alexis, M. and Rigos, G. (2017) Effects of graded dietary levels of soy protein concentrate supplemented with methionine and phosphate on the immune and antioxidant responses of gilthead sea bream (Sparus aurata L.). *Fish & Shellfish Immunology*, Academic Press. **64**, 111–21. https://doi.org/10.1016/J.FSI.2017.03.017

[96] Estensoro, I., Ballester-Lozano, G., Benedito-Palos, L., Grammes, F., Martos-Sitcha, J.A., Mydland, L.T. et al. (2016) Dietary butyrate helps to restore the intestinal status of a marine teleost (Sparus aurata) fed extreme diets low in fish meal and fish oil. *PLoS ONE*, Public Library of Science. **11**. https://doi.org/10.1371/journal.pone.0166564

[97] Kiela, P.R. and Ghishan, F.K. (2016) Physiology of intestinal absorption and secretion. *Best Practice and Research: Clinical Gastroenterology*, Bailliere Tindall Ltd. **30**, 145–59. https://doi.org/10.1016/j.bpg.2016.02.007

[98] Peñaranda, D.S., Bäuerl, C., Tomás-Vidal, A., Jover-Cerdá, M., Estruch, G., Martínez, G.P. et al. (2020) Intestinal explant cultures from gilthead seabream (Sparus aurata, L.) allowed the determination of mucosal sensitivity to bacterial pathogens and the impact of a plant protein diet. *International Journal of Molecular Sciences*, MDPI AG. **21**, 1–20. https://doi.org/10.3390/ijms21207584

[99] Ferreira, M., Machado, M., Mota, C.S.C., Abreu, H., Silva, J., Maia, M.R.G. et al. (2023) Micro- and macroalgae blend modulates the mucosal and systemic immune responses of European seabass (Dicentrarchus labrax) upon infection with Tenacibaculum maritimum. *Aquaculture*, Elsevier. **566**. https://doi.org/10.1016/J.AQUACULTURE.2022.739222

[100] Liu, W.C., Guo, Y., Zhao, Z.H., Jha, R. and Balasubramanian, B. (2020) Algae-Derived Polysaccharides Promote Growth Performance by Improving Antioxidant Capacity and Intestinal Barrier Function in Broiler Chickens. *Frontiers in Veterinary Science*, Frontiers Media S.A. **7**. https://doi.org/10.3389/fvets.2020.601336

[101] Piro, G., Lenucci, M., Dalessandro, G., La Rocca, N., Rascio, N., Moro, I. et al. (2000) Ultrastructure, chemical composition and biosynthesis of the cell wall in koliella antarctica (klebsormidiales, chlorophyta). *European Journal of Phycology*, **35**, 331–7. https://doi.org/10.1080/09670260010001735931

[102] Suzuki, H., Hulatt, C.J., Wijffels, R.H. and Kiron, V. (2019) Growth and LC-PUFA production of the cold-adapted microalga Koliella antarctica in photobioreactors. *Journal of Applied Phycology*, Springer Netherlands. **31**, 981–97. https://doi.org/10.1007/s10811-018-1606-z

[103] Yakimovich, K.M., Gauthier, N.P.G., Engstrom, C.B., Leya, T. and Quarmby, L.M. (2021) A Molecular Analysis of Microalgae from Around the Globe to Revise Raphidonema

(Trebouxiophyceae, Chlorophyta). *Journal of Phycology*, John Wiley and Sons Inc. **57**, 1419–32. https://doi.org/10.1111/jpy.13183

[104] Andreoli, C., Lokhorst, G.M., Mani, A.M., Scarabel, L., Moro, I., La Rocca, N. et al. (1998) Koliella antarctica sp. nov. (Klebsormidiales) a new marine green micro alga from the Ross Sea (Antarctica). *Algological Studies*, Schweizerbart. **90**, 1–8. https://doi.org/10.1127/algol_stud/90/1998/1

[105] Vona, V., Rigano, V.M., Andreoli, C., Lobosco, O., Caiazzo, M., Martello, A. et al. (2018) Comparative analysis of photosynthetic and respiratory parameters in the psychrophilic unicellular green alga Koliella antarctica, cultured in indoor and outdoor photo-bioreactors. *Physiology and Molecular Biology of Plants*, Springer. **24**, 1139–46. https://doi.org/10.1007/s12298-018-0595-3

[106] Fogliano, V., Andreoli, C., Martello, A., Caiazzo, M., Lobosco, O., Formisano, F. et al. (2010) Functional ingredients produced by culture of Koliella antarctica. *Aquaculture*, Elsevier. **299**, 115–20. https://doi.org/10.1016/J.AQUACULTURE.2009.11.008

[107] Lima, S., Schulze, P.S.C., Schüler, L.M., Rautenberger, R., Morales-Sánchez, D., Santos, T.F. et al. (2021) Flashing light emitting diodes (LEDs) induce proteins, polyunsaturated fatty acids and pigments in three microalgae. *Journal of Biotechnology*, Elsevier B.V. **325**, 15–24. https://doi.org/10.1016/j.jbiotec.2020.11.019

[108] Shramko, V.S., Polonskaya, Y. V., Kashtanova, E. V., Stakhneva, E.M. and Ragino, Y.I. (2020) The short overview on the relevance of fatty acids for human cardiovascular disorders. *Biomolecules*, MDPI AG. **10**, 1–24. https://doi.org/10.3390/biom10081127

[109] Buscemi, S., Corleo, D., Di Pace, F., Petroni, M.L., Satriano, A. and Marchesini, G. (2018) The effect of lutein on eye and extra-eye health. *Nutrients*, MDPI AG. **10**. https://doi.org/10.3390/nu10091321

[110] Tlais, A.Z.A., Fiorino, G.M., Polo, A., Filannino, P. and Cagno, R. Di. (2020) High-value compounds in fruit, vegetable and cereal byproducts: An overview of potential sustainable reuse and exploitation. *Molecules*, MDPI AG. **25**. https://doi.org/10.3390/molecules25132987

[111] Balasubramanian, B., Liu, W.C. and Kim, I.H. (2023) Editorial: Application of natural bioactive compounds in animal nutrition. *Frontiers in Veterinary Science*, Frontiers Media S.A. **10**. https://doi.org/10.3389/fvets.2023.1204490

[112] Maffei, G., Bracciale, M.P., Broggi, A., Zuorro, A., Santarelli, M.L. and Lavecchia, R. (2018) Effect of an enzymatic treatment with cellulase and mannanase on the structural properties of Nannochloropsis microalgae. *Bioresource Technology*, Elsevier Ltd. **249**, 592–8. https://doi.org/10.1016/j.biortech.2017.10.062

[113] Zhang, Y., Kong, X., Wang, Z., Sun, Y., Zhu, S., Li, L. et al. (2018) Optimization of enzymatic hydrolysis for effective lipid extraction from microalgae Scenedesmus sp. *Renewable Energy*, Pergamon. **125**, 1049–57. https://doi.org/10.1016/J.RENENE.2018.01.078

[114] Gonçalves, C., Rodriguez-Jasso, R.M., Gomes, N., Teixeira, J.A. and Belo, I. (2010) Adaptation of dinitrosalicylic acid method to microtiter plates. *Analytical Methods*, **2**, 2046–8. https://doi.org/10.1039/c0ay00525h

[115] Nielsen, P.M., Petersen, D. and Dambmann, C. (2001) Improved Method for Determining Food Protein Degree of Hydrolysis. *Food Chemistry and Toxicology*, **66**. https://doi.org/10.1111/j.1365-2621.2001.tb04614.x

[116] Lowry, O.H., Rosebrough, N.J., Farr, A.L. and Randall, R.J. (1951) Protein measurement with the Folin phenol reagent. *The Journal of Biological Chemistry*, **193**, 265–75. https://doi.org/10.1016/s0021-9258(19)52451-6

[117] Dubois, M., Gilles, K.A., Hamilton, J.K., Rebers, P.A. and Smith, F. (1956) Colorimetric Method for Determination of Sugars and Related Substances. *American Chemical Society*, **28**, 350–6. https://doi.org/10.1021/ac60111a017

[118] Pereira, H., Barreira, L., Mozes, A., Florindo, C., Polo, C., Duarte, C. V et al. (2011) Microplate-based high throughput screening procedure for the isolation of lipid-rich marine microalgae. *Biotechnology for Biofuels*, **4**. https://doi.org/10.1186/1754-6834-4-61

[119] Bligh, E.G. and Dyer, W.J. (1959) A rapid method of total lipid extraction and purification. *Canadian Journal of Biochemistry and Physiology*, **37**, 911–7. https://doi.org/10.1139/o59-099

[120] Templeton, D.W. and Laurens, L.M.L. (2015) Nitrogen-to-protein conversion factors revisited for applications of microalgal biomass conversion to food, feed and fuel. *Algal Research*, Elsevier B.V. **11**, 359–67. https://doi.org/10.1016/j.algal.2015.07.013

[121] Pereira, H., Barreira, L., Figueiredo, F., Custódio, L., Vizetto-Duarte, C., Polo, C. et al. (2012) Polyunsaturated fatty acids of marine macroalgae: Potential for nutritional and pharmaceutical applications. *Marine Drugs*, MDPI AG. **10**, 1920–35. https://doi.org/10.3390/md10091920

[122] Lichtenthaler, H.K. and Wellburn, A.R. (1983) Determinations of total carotenoids and chlorophylls a and b of leaf extracts in different solvents. *Biochemical Society Transactions*, **11**, 591–2.

[123] Schüler, L.M., Gangadhar, K.N., Duarte, P., Placines, C., Molina-Márquez, A.M., Léon-Bañares, R. et al. (2020) Improvement of carotenoid extraction from a recently isolated, robust microalga, Tetraselmis sp. CTP4 (chlorophyta). *Bioprocess and Biosystems Engineering*, Springer. **43**, 785–96. https://doi.org/10.1007/s00449-019-02273-9

[124] Couso, I., Vila, M., Vigara, J., Cordero, B.F., Vargas, M.Á., Rodríguez, H. et al. (2012) Synthesis of carotenoids and regulation of the carotenoid biosynthesis pathway in response to high light stress in the unicellular microalga Chlamydomonas reinhardtii. *European Journal of Phycology*, **47**, 223–32. https://doi.org/10.1080/09670262.2012.692816

[125] Pfaffl, M.W. (2001) A new mathematical model for relative quantification in real-time RT-PCR. *Nucleic Acids Research*, **29**. https://doi.org/10.1093/nar/29.9.e45

[126] Tian, H., Lu, Z. and Chen, S. (2022) Predictive Modeling of Thermally Assisted Machining and Simulation Based on RSM after WAAM. *Metals*, MDPI. **12**. https://doi.org/10.3390/met12040691

[127] Ferreira, A., Figueiredo, D., Ferreira, F., Ribeiro, B., Reis, A., da Silva, T.L. et al. (2022) Impact of High-Pressure Homogenization on the Cell Integrity of Tetradesmus obliquus and Seed Germination. *Molecules*, MDPI. **27**. https://doi.org/10.3390/molecules27072275

[128] Zhang, Y., Kang, X., Zhen, F., Wang, Z., Kong, X. and Sun, Y. (2022) Assessment of enzyme addition strategies on the enhancement of lipid yield from microalgae. *Biochemical Engineering Journal*, Elsevier. **177**, 108–98. https://doi.org/10.1016/J.BEJ.2021.108198

[129] Pancha, I., Chokshi, K., Maurya, R., Bhattacharya, S., Bachani, P. and Mishra, S. (2016) Comparative evaluation of chemical and enzymatic saccharification of mixotrophically grown de-oiled microalgal biomass for reducing sugar production. *Bioresource Technology*, Elsevier. **204**, 9–16. https://doi.org/10.1016/J.BIORTECH.2015.12.078

[130] Tacias-Pascacio, V.G., Morellon-Sterling, R., Siar, E.H., Tavano, O., Berenguer-Murcia, Á. and Fernandez-Lafuente, R. (2020) Use of Alcalase in the production of bioactive peptides: A review. *International Journal of Biological Macromolecules*, Elsevier B.V. **165**, 2143–96. https://doi.org/10.1016/j.ijbiomac.2020.10.060

[131] Wang, M., Lee, E., Dilbeck, M.P., Liebelt, M., Zhang, Q. and Ergas, S.J. (2017) Thermal pretreatment of microalgae for biomethane production: experimental studies, kinetics and energy analysis. *Journal of Chemical Technology and Biotechnology*, John Wiley and Sons Ltd. **92**, 399–407. https://doi.org/10.1002/jctb.5018

[132] Bleakley, S. and Hayes, M. (2021) Functional and bioactive properties of protein extracts generated from spirulina platensis and isochrysis galbana T-Iso. *Applied Sciences*, MDPI AG. **11**. https://doi.org/10.3390/app11093964

[133] Vilg, J.V. and Undeland, I. (2017) pH-driven solubilization and isoelectric precipitation of proteins from the brown seaweed Saccharina latissima—effects of osmotic shock, water volume and temperature. *Journal of Applied Phycology*, Springer Netherlands. **29**, 585–93. https://doi.org/10.1007/s10811-016-0957-6

[134] Cavonius, L.R., Albers, E. and Undeland, I. (2015) pH-shift processing of Nannochloropsis oculata microalgal biomass to obtain a protein-enriched food or feed ingredient. *Algal Research*, Elsevier B.V. **11**, 95–102. https://doi.org/10.1016/j.algal.2015.05.022

[135] Vasić, K., Knez, Ž. and Leitgeb, M. (2021) Bioethanol production by enzymatic hydrolysis from different lignocellulosic sources. *Molecules*, MDPI AG. **26**. https://doi.org/10.3390/molecules26030753

[136] Soto-Sierra, L., Wilken, L.R., Mallawarachchi, S. and Nikolov, Z.L. (2021) Process development of enzymatically-generated algal protein hydrolysates for specialty food applications. *Algal Research*, Elsevier. **55**, 102248. https://doi.org/10.1016/J.ALGAL.2021.102248

[137] Horst, I., Parker, B.M., Dennis, J.S., Howe, C.J., Scott, S.A. and Smith, A.G. (2012) Treatment of Phaeodactylum tricornutum cells with papain facilitates lipid extraction. *Journal of Biotechnology*, **162**, 40–9. https://doi.org/10.1016/j.jbiotec.2012.06.033

[138] Weiss, I.M., Muth, C., Drumm, R. and Kirchner, H.O.K. (2018) Thermal decomposition of the amino acids glycine, cysteine, aspartic acid, asparagine, glutamic acid, glutamine, arginine and histidine. *BMC Biophysics*, BioMed Central Ltd. **11**. https://doi.org/10.1186/s13628-018-0042-4

[139] Körner, P. (2021) Hydrothermal Degradation of Amino Acids. *ChemSusChem*, John Wiley and Sons Inc. **14**, 4947–57. https://doi.org/10.1002/cssc.202101487

[140] Juul, L., Haue, S.K., Bruhn, A., Boderskov, T. and Dalsgaard, T.K. (2023) Alkaline pH increases protein extraction yield and solubility of the extracted protein from sugar kelp (Saccharina latissima). *Food and Bioproducts Processing*, Institution of Chemical Engineers. **140**, 144–50. https://doi.org/10.1016/j.fbp.2023.05.008

[141] Sari, Y.W., Sanders, J.P.M. and Bruins, M. (2016) Techno-economical evaluation of protein extraction for microalgae biorefinery. *IOP Conference Series: Earth and Environmental Science*, Institute of Physics Publishing. https://doi.org/10.1088/1755-1315/31/1/012034

[142] Whitaker, J.R., Feeney, R.E. and Sternberg, M.M. (1983) Chemical and physical modification of proteins by the hydroxide ion. *Food Science and Nutrition*, **19**, 173–212. https://doi.org/10.1080/10408398309527375

[143] Markou, G., Angelidaki, I. and Georgakakis, D. (2012) Microalgal carbohydrates: An overview of the factors influencing carbohydrates production, and of main bioconversion technologies for production of biofuels. *Applied Microbiology and Biotechnology*, **96**, 631–45. https://doi.org/10.1007/s00253-012-4398-0

[144] Pace, C.N., Treviño, S., Prabhakaran, E. and Scholtz, J.M. (2004) Protein structure, stability and solubility in water and other solvents. *Philosophical Transactions of the Royal Society*, Royal Society. **359**, 1225–35. https://doi.org/10.1098/rstb.2004.1500

[145] Morr, C. V. and Lin, S.H.C. (1970) Preparation and Properties of an Alcohol-Precipitated Whey Protein Concentrate. *Journal of Dairy Science*, Elsevier. **53**, 1162–70. https://doi.org/10.3168/JDS.S0022-0302(70)86362-7

[146] Tai, Y., Shen, J., Luo, Y., Qu, H. and Gong, X. (2020) Research progress on the ethanol precipitation process of traditional Chinese medicine. *Chinese Medicine*, BioMed Central Ltd. **15**. https://doi.org/10.1186/s13020-020-00366-2

[147] Kagan, I.A. (2022) Water- and Ethanol-Soluble Carbohydrates of Temperate Grass Pastures: a Review of Factors Affecting Concentration and Composition. *Journal of Equine Veterinary Science*, W.B. Saunders. **110**, 103866. https://doi.org/10.1016/J.JEVS.2022.103866

[148] Alves, L.A., Almeida E Silva, J.B. and Giulietti, M. (2007) Solubility of D-glucose in water and ethanol/water mixtures. *Journal of Chemical and Engineering Data*, **52**, 2166–70. https://doi.org/10.1021/je700177n

[149] Kumar, N.G., Contaifer, D., Madurantakam, P., Carbone, S., Price, E.T., Tassell, B. Van et al. (2019) Dietary bioactive fatty acids as modulators of immune function: Implications on human health. *Nutrients*, MDPI AG. **11**. https://doi.org/10.3390/nu11122974

[150] Kris-Etherton, P., Hecker, K., Taylor, D.S., Zhao, G., Coval, S. and Binkoski, A. (2001) Dietary Macronutrients and Cardiovascular Risk. *Nutrition in the Prevention and Treatment of Disease*, Academic Press. p. 279–90. https://doi.org/10.1016/B978-012193155-1/50020-9

[151] Zárate, R., Jaber-Vazdekis, N., Tejera, N., Pérez, J.A. and Rodríguez, C. (2017) Significance of long chain polyunsaturated fatty acids in human health. *Clinical and Translational Medicine*, Wiley. **6**. https://doi.org/10.1186/s40169-017-0153-6

[152] Schmitz, G. and Ecker, J. (2008) The opposing effects of n-3 and n-6 fatty acids. *Progress in Lipid Research*, Elsevier Ltd. **47**, 147–55. https://doi.org/10.1016/j.plipres.2007.12.004

[153] Bagga, D., Wang, L., Farias-Eisner, R., Glaspy, J.A. and Reddy, S.T. (2003) Differential effects of prostaglandin derived from-6 and-3 polyunsaturated fatty acids on COX-2 expression and IL-6 secretion. *Proceedings of the National Academy of Sciences of the United States of America*, **100**, 1751–6. https://doi.org/10.1073/pnas.0334211100

[154] Van Ginneken, V.J.T., Helsper, J.P.F.G., De Visser, W., Van Keulen, H. and Brandenburg, W.A. (2011) Polyunsaturated fatty acids in various macroalgal species from north Atlantic and tropical seas. *Lipids in Health and Disease*, **10**. https://doi.org/10.1186/1476-511X-10-104

[155] Sánchez-Machado, D.I., López-Cervantes, J., López-Hernández, J. and Paseiro-Losada, P. (2004) Fatty acids, total lipid, protein and ash contents of processed edible seaweeds. *Food Chemistry*, Elsevier. **85**, 439–44. https://doi.org/10.1016/J.FOODCHEM.2003.08.001

[156] Gouda, M., Tadda, M.A., Zhao, Y., Farmanullah, F., Chu, B., Li, X. et al. (2022) Microalgae Bioactive Carbohydrates as a Novel Sustainable and Eco-Friendly Source of Prebiotics: Emerging Health Functionality and Recent Technologies for Extraction and Detection. *Frontiers in Nutrition*, Frontiers Media S.A. **9**. https://doi.org/10.3389/fnut.2022.806692

[157] Gao, F., Cabanelas, I.T.D., Wijffels, R.H. and Barbosa, M.J. (2022) Fucoxanthin and docosahexaenoic acid production by cold-adapted Tisochrysis lutea. *New Biotechnology*, Elsevier. **66**, 16–24. https://doi.org/10.1016/J.NBT.2021.08.005

[158] Pandohee, J. (2022) Alpha-linolenic acid. *Nutraceuticals and Health Care*, Academic Press. 279–88. https://doi.org/10.1016/B978-0-323-89779-2.00003-X

[159] Chen, W., Li, T., Du, S., Chen, H. and Wang, Q. (2023) Microalgal polyunsaturated fatty acids: Hotspots and production techniques. *Frontiers in Bioengineering and Biotechnology*, Frontiers Media S.A. **11**. https://doi.org/10.3389/fbioe.2023.1146881

[160] Schüler, L., de Morais, E.G., Trovão, M., Machado, A., Carvalho, B., Carneiro, M. et al. (2020) Isolation and Characterization of Novel Chlorella Vulgaris Mutants With Low Chlorophyll and Improved Protein Contents for Food Applications. *Frontiers in Bioengineering and Biotechnology*, Frontiers Media S.A. **8**. https://doi.org/10.3389/fbioe.2020.00469

[161] Wiltshire, K.H., Boersma, M., Möller, A. and Buhtz, H. (2000) Extraction of pigments and fatty acids from the green alga Scenedesmus obliquus (Chlorophyceae). *Aquatic Ecology*, **34**, 119–26. https://doi.org/10.1023/A:1009911418606

[162] Giossi, C., Cartaxana, P. and Cruz, S. (2020) Photoprotective role of neoxanthin in plants and algae. *Molecules*, MDPI AG. **25**. https://doi.org/10.3390/molecules25204617

[163] Stahl, W. and Sies, H. (2005) Bioactivity and protective effects of natural carotenoids. *Biochimica et Biophysica Acta (BBA) - Molecular Basis of Disease*, Elsevier. **1740**, 101–7. https://doi.org/10.1016/J.BBADIS.2004.12.006

[164] Chen, D., Zhao, C.X., Lagoin, C., Hai, M., Arriaga, L.R., Koehler, S. et al. (2017) Dispersing hydrophobic natural colourant β-carotene in shellac particles for enhanced stability and tunable colour. *Royal Society Open Science*, Royal Society Publishing. **4**. https://doi.org/10.1098/rsos.170919

[165] Cummins, P.M. (2012) Occludin: One Protein, Many Forms. *Molecular and Cellular Biology*, Informa UK Limited. **32**, 242–50. https://doi.org/10.1128/mcb.06029-11

[166] Srdanovic, I., Yang, N. and Ray, S. (2022) Cell proliferation. *Reference Module in Biomedical Sciences*, Elsevier. https://doi.org/10.1016/B978-0-12-824315-2.00216-5

[167] Burk, R.F. and Hill, K.E. (2010) Glutathione Peroxidases. *Comprehensive Toxicology, Second Edition*, Elsevier. **4**, 229–42. https://doi.org/10.1016/B978-0-08-046884-6.00413-9

[168] Sarıkaya, E. and Doğan, S. (2020) Glutathione Peroxidase in Health and Diseases. *Glutathione System and Oxidative Stress in Health and Disease*, IntechOpen. https://doi.org/10.5772/intechopen.91009

[169] Jiang, W., Ye, Q., Wu, Z., Zhang, Q., Wang, L., Liu, J. et al. (2023) Analysis of CAT Gene Family and Functional Identification of OsCAT3 in Rice. *Genes*, MDPI. **14**. https://doi.org/10.3390/genes14010138

[170] Chen, C. (2010) COX-2's new role in inflammation. *Nature Chemical Biology*, **6**. https://doi.org/10.1038/nchembio.375

[171] Sutcliffe, S. and Pontari, M.A. (2016) Inflammation and Infection in the Etiology of Prostate Cancer. *Prostate Cancer: Science and Clinical Practice: Second Edition*, Academic Press. 13–20. https://doi.org/10.1016/B978-0-12-800077-9.00002-5

[172] Ricciotti, E. and Fitzgerald, G.A. (2011) Prostaglandins and inflammation. *Arteriosclerosis, Thrombosis, and Vascular Biology*, **31**, 986–1000. https://doi.org/10.1161/ATVBAHA.110.207449

[173] Boraschi, D. (2022) What Is IL-1 for? The Functions of Interleukin-1 Across Evolution. *Frontiers in Immunology*, Frontiers Media S.A. **13**. https://doi.org/10.3389/fimmu.2022.872155

[174] Cerezo-Ortega, I.M., Di Zeo-Sánchez, D.E., García-Márquez, J., Ruiz-Jarabo, I., Sáez-Casado, M.I., Balebona, M.C. et al. (2021) Microbiota composition and intestinal integrity remain unaltered after the inclusion of hydrolysed Nannochloropsis gaditana in Sparus

aurata diet. *Scientific Reports*, Nature Research. **11**. https://doi.org/10.1038/s41598-021-98087-5

[175] Abdel-Latif, H.M.R., El-Ashram, S., Yilmaz, S., Naiel, M.A.E., Abdul Kari, Z., Hamid, N.K.A. et al. (2022) The effectiveness of Arthrospira platensis and microalgae in relieving stressful conditions affecting finfish and shellfish species: An overview. *Aquaculture Reports*, Elsevier. **24**, 101135. https://doi.org/10.1016/J.AQREP.2022.101135

[176] Reis, B., Gonçalves, A.T., Santos, P., Sardinha, M., Conceição, L.E.C., Serradeiro, R. et al. (2021) Immune status and hepatic antioxidant capacity of gilthead seabream sparus aurata juveniles fed yeast and microalga derived β-glucans. *Marine Drugs*, MDPI. **19**. https://doi.org/10.3390/md19120653

[177] Beutner, S., Bloedorn, B., Frixel, S., Blanco, I.H., Hoffmann, T., Martin, H.-D. et al. (2001) Quantitative assessment of antioxidant properties of natural colorants and phytochemicals: carotenoids, flavonoids, phenols and indigoids. The role of b-carotene in antioxidant functions. *Science of Food and Agriculture*, **81**, 559–68. https://doi.org/10.1002/jsfa.849

[178] Jergensen, K. and Skibsted, L.H. (1993) Carotenoid scavenging of radicals: Effect of carotenoid structure and oxygen partial pressure on antioxidative activity. *Z Lebensm Unters Forsch*, **196**, 423–9. https://doi.org/10.1007/bf01190806

[179] Goiris, K., Muylaert, K., Fraeye, I., Foubert, I., De Brabanter, J. and De Cooman, L. (2012) Antioxidant potential of microalgae in relation to their phenolic and carotenoid content. *Journal of Applied Phycology*, Kluwer Academic Publishers. **24**, 1477–86. https://doi.org/10.1007/s10811-012-9804-6

[180] Guedes, A.C., Amaro, H.M. and Malcata, F.X. (2011) Microalgae as sources of carotenoids. *Marine Drugs*, MDPI AG. **9**, 625–44. https://doi.org/10.3390/md9040625

[181] Carballo, C., Pinto, P.I.S., Mateus, A.P., Berbel, C., Guerreiro, C.C., Martinez-Blanch, J.F. et al. (2019) Yeast β-glucans and microalgal extracts modulate the immune response and gut microbiome in Senegalese sole (Solea senegalensis). *Fish & Shellfish Immunology*, Academic Press. **92**, 31–9. https://doi.org/10.1016/J.FSI.2019.05.044

[182] Cerezuela, R., Meseguer, J. and Esteban, M.Á. (2013) Effects of dietary inulin, Bacillus subtilis and microalgae on intestinal gene expression in gilthead seabream (Sparus aurata L.). *Fish & Shellfish Immunology*, Academic Press. **34**, 843–8. https://doi.org/10.1016/J.FSI.2012.12.026

[183] Nayak, S., Al Ashhab, A., Zilberg, D. and Khozin-Goldberg, I. (2020) Dietary Supplementation with Omega-6 LC-PUFA-Rich Microalgae Regulates Mucosal Immune Response and Promotes Microbial Diversity in the Zebrafish Gut. *Biology*, MDPI AG. **9**, 119. https://doi.org/10.3390/biology9060119

Annex

Supplementary Data 1: Experimental matrix suggested by Design Expert version 11, for the 2 factors and range values selected for the experiment, including biomass concentration between 60 and 150 g/L and pressure between 300 and 1200 bar.

Run	A: [Biomass] (g/L)	B: Pressure (bar)
1	105	750
2	105	1200
3	105	300
4	105	750
5	105	750
6	73	432
7	73	1068
8	105	750
9	150	750
10	137	1068
11	60	750
12	105	750
13	137	432

Supplementary Data 2: Experimental matrix suggested by Design Expert version 11, for the 4 factors and range values selected for the experiment, including biomass concentration between 20 and 60 g/L, alcalase concentration between 0 and 6% (w/w), viscozyme concentration between 0 and 6% (w/w) and pH between 6 and 8.

Run	A: [Biomass] g/L	B: [Alcalase] % (w/w)	C: [Viscozyme] % (w/w)	D: pH
1	40	6	3	7
2	60	0	6	6
3	20	0	6	8
4	60	0	6	8

5	20	3	3	7
6	60	6	6	8
7	20	0	0	6
8	40	3	3	7
9	40	0	3	7
10	40	3	3	7
11	40	3	3	7
12	20	6	0	8
13	20	6	6	6
14	20	6	0	6
15	40	3	3	7
16	40	3	6	7
17	20	0	6	6
18	40	3	0	7
19	60	6	6	6
20	40	3	3	6
21	20	0	0	8
22	60	0	0	8
23	40	3	3	7
24	40	3	3	7
25	60	3	3	7
26	20	6	6	8
27	60	6	0	6
28	40	3	3	8
29	60	0	0	6
30	60	6	0	8